Fibers-based Porous Structures for Oil Absorption Applications

by

Syed Ali Shahid

A thesis
presented to the University of Waterloo
in fulfillment of the
thesis requirement for the degree of
Master of Applied Science
in
Chemical Engineering (Water)

Waterloo, Ontario, Canada, 2017

I hereby declare that I am the sole author of this thesis. This is a true copy of the thesis, including any required final revisions, as accepted by my examiners.

I understand that my thesis may be made electronically available to the public.

Abstract

In the age of environmental awareness the persistent problem of oil spills and their frequent occurrences have urged researchers to advance and innovate the methods for oil spill remediation. Besides being a significant economic loss oil spills have devastating impact on the environment that lasts for decades. Current oil spill clean up methods like: skimming, onsite burning and dispersants are often deemed as ineffective and are not eco- and environment friendly. Alternatively porous materials with their excellent innate proprieties are being considered as an enticing avenue for developing clean, inexpensive and an environment friendly solution to the problem of oil spills.

This work examines the use of short polymer fibers derived from recycled waste streams which can be enclosed in a suitable containment and used for oil absorption applications. Preventing fiber waste occupying valuable landfill sites and instead using them to solve another environmental problem makes this an environment friendly and a sustainable solution. The recycled short polymer fibers were used to build a porous medium with varying porosity.

Methods for characterizing the fiber material were studied and experiments were preformed to evaluate the feasibility of these fibers and prove that they indeed are an excellent choice for oil absorption. The hydrophobic and oleophilic character of the recycled fiber material was confirmed by contact angle measurements which also supplemented the study of spontaneous imbibition. The method for water-air capillary pressure curve was also obtained which showed that positive pressure is required to force water into the porous structure which further verified the non-wetting behavior of water on the fiber material.

Spontaneous imbibition experiment was performed to characterize the porous media sample to determine the wetting behavior of a range of low bulk densities porous samples with different hydrocarbon oils. The sorption behavior was studied as an immiscible displacement phenomena and the competing mechanisms for oil sorption were discussed

while interpreting results. The sorption kinetics of hydrocarbon oils inside the porous media were monitored using a load cell arrangement, thus resulting in the calculation of gravimetric and volumetric absorbency. It was found that certain hydrocarbons reached their peak absorbency at a particular bulk density. The effect of changing bulk density, oil properties and their subsequent effects were evaluated which afforded a fundamental analysis of the sorption mechanism. Wetting phase saturation was used as a criterion for comparing performance of varying bulk densities.

Traditional models like the Lucas-Washburn and the Darcy-based model were used to validate the experimental data. Due to considerable differences in the viscosities of the displacing (invader) and the displaced fluid (defender) the invasion front was assumed as compact and a stable sharp front. Under this assumption the fluid flow was modeled as single phase flow and the pore level physics was ignored. These models provide simple phenomenological macroscopic description of flow and with their mathematical simplicity can be conveniently applied on the experimental data. The driving force arising due to the interfacial pressure difference between the wetted and non-wetted regions was found to be an important parameters to derive some useful understanding of the porous structure. Since these models assume porous media to be a bundle of vertically aligned capillary tubes, the capillary pressure as described by the Young-Laplace equation was imposed as the pressure boundary condition at the moving liquid front. The governing equations thus derived gives a relationship between the front height, time and some macroscopic parameters like permeability, effective capillary radius and capillary pressure.

It was determined that porosity and wettability changes alone does not correlate with the observed data, hence to evaluate the performance of the sorbents correctly requires further studies on pore connectivity and pore size distributions. This was proposed as future work to analyze the porous structure by obtaining tomographic images and forming a 3-D structure of the real porous media sample. Moving forward the imbibition data could be simulated as two-phase flow directly in these 3-D pore network models. Moreover,

accurate relative permeabilities could be used to know the exact front saturation. Using this approach fluid behavior could be predicted much more accurately which would enable to design optimal porous structures for specific applications like sorbent booms for recovery of hydrocarbons from water.

Acknowledgements

First and foremost I would like to express my sincere gratitude to my supervisors Prof. Leonardo Simon and Prof. Marios Ioannidis for giving me this great opportunity to become a part of this project. I thank them for their continuous support, patience and guidance all along without which completion of this work would not have been possible.

I would like to thank to Prof. Jeff Gostick for his valuable support and kind help in providing access to his laboratory and also helping out with other matters. I would also thank him and Prof. Boxin Zhao for giving their valuable time and agreeing to become evaluators for my thesis.

Financial support from the Natural Sciences and Engineering Research Council of Canada (NSERC), Ontario Center of Excellence, Clear Blue Sorbents, the Collaborative Graduate Program for Water and the Department of Chemical Engineering is also gratefully acknowledged. I would also thank Mr. Michael Duffy and Mr. Clair Shoemaker from Clear Blue Sorbents for providing samples and essential support to this research.

Dedication

To my parents and siblings for their endless love, support and encouragement.

Table of Contents

List of Tables

List of Figures

Chapter 1

Introduction

1.1 General Overview

In a world so profoundly reliant on oil for sustaining its industrial and social economies the inevitability of a catastrophic oil spill is significant. The fact that oil still remains the most affordable, efficient and concentrated form of energy source downplays many of the adverse effects it has on our environment. In addition to being an important fossil fuel our addiction to oil, dubbed sometimes as black gold can be realized by considering how much of our daily use in transportation, housing, communication and entertainment are so dependent on oil-derived products. The conventional notion of oil to run out soon has incentivized scientists and engineers to develop even better technologies of oil exploration. As a result oil production continues to increase as global energy trends show. In Canada approximately 260000 tons of oil are consumed everyday. About ten times of this amount is used in USA per day and a total of 10 million tons used per day worldwide [1]. Therefore oil pollution is becoming an ever increasing concern amongst oil regulating authorities, environmental groups and society in general. More stringent legislation, guidelines and

operational procedures are being put in place to minimize the risks of a possible oil accident leading to a spill and subsequent environmental repercussions.

The supply chain of oil starting from crude oil wells moving to the consumer end is very complex. Oil products used for transportation, industrial machineries and various oil based industries can involve as many as ten to fifteen points of transfer of hydrocarbons using different transportation modes. These modes could be oil tankers, rail cars, pipelines. Despite best industrial practices for safe handling of oil the inherent risk involving human error and equipment failure cannot be eliminated. Therefore it is necessary for response organizations and researchers to develop advanced methods for controlling and cleaning up oil spills. The Deepwater horizon disaster in 2010 is a recent example and the largest oil spill to date which spilled nearly 5 million barrels of oil into the Gulf of Mexico. Other examples include the deliberate release of 4 million barrels in Suez Gulf and the Exxon Valdez which released 260 thousand barrels in the Gulf of Alaska. These accidents though very rare sends reminders of the dreadful ecological and environmental consequences oil spills have. Besides causing adverse impacts on the ecosystem that lasts for decades these occurrences results in great economic loss [2]. Therefore it has become really important for advancing oil spill remediation technologies.

In Canada oil spill statistics are collected by provincial offices and the complete database is maintained by Environment Canada. The minimum criterion for reporting an oil spill is 4000 liters and currently about 12 such spills occur every day. The figure below summarizes the oil spillage situation in Canada [1].

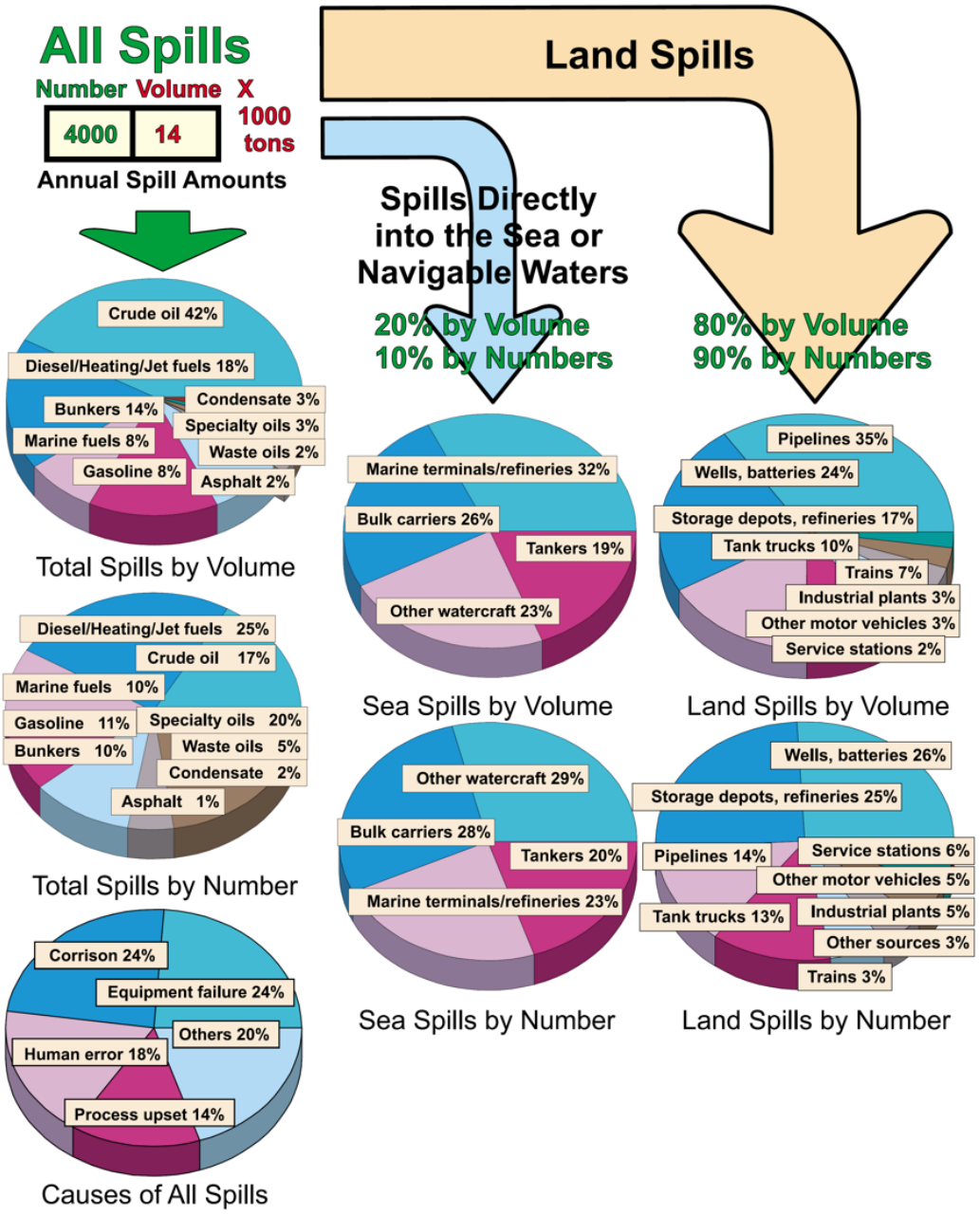

Figure 1.1: Oil spill summary in Canada [1]

Existing oil spill remediation includes a number of physio-chemical techniques that are employed for spill clean-up. These methods can generally be categorized into chemical, physical, thermal and biological methods and have been reviewed extensively in literature [3]. The clean up strategy depends on a number of factors: oil type, spill size and whether spill has occurred on water or land [3, 4]. This study will mainly emphasize spill clean-up from marine/aquatic systems. Amongst the different countermeasures the most typical ones include use of dispersants to break and mobilize the thick oil slick, controlled on-site burning of the oil, suction skimmers, physical containment and absorbent booms [5, 6]. All these techniques have their own pros and cons and usually a combination of these methods are used for an effective clean up. However most of these methods cause either secondary pollution problems like CO_2 emission in case of onsite burning or they are simply expensive and inefficient. In recent times it has become an interesting prospect for companies to not just remove the oil from the water but also recover it as much as possible. Therefore the science of oil/water separation through the use of absorbent materials has gained particular attention. Materials with special wettability characteristics are being fabricated to selectively and preferentially soak up oil in large amounts and at a fast rate.

Absorbent materials with opposite chemical affinities towards oil and water has become a very promising avenue for research on oil water separation. Porous materials with intrinsic hydrophobic and oleophilic properties have been shown to exhibit efficient oil sorbing characteristics. Wettability of a solid surface by different fluids like oil and water is a hot topic in material and interfacial science. Properties like hydrophobicity and oleophilicity is a direct result of the surface chemistry and surface morphology of the solid substrate. Jiang et al [7] prepared a mesh film with super-hydrophobic and super-oleophilic characteristics and demonstrated the effects of surface roughness on the wettability of the film. This increased interest not only on the fundamental level but also practical applications like oil/water separation. A large range of material have been studied and reported in literature that has useful properties for selective oil absorption. These materials are gen-

erally being categorized into 3 types: natural organic, natural inorganic and synthetic [8]. Characteristics of synthetic sorbents which are mainly polymers will be main focus of this study. A lot of polymers like polyurethane or polypropylene are now being commercially produced for oil separation applications.

This study will evaluate the fundamentals of absorption characteristics that enable these materials to be used in hydrocarbon spill clean up applications. Some of these properties that would be investigated are porosity, uptake rate, buoyancy on water, oil retention and oleophilicity/hydrophobicity. The material used in this study is a recycled polymer short fiber coming from different recycled waste streams.

As mentioned before these synthetic polymer fibers are considered as highly porous structures which can absorb liquids based on their preference. The main focus here therefore would be to study the fundamentals of liquid absorption into the short-fiber porous structure, surface preference, the relationship between liquid properties and the microstructure and lastly to mathematically model the absorption behavior that would allow design of efficient porous structures for hydrocarbon/water separation.

1.2 Motivation

Waste utilization is a key ingredient for industries investing in green and sustainable practices and moving towards a circular economy. Disposal of plastic waste which include all types of polymer fibers has become an increasing environment concern [9, 10]. Of the total plastic ever made till 2015 , 79% is accumulated in landfills [11]. Due to limited landfills available, increasing cost of raw materials the reuse of waste is an excellent option and in best interest for the environment. Polymer fiber waste is generated from various sources like tires, carpets, textiles, fishing lines etc.. Instead of dumping the waste fiber in to the environment efforts have to be made to realize some useful applications for them [10, 12].

Therefore considering these environmental constrains in mind the aim is to incorporate the polymer fiber waste stream and convert them to absorbent materials that could be used for cleaning of oil from surfaces of water or any scenario of oil/water separation in general. Moreover the fact that this developed material from waste would be used to solve another environment nuisance that of oil spill makes it a perfect fit to be classified as an environment friendly and a sustainable product. This research is to evaluate the properties of recycled polymer fiber and through relevant experiments validate that they indeed are an excellent alternate material for oil spill remediation.

The research methodology employed here to study hydrocarbon absorption comprises of phenomenological laws describing the physics of flow through porous media. Here porous media refers to the random polymer short fibers. Liquid penetration is a function of the microstructure of the porous medium, time and the wettability. The absorption is driven by the capillary forces arising from the difference in surface energies of the dry and wet solid (polymer fiber). In the field of interfacial phenomena this process is referred to as imbibition which is defined as the displacement of one less viscous and non wetting fluid by another immiscible, viscous and wetting fluid [13]. There are many examples where this phenomena of imbibition could be seen. Penetration of ink into an napkin, transport of water inside plants, recovering oil from reservoirs are some simple examples of a liquid invading a porous medium and displacing the immiscible phase. This displacement is characterized by the contrast of the fluid's viscosities and their interfacial tensions. This will be discussed in great detail in Chapter 2 where this subject will be introduced as spontaneous imbibition in porous media which is a vast field combining the physics of flow with the surface chemistry of the solid substrate.

In this thesis the aim is to understand the characteristics of the imbibition process, the interplay between the fluid properties and surface chemistry and to characterize the pore structure. Design of efficient porous structures has been of great interest for engineers because of their applications in a wide range of technological fields like oil recovery from

reservoirs, food industry, moisture management fabrics, filtration and fuel cells [14]. Qualitative assessment of the process can be done conveniently by the help of well-established theory however quantitative characterization that leads to insights of the microporous structure still remains a challenge. It is the intent in this work to probe these challenges of flow though disordered porous media and interpret the experiential results to aid in development of better predictive models for imbibition. The challenges of developing reliable pore scale models and to correlate properties measured on macroscale like absorption kinetics, bulk densities to characteristics like pore radius and permeability is one of the primary motive for the majority of the work that is reported here.

1.3 Objective and Scope of this Thesis

The aim of this thesis is to investigate the absorption characteristics of short polymer fiber used to create porous structures. To better comprehend the experimental data the research problem has been divided into 3 parts:

i) Wettability of the polymer material and its importance for the imbibition phenomenon

ii) Characterize the imbibition process and

iii) Combine the experimental data to fit theoretical models that would allow development of efficient absorbent products

These are the research activities that were done to meet these objectives:

- Evaluate wettability by measuring contact angles of water and a range of hydrocarbon oils on solid substrates prepared from polymer fibers.
- Study the effect of roughness on the magnitude of contact angles.

- Perform spontaneous imbibition experiments with a range of hydrocarbon oils and evaluate the efficiency of a sorbate-sorbent system
- Compare performance of sorbents of different bulk densities.
- Perform water/air capillary pressure test on the polymer porous media to study the saturation behavior in relation to capillary pressure and porosity
- Perform computerized tomography scan (CT-scan) for 3D visualization of the pore structure and a measure of its size distribution inside the fibrous media

Chapter 2

Literature Review

2.1 Oil on Water Clean-Up - An Overview

In an increasingly oil dependent world various anthropogenic causes from oil based activities pose severe threats to the environment on various levels. Accidental oil spills are a common occurrence which has significant short and long term consequences on the overall health of our ecosystem. As oil exploration continues to grow in more vulnerable and extreme environments, the risks of spill accidents is becoming ever more prevalent. The catastrophic oil spills in the past reminds of a pressing need for the scientific community to match upto these risks and improve and design new methods of oil spill remediation.

One third of the total oil consumed worldwide comes from marine reservoirs. According to a study on marine oil incidents every 30 meter depth increase of the offshore platform increase the chances of oil spill incident by nearly 9% [15]. However quantitatively speaking only 10 % of the oil polluting the environment originates from marine oil spills. The major contribution comes as run off from land based activities. The clean up strategy would differ based on the spill type, location and weather conditions. Land based spill for instance

would require a different approach than a spill on an ocean. One needs to appreciate these differences at the fundamental level and come up with suitable technologies accordingly. This thesis aims to look at the oil/water scenario in particular, therefore characteristics of a land based spill would not be discussed here. According to one estimate annually 2 million tonnes of oil enter the marine environment. It is believed that oil spill is a complex multi-faceted problem and an efficient and cost effective response strategy is the need of the time.

Currently there are four oil remediation technologies that are commonly deployed by the response organizations. These methods are not standalone and usually a combination of them is used for an effective clean-up. Developing materials with special wetting characteristics capable of selectively absorbing large quantities of oil has aroused great interest in the materials science community. The working principle of these materials is based on the surface energetics of the solid material and its preference for one of the liquid between oil and water. A parameter which measures this preference is the contact angle which will be discussed in section 2.7.1. These class of selective materials are generally being classified into two types: filtration and absorption materials [16]. Examples of filtration are membranes, fabrics and meshes; they have thinner cross-sections and allow either water or oil to pass/permeate through them. Absorbent systems selectively picks up the wetting liquid (oil or water) and fills up its internal void porous structure by capillary forces causing a selective separation. Wetting (in terms of the contact angle) is just one requirement and the most important one too, but other factors like liquid properties, internal void structure, its size ratio, surface topology makes the whole absorption process a very dynamic one with several parameters to alter for an optimized separation.

There are different mechanism through which a liquid can penetrate, flow and retain itself inside a solid material. However there are inconsistencies in the terminology used to describe these processes of fluid flow inside a porous structure. The terms 'Absorption' and 'Adsorption' are interchangeably used very frequently. In context of this thesis it is better

to elaborate the differences between them and adopt a generic term that encompasses both of them together.

2.1.1 Absorption, Adsorption and Sorption

Although absorption and adsorption do have subtle diffirences, researchers have tend to use them indistinguishably. For instance the process of oil uptake in porous medium has been referred to in some research articles as absorption [17] while adsorption in others [18]. Absorption occurs when a liquid get physically transported into and throughout the bulk of the porous material. Whereas adsorption is when liquid molecules get physically attached at the solid interface due to molecular interactions like Van der Waals forces. For a particular liquid that wets a solid material the uptake mechanism is believed to be a mechanism of both phenomena in succession. For example oil uptake would proceed by first getting physically adhered with the solid substrate and fills up the surface pores. From there due to capillary forces the oil would transport itself into the interior pores and voids [19, 20].

2.2 Sorbent Materials for Oil Absorption

Use of sorbents for combating oil spills is considered an inexpensive and effective method. Active research on oil sorbent materials has been going on for many decades. These materials with their oleophilic and hydrophobic character provides natural ability for oil to adhere to their surfaces. The highly porous structure allows the oil to penetrate by capillary action and to be held within the void by the adhesive forces on the surface of the sorbent materials. Other desirable properties for sorbents are buoyancy on water, retention of oil over time, recoverability of oil and reusability of the sorbent. These sorbent materials are generally categorized into 3 types: organic, mineral and synthetic. Previously

natural organic materials like cotton, milkweed and kapok have been evaluated as suitable materials for oil absorption. However these materials also possess high water sorption which is not desirable. The most commonly used materials are organic synthetic polymers like: polypropylene, polystyrene and polyurethane. These materials are mostly used in their non woven forms which makes them different from conventional textiles. These materials are produced as long fibers which form into fibrous webs with pores for liquids to penetrate.

Figure 2.1: 4 types of sorbents; a)Type 1 (sheets), b)Type 2 (loose) , c) Type 3 (booms) and d)Type 4 (pom-poms)

The ASTM standard (F726-12) categorizes the sorbents into 4 types: Type 1 have length and width much greater than their thickness, like pads, sheets and films for example. Type 2 are unconsolidated loose particulate materials that has no form and are handled with scoops. Type 3 are those in which the sorbent materials is enclosed in a suitable fabric which has small holes to permeate oil. These are called booms and are typically the most used type for picking up light oil from surfaces of open waters. Type 4 have open structures formed from a bundle of fibers that are called 'pom poms' and used as sweeps that provide a large surface area to adhere very viscous heavy oil. Figure 2.1 shows the different type of sorbents in use.

2.3 Characteristics of a Porous Material

A wide range of technological and natural processes around us are dependent on porous materials. Textiles, insulating materials, diapers, tissue papers and filters are some common examples of porous material in our everyday life. Technological examples include hydrology and petroleum production. These processes owe their properties to the unique internal pore structure and their interaction with a moving fluid. A material is said to be porous if it satisfies at least one of the following two conditions [21]:

1. It should contain empty space embedded within a solid and occupied by some fluid like air, oil, water etc..
2. It should be capable of transferring a fluid across its cross section.

The ability of a fluid to get sorbed and get transported through a porous solid fundamentally covers 3 aspects: transport phenomena, interfacial phenomena and the pore structure. In analyzing flow through a porous media it is desired to understand the synergistic effects of the three aspects together. However an attempt to describe the physics of

flow requires an accurate mathematical description of a pore. A porous material is said to consist of a network of interconnected voids, capillaries and pores of various size. Due to the complex geometry and irregularity of this network of void/pore space within a porous material no one has been able to present a unique mathematical definition of a pore. All definitions that aims to characterize a pore size and its distribution depends on a pore model and are termed as operational definitions. These models are further categorized as one, two or three dimensional models.

Pore network models are of great practical advantage to get insight of the microscopic pore structure that would be useful in interpreting and predicting macroscopic fluid behavior. However increasing the dimensionality of the network model increase the mathematical complexity which has little practical importance. The simplest approach in modelling fluid flow is the one dimensional "bundle of capillary tube" model which assumes the porous space to be composed of aligned capillary tubes of the same radius. The theory despite depicting a false image of the real porous medium has gained wide popularity in the porous medium community. This is because of its mathematical simplicity, easily measured parameters and ability to validate experimental data accurately in most cases of immiscible displacement of fluids [22]. The mathematical theory of the model and its simple macroscopic parameters would be discussed in section 2.8.

The discussion of pore structure at the microscopic level is not in the scope of this thesis. This is mainly because when the viscosity of the displacing fluid (oil) is significantly larger than the displaced fluid (air), the soprtion phenomena can be described by macroscopic models. Therefore this theses will not incorporate pore level physics; it will be limited to models that describe macroscopic properties influenced by the porous microstructure.

2.4 Macroscopic Properties of the Porous Medium

The most important properties characterizing a pore structure at the macro-scale are *a*) permeability *b*) porosity *c*) capillary pressure *d*) formation factor and *e*) specific surface area.

2.4.1 Permeability

Permeability is a unique property of a porous material indicative of its ability to transfer fluids. Its a material property governed by the porous structure and is independent of the conducting fluid property. The defining equation that relates permeability (K) to measurable quantities and that has become a standard mathematical tool for porous media flow is the Darcy's Law:

$$Q = \frac{K\,A}{\eta}\,\frac{\Delta P}{L} \tag{2.1}$$

where Q is the volumetric flow rate, A the cross-sectional area, ΔP/L is the pressure drop per unit length in the direction of the flow and η is the viscosity of the fluid. The unit has been assigned the name Darcy after the name of the scientist who developed this theory. The unit 1 darcy is defined as :

$$1\,darcy = \frac{1\,(cm^3/s)\,1\,(cP)}{1\,(cm^2)\,1(atm/cm)} \tag{2.2}$$

1 darcy is a considerably larger value for permeability as many practical porous materials have values much less than 1. Permeability measurements are done experimentally on a porous sample arranged in a cylindrical geometry like a tube. Both gas and liquids can be made to pass in plane or through plane to measure permeability. The experimental setup called permeameter is different for different fluids and extra caution is taken to make sure

that the fluid doesn't leak or by pass the porous material. It is believed that liquids tend to change the microstructure of the sample which compromises the accuracy of the results.

The procedure to find the permeability is simple. A steady flow rate of the fluid is passed through a sample of a precisely known length and a pressure drop is measured. A suitable sequence of flow rates is used which gives a corresponding pressure drop. A graph is plotted for these flow rates against pressure drop and the line of best fit is made to pass through the origin. The slope of the straight line gives the value for permeability of that sample. In case the data points do not fall on a straight line, the Darcy law does not validate the data and the experimental system must be further investigated. For the case of gases the procedure remains the same but the equation becomes slight different due to the compressibility factor of the gas. This happens because when a pressure drops in a gas flow its volume and velocity both changes from one face of the porous medium to another. Whereas in Equation 2.1 these quantities are constant for a steady state. Therefore to resolve this the differential form of Darcy equation is integrated with the condition that in gas flow the product of velocity and pressure through a sample is a constant. Darcy's law for compressible fluids becomes

$$\upsilon_2 = -(k/\eta)\,(P_2^2 - P_1^2)/(2P_2\,L) = -(k/\eta)(P_m/P_2)(\Delta P/L) \tag{2.3}$$

2.4.2 Porosity

Porosity is a measure of the total void space inside a porous solid. It can be written as the ratio of pore (void) volume to the solid volume. There are different types of voids inside a porous medium and terms like absolute and effective porosity are used to distinguish them. If the voids/pores are interconnected the porosity is termed as effective porosity. Whereas some porous solids have isolated pores and those cannot be used for transferring fluid through them; in such case the porosity is absolute porosity.

There are several experimental techniques to calculate the porosity. The one used in thesis is the density method. This methods depends on knowing the density of the sample and the density of the material in the sample. Since the mass and the volume of the porous sample are known, the bulk density can be calculated. By knowing the material density it follows that one can find the porosity using the relationship shown:

$$\phi = 1 - (\rho_{bulk}/\rho_{material}) \tag{2.4}$$

.

2.4.3 Capillary Suction Pressure and Effective Capillary Diameter

Considering porous structure as a bundle of aligned capillary tubes one can find the suction pressure responsible for pulling (imbibing) a liquid to a certain height in a porous medium. The rate at which the liquid imbibes inside the hypothetical capillaries is described by the famous Lucas-Washburn model. The capillary pressure across the wet and dry interface is given by the Young-Laplace equation which relates it to surface tension and radius of the capillary. The model has several assumptions that makes it far from reality, however its easy experimental validation and macroscopic flow description (in terms of effective capillary) makes it a suitable tool for interpreting experimental imbibition data.

These macroscopic properties influenced by the microporous structure enables one to make performance comparisons between different sorbent based on their fluid behavior. For instance one can compare the performance of two sorbents material by the rate of liquid uptake and the total mass sorbed. The material property that characterizes this would be macroscopic parameters discussed above. The next section will discuss the characteristics and properties that an oil absorbent should possess.

2.5 Characteristics for Optimal Design of Sorbents

Sorption is a general term that describes fluid uptake by a porous medium and essentially encompasses the mechanism of both absorption and adsorption concomitantly. In this thesis the term sorption and imbibition and the terms sorbents, booms and porous medium will be used interchangeably through out the text. In context of the research objective, that is to develop qualitative and quantitative basis for efficient boom development one must understand the dynamics of the process. Designing an efficient sorbent implies to maximize liquid uptake and minimize the uptake time. A third parameter would be to minimize the amount of porous material for a given sorbent job so that all the effective porosity is utilized meaning that all the air is displaced by the invading liquid.

The preceding section discussed the driving force for pulling the liquid into the pores; that is the capillary pressure as a macroscopic property described by the Young-Laplace equation. The equation implies that to increase the suction force for the same liquid would require to decrease the effective diameter of the hypothetical capillary in the Lucas-Washburn model. Since the porosity is depicted by the capillary diameter one would consider decreasing the porosity (void space) to increase the driving force for liquid uptake. However on the other hand the permeability of the porous medium as described by the Darcy law scales with the square of the pore size. Therefore due to these superimposing mechanisms a dynamic competition exists which would lead to an optimization problem with an aim to minimize the sorption time for a specific pore size/volume.

The sorption time is a function of the porous structure, liquid property and the wetting characteristic of the system. According to Jiang et al [19] desirable properties for an oil sorbent are high sorption capacity, high sorption rate, hydrophobicity and oleophilicity, buoyancy on water, good oil retention, durability and oil recoverability. Some of the important factors that have a synergistic effect on the efficacy of this optimization problem are outlined below with a brief description.

2.5.1 Voids between Fiber Filaments

It has been shown through analyzing scanning electron microscopy (SEM) images of sorbents made with polymer fibers that the interconnected void space forms capillary bridges that generates the effective capillary pull responsible for pulling the oil inwards and the adhesive forces (wettability) keeps the oil intact within the porous space [23].

2.5.2 Fiber Porosity and Fiber Diameter

In some cases even the fiber filament have hollow cross sections called lumens. This is especially true for natural fibers like cotton and milkweed [24]. It is shown by Lin et al using BET analysis that these pores could be in the range of mesopores (5-50 nm) to macropores (>50 nm) [25]. It is believed that one of the reasons for a non-Washburn behavior, despite showing sharp saturation liquid front, is due to the fact that these porous fibers act as sinks. It is therefore advisable to investigate not just voids but also the structure of the fiber itself before modeling the sorption behavior.

A large diameter fiber would negatively affect the sorbent performance as it would have less void space for the oil to occupy. It was shown that small fiber diameter favors adhesion of high visocisty oil [26, 25]. Zhu et al. [27] were the first to fabricate elecltrospun fibers specially made for oil spill absorbent application. They showed through absorption studies done under SEM analysis that an appropriated void size and fiber diameters are needed for maximum sorption capacity. To have larger voids and oil capacity it was shown that electrospun fibers made in the range of 1-3 µm were best suited for sorbing certain oils better than others. These results were in contrast to fibers prepared with the conventional meltblown techniques in which the fiber diameters were in the range of 10-50 µm [28]. Other factors that need to be researched alongside are the effect of oil viscosity and density in relation to the appropriate fiber porosity and diameter.

2.5.3 Surface Energy of the Fiber Material and the Liquid

The surface energy arises due to unbalanced force on molecules residing on the surface of a solid or a liquid. These molecules want to minimize their free energy and want to form intermolecular bonds with other neighboring molecules. For a liquid this means that it would try to ball up voluntarily to reduce its surface to a minimum. These forces which contracts the liquid into a droplet are cohesive forces. For a solid its surface energy stabilizes by allowing a liquid to spread on its surface by displacing air. These forces that allows the liquid to spread on the solid are the adhesive force acting on the solid-liquid interface. Wettability as measured by contact angle is the competition between these two forces. For a fiber material to get preferably wet with oil and repel water it must have a critical surface tension in between the surface tension of oil and water. This point is explained further in sec 2.7.1.

2.5.4 Viscosity of the Hydrocarbon Oils

Viscosity is a key parameter that can affect the sorption in different ways. Some researchers have reported opposing effects of increasing the viscosity on oil sorption capacity [29, 27]. They have observed that in some cases sorption increases as viscosity increases and this behavior is attributed to enhanced adherence of highly viscous oils to the surface of the fiber. On the other hand the low sorption is attributed to the inability of the high viscous oil to penetrate further into the porous matrix. From a practical standpoint the effect of different viscosity is important to study since in oil spill scenarios due to weathering and evaporation the volatile component of the oil evaporates leaving behind the viscous oil. Emulsification is another process which changes the oil viscosity significantly from when the oil was spilled. Therefore according to the lifecycle of the spilled oil it will require sorbent with different porous medium properties.

The difference in viscosity of the fluids is also an important parameter in modeling immiscible displacement (sorption). The viscosities of the fluids have to be sufficiently different for the displacement process to be assumed as stable displacement in which case single phase modeling can applied to the experimental data.

2.6 Spontaneous Imbibition

Fluid flow in porous media is an ubiquitous and important phenomena because of its presence in a wide range of practical applications like petroleum engineering, filtration and contaminant cleanup. The complex nature of the porous media and the demands of developing better theories or models to predict flow has gained wide interest from scientists till date [22]. In fluid mechanics this field of study is also referred to as multiphase transport in permeable media.

A subset of multiphase transport is immiscible displacement where one fluid displaces the other and the process is characterized by properties of the fluid, porous structure and the wetting behavior of the system. If the wetting fluid displaces the non-wetting the process is termed as imbibition and the reverse process is drainage. Further if the imbibition is not aided externally and happens solely due to capillary forces it is referred to as spontaneous imbibition. As a convention the fluid which displaces the other fluid is called the invader and the displaced fluid is called the defender [30].

In spontaneous imbibition the invader will always be the wetting fluid. The immiscible displacement process is governed by several factors: physical properties of the fluids; viscosities of the invader and defender, their densities and the interfacial tensions. They also depend on the saturation of the defender (S_2) and its distribution inside the porous medium. Saturation of a fluid is defined as the fraction of pore volume occupied by that fluid, so that $S_2 + S_1 = 1$ where S_1 is the saturation of the invader. All these aspects play

a decisive role in describing the physics of the imbibition process.

There are many challenges to analyze and predict fluid flow in porous medium. The complexity arise because of the different length and time scales that are encountered. The length scale of interest is usually that of a pore of sub-micrometer range, where as properties of interest like permeability, capillary pressure are at the macroscale. It is difficult to find quantitative relationships between pore level events to fluid flow occurring over a macroscale sample of porous media. However for practical applications it is really useful to find such relationships as it helps in developing controlled imbibition process. [13].

The physics of flow is determined by a combination of capillary and viscous forces. The geometry or shape of the moving front is governed by the relative magnitudes of these forces and it is this particular aspect that makes the modeling a very complex subject. In two phase flow the measure of these forces is characterized by two dimensionless numbers:

1. Capillary number $C_a = \frac{\eta v}{\gamma}$, which is a ratio of viscous to capillary forces
2. Mobility ratio $k = \frac{\eta_2}{\eta_1}$ which is the ratio of the viscosities of the two fluids

Based on the magnitudes of these numbers the flow can take either of the three forms [31]. :

a) Capillary fingering

b) Viscous fingering and

c) Stable displacement

Imbibition has long been studied as a two phase flow phenomena and understanding the pore level invasions has been of great interest in ascertaining the different shapes of the

boundaries between invader and the defender. However pioneering work by Lenormand et al [31] changed directions of further research and made some aspects easier to study than before. Their work experimented with several porous networks and fluids and verified that for certain values of the dimensionless numbers the pore level physics become irrelevant and the flow can essentially be modelled as single phase flow. Such a case was observed when the invading fluid (imbibing) has sufficiency larger viscosity than the defender or the displaced fluid.

In other words when the capillary number or the mobility ratio was high the flow regime was that of stable displacement of the moving liquid front. This regime is characterized by a well defined boundary between the wet and the dry regions of the porous medium. There is no entrapment of any blob of non wetting fluid also called ganglion behind the wetting front. This kind of stable displacement also has other names like saturated flow, piston flow or plug flow.

The benefit of assuming saturated flow is that it allows one to move from the continuum approach at the microscopic pore level to porous continuum approach at the macroscopic level. This 'upscaling' process implies that instead of infinitesimal averaging at the pore level the porous continuum model would average the flow properties over a representative elementary volume of the porous medium [32, 33]. Subsequently for stable displacement this means the interface position would be averaged out as one so that the description of flow and the governing equations would be macroscopic in nature.

Assumption of sharp moving front simplifies the flow as single phase and average properties derived like average permeability, capillary pressure could be useful performance indicators in practical applications. A vast amount of work has been done on single phase flow modelling; they are useful starting point for modelling experimental imbibition data as some of those produce very reliable results.

Two of the prominent models to study saturated or sharp moving front flow are Lucas-

Washburn and the Darcy law. Both these models are robust and involve easily measurable parameters. They both relate imbibition rate with the fluid properties and some representative pore size information. These models are deficient in providing realistic view of the porous microstructure. Several researchers have modified these models to include some complex geometry factor to account for the tortuosity and random nature of the real porous medium [34]. This thesis will evaluate the validity of these two models by fitting experimental imbibition data and shed some useful insight of the flow properties and their dependence on some easily measurable properties for the short polymer fiber porous material.

2.7 Wettability

2.7.1 Contact Angle

Wettability is defined as the tendency of a liquid to be attracted towards a solid surface [35]. The process commonly involves displacement of air by a liquid spreading along the solid. The interface between spreading liquid, air and the solid surface is referred to as the three phase contact line. It is the geometry of contact and its rate of change that determines the extent of wetting. The parameter that quantifies this degree of wetting is the contact angle. It is dependent on the interfacial energies at the 3 phase contact line and is defined as the angle formed at the intersection of solid/liquid and liquid/vapor interface. By assuming mechanical equilibrium of the three interfacial energies acting on the liquid drop, Thomas Young expressed the contact angle as a trigonometric function:

$$\cos\theta = \left(\gamma_{SV} - \gamma_{SL}\right)/\gamma_{LV} \tag{2.5}$$

Figure 2.2 illustrates the contact angle of a sessile drop resting against a solid surface

where γ represents the interfacial tension and S, L and V indicate the solid, liquid and the vapour phase respectively.

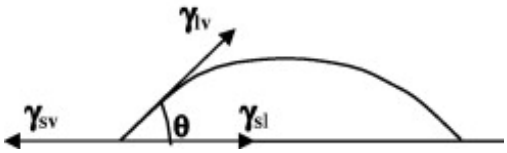

Figure 2.2: Contact angle as a function of 3 interfacial tensions

Young's equation assumes the solid surface in contact with the liquid droplet to be rigid, homogeneous and smooth. Also there should be no physical/ chemical interaction between the solid, liquid and vapor phase. Theoretically speaking this implies that Equation 2.5 based on the 3 thermodynamic properties γ_{SV} , γ_{SL} and γ_{LV} will give a unique value for the contact angle θ_Y or the Young contact angle [36].

However real solids are generally not smooth, homogeneous surface and therefore the observed contact angle may or may not be just a function of surface energetics as described by Young [37]. Infact this proposition is further verified by measuring dynamic contact angles and comparing the advancing and receding contact angles as a function of time. For non-ideal surfaces these values differ owing to surface heterogeneities and this is referred to as contact angle hysteresis. This apparent complexity has inspired indepth research on the thermodynamic status of contact angles [38, 39]. Therefore the topic of contact angles and its proper use in characterizing wettability is a hotly debated topic till date. It is imperative for researchers to measure contact angles so as to closely approximate Young's ideal surface i.e preparing as rigid and smooth samples as possible.

Resolving the controversy surrounding the proper use of of contact angles is beyond the scope of this thesis. The experimental methodology discussed in Chapter 3 will use two different types of surfaces from the same polymer fiber material. For practical purposes the general guidelines for degree of wetting by reporting contact angles as received from

the goniometer will be used here nonetheless. Therefore as a rule of thumb contact angles $\theta \ll 90^0$ implies high wettability and $\theta \gg 90^0$ implies low wettability. Figure 2.3 below illustrates the 3 cases of wetting.

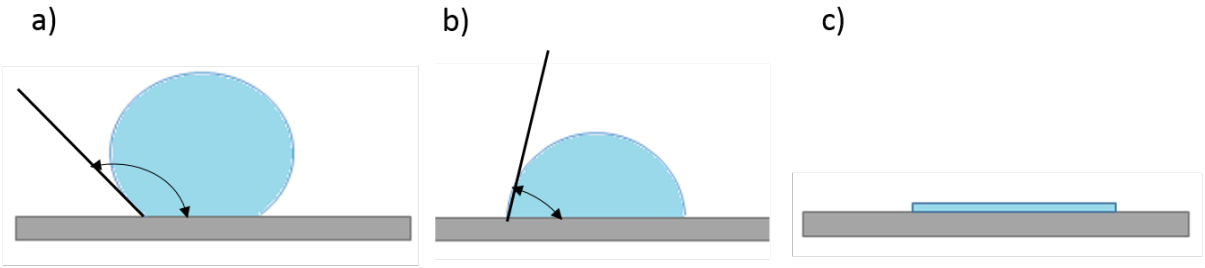

Figure 2.3: a) Non-wetting $\theta > 90^0$, b) Partial wetting $\theta < 90^0$ and c) Complete wetting $\theta = 0^0$

Relating contact angles to the surface tension of solids is of great importance in fundamental research and applied fields in material science [38, 37]. By looking at the Young's equation it is possible to realize that there are only two measurable quantities: the liquid/vapour surface tension γ_{LV} and the contact angle θ. It is desirable to find a suitable parameter to quantify wettability of a solid. Contact angle is one of them, however in order to predict which solids are going to be wetted more by a liquid without knowledge of the surface tension the other two quantities in the Young equation have to be known as well. Unfortunately there is no direct way of measuring γ_{SV} and γ_{SL} [37, 40]. Infact researchers have found them to be inseparable quantities.

Different approaches have been used to calculate the solid surface tension. The contact angle approach has been favored as a good starting point to study surface tension of solids. Difference theories have been proposed ranging from simple to complex ones. The three most regarded theories in this area are Owens/Wendt, Wu and the Zisman method. The

two latter methods are presented in mathematically complex forms and takes into account surface chemistry by dividing the surface contributions into polar and non polar parts. Zisman method is a popular method with very straightforward mathematical form.

Zisman defined $\gamma_{SV} - \gamma_{SL}$ as one single quantity for the case that $\theta \to 0$. The importance of this definition quickly becomes useful when considering the Young equation for the case that liquid forms a contact angle equal to zero. Then the Young equation becomes:

$$1 = (\gamma_{SV} - \gamma_{SL}) / \gamma_{LV}$$

Therefore this implies that theoretically speaking for liquids that 'just' forms a contact angle of 0^0, the γ_{LV} is equal to the surface tension of solid [40, 41]. The surface energy found this way came to be known as critical surface tension of the solid, or in other words it is the maximum possible surface tension of a liquid which will still wet the solid completely. The apparent simplicity of this method allowed determination of surface energy of solids by measuring contact angles of different liquids with known γ_{LV} and then plotting the corresponding values on a $\cos\theta$ versus γ_{LV} graph. It followed that a general linear trend was observed. This allowed data to be extrapolated so that γ_{LV} will be the surface tension of the solid as $\cos\theta$=1. This critical surface tension of the solid thus becomes an important parameter characterizing the ability of the solid to be wetted by a particular liquid.

Since this thesis focused on oil/water separation, it is expected that the critical surface energy of the solid prepared from polymer fiber to be in between that of hydrocarbon oil and water.

2.7.2 Capillarity

Fluid flow in porous medium is a process driven by capillary pressure. In fluid statics when two immiscible fluids comes in contact a discontinuity exist because of the pressure

difference across the interface [42]. This pressure difference is called the capillary pressure and is a function of the curvature, interfacial tensions and the wetting characteristics of the system. This differences arise because of the intermolecular attractions of the fluids involved with a solid phase. The cohesive and the adhesive forces determine wettability of the system. For instance when the adhesive forces between the liquid and the solid is greater than the cohesive force within the liquid, the solid would prefer to displace air and become wetted by the liquid. This difference in surface energies of the wet and dry solid leads to the capillary pull resulting in the concave shape of the meniscus. As stated earlier this phenomena where one fluids invades and displace the other fluid is called spontaneous imbibition, where spontaneous refers to thermodynamic spontaneity. Consider a vertical capillary placed on a liquid reservoir (see Figure 2.4). The pressure of the wetting phase (liquid) is denoted by P_w and that of the non wetting phase as P_{nw}: Then by definition

$$P_c = P_{nw} - P_w \tag{2.6}$$

Thus, capillary pressure is the excess pressure inside the non-wetting phase and is a function of the saturation at the liquid front. In this approach full saturation is assumed so that it resembles the so called piston like displacement. The liquid inside the capillary tends to rise and the balance of different forces will determine the rate of the moving front whereas final potion of the meniscus after a long time is essentially the balance between the capillary suction forces driving the flow up and the counter force of gravity. Assuming the radius of capillary as R_c and taking all the forces acting on the moving liquid front inside the capillary as follows:

- gravity: $\rho g A h$
- Surface Tension: $2\pi R_c \cos\theta$
- Inertia: $\partial/\partial t \left[A\rho(h + h_0)\partial h/\partial t\right]$

- Viscous : $k(h + h_0)\partial h/\partial t$

The inertial term comes as result of Newton's second law and is written in terms of the average velocity $\partial x/\partial t$ of the meniscus. The viscous term comes from the streamline flow condition of Newtonian flow with no slip boundary condition at the walls of the capillary. Consider a capillary tube immersed in a reservoir of a wetting liquid (oil in the case considered here) at atmospheric pressure. The combination of adhesive forces and liquid surface tension cause the liquid to rise inside the capillary and reaches to a height when the upward and downward forces balance each other out.

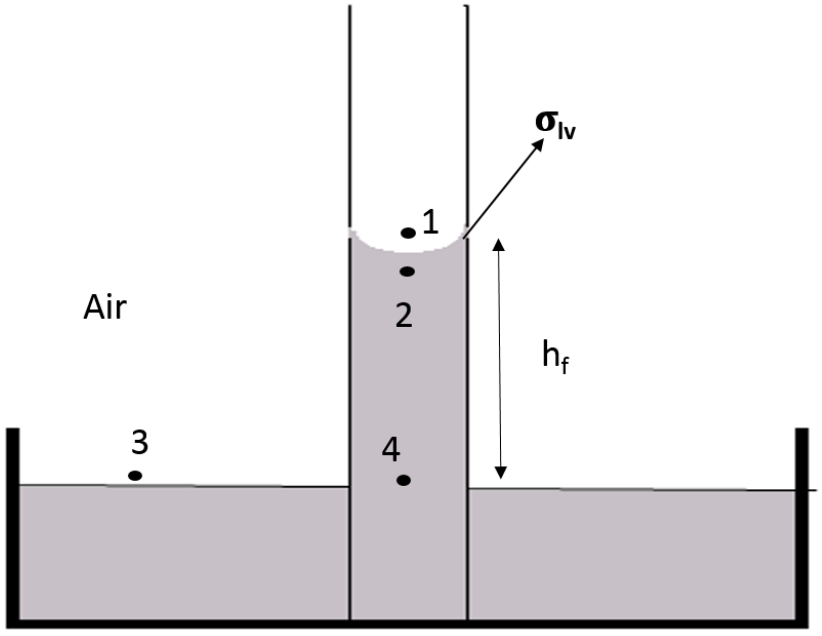

Figure 2.4: Capillary tube immersed in a wetting fluid reservoir

The force balance on the meniscus is written as:

$$-2\pi r\cos\theta + \rho g A h + \partial/\partial t\left[A\rho(h + h_0)\partial h/\partial t\right] + k(h + h_0)\partial h/\partial t = 0 \qquad (2.7)$$

As the meniscus reaches to its final steady state height characterized by the contact angle θ as given by equation 2.5, the time component goes away and equation 2.7 becomes

$$\mathrm{h}_\infty = \frac{2\gamma_{lv}\cos\theta}{R_c\rho_{liq}g} \tag{2.8}$$

where h_∞ is the steady state height reached by the meniscus when capillary pull is balanced by the hydrostatic force of the liquid column. The interfacial pressure difference between the wetting and the non-wetting phase as defined by the capillary pressure definition can be written as referring to the above diagram:

$$P_c = P_1 - P_2 \tag{2.9}$$

The pressure at point 2 is equal to the pressure at point 4 minus the hydrostatic pressure of the liquid:

$$P_2 = P_4 - \rho_{liq}gh_\infty \tag{2.10}$$

and similarly pressure at point 1 is:

$$P_1 = P_3 - \rho_{air}gh_\infty \tag{2.11}$$

Therefore subtracting the above two equations and knowing that P_3 and P_4 are the same results in :

$$P_c = \rho_{liq}gh_\infty - \rho_{air}gh_\infty = (\rho_{liq} - \rho_{air})gh_\infty \tag{2.12}$$

Knowing that density of air is negligible and using expression for h_∞ in the above equation leads to the well known Young-Laplace equation.

$$P_c = \frac{2\gamma_{lv}\cos\theta}{R_c} \tag{2.13}$$

Where R_c is the capillary radius. The importance of determining the capillary pressure pertaining to the different macroscopic flow models will be discussed next.

2.8 Single Phase Flow Models

Different approaches can be used to analyze and to model the imbibition in porous media. The models that have been used over the past many years for mathematical description of the flow can be broadly categorized into [22]

1. Capillary based models
2. Porous continuum models
3. Discrete models (for e.g pore network modelling) and
4. Statistical models

This thesis will discuss the first two models in some detail. It is greatly desired by the imbibition community to find a mathematical theory that is amenable and which can relate the flow quantities with time, the characteristic of the fluids and the porous medium. First the capillary model called the Lucas-Washburn model will be discussed and some of its basic assumptions will be stated before detailing the mathematical theory behind it. Some reasons why the capillary model fails in some cases will be discussed. In porous continuum models the flow as described by Darcys law will be discussed, which relates the averaged flow quantities to the macroscopic properties of porous media and the fluid. Using volume averaged properties allows one to upscale from microscopic pore level physics

to macroscopic flow description which is easier to implement and much useful for practical applications. Darcy based models can be extended to single phase and multiphase flow, however only the former will be discussed here and applied to the experimental data in this thesis. Necessary conditions for assuming single phase flow will also be discussed in the forthcoming section.

2.8.1 Lucas-Washburn Model

The simplest geometrical representation of a porous medium that has been used traditionally to model imbibition is the "Bundle of capillary tubes" model. This model assumes that flow occurring in a complex porous medium could be approximated by flow in an appropriated size of capillary tube (see figure 2.5). The tubes are considered to be of same constant size through its length and therefore the mathematical theory will consider the fluid flow in a single capillary tube.

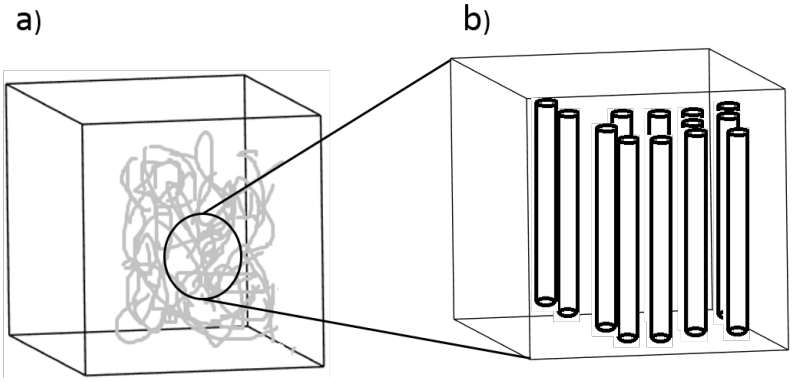

Figure 2.5: a) Fibers in disordered porous media and b) Bundle of capillary tube model

Describing the mechanics of an advancing menisci inside a capillary dates back to early 20th century when Lucas and Washburn independently developed the mathematical theory of liquid rise in a capillary [43]. The model is based on momentum balance on the moving

meniscus and by balancing the capillary force with the viscous force leads to an analytical solution relating the meniscus height with time. This model is extensively applied in predicting flow dynamics in porous medium and getting some macroscopic pore size information like capillary pressure and effective capillary diameter; these are useful performance parameters for practical applications as in sorbents. The complex microstructure is replaced by an imaginary bundle of aligned capillary tubes of constant diameter and in which the flow occurs in only one dimension.

A complete balance of forces on the moving meniscus as in Equation 2.7 involves the capillary suction force being balanced by the inertial, viscous and gravity effects. The equation can be solved analytically for two simple cases. In the first case capillary forces is balanced by only the viscous forces which results in the classical Lucas-Washburn equation. The second case takes both gravity and viscous effect which leads to a non-linear ordinary differential equation that can be solved analytically. Before discussing them individually let's first review the simplistic assumptions of this model [22, 44]:

1. Flow is one dimensional and therefore could not be used to model two or 3 dimensional flows.

2. The real complex microstructure is replaced with a hypothetical bundle of straight capillaries and the flow is considered representative of the porous medium flow.

3. Unlike real porous medium with a distribution of pore/void sizes this model assumes capillaries of a constant diameter.

4. There is no inter-connection between capillaries unlike real porous medium in which pores are connected.

5. There is not tortuosity factor.

6. Above assumption are needed to fit model parameters that could represent pore size information for example the effective capillary diameter.

From above assumption it becomes clear that this model is not a true representation of a real porous medium however it is still extensively used to model imbibition process. The reason for its continued popularity are its mathematical simplicity, easily measured parameters, vast literature and most importantly in many cases the experimental data does follow the Lucas-Washburn law. Many studies have been devoted to include additional terms to the basic version proposed by Lucas-Washburn which includes adding acceleration terms and accounting entrance effects [14]. Some researchers proposed that for porous media that swells when in contact with liquid the effective capillary radius change (decrease) with time linearly.

2.8.1.1 Mathematical Theory

Consider the schematic shown in Figure 2.4. The fluid motion inside a pore space of a real porous medium is emulated here to be taking place inside a single capillary tube. The integral analysis on the moving liquid column depicted as control volume (CV) is based on the average velocity of the meniscus. It follows that the mass balance of the deforming or growing control volume can be writte[22]:

$$\left(\frac{\mathrm{d}m}{\mathrm{d}t}\right)_{CV} = 0 = \frac{\mathrm{d}}{\mathrm{d}t}\int_V \rho \,\mathrm{d}V + \int_A \rho \,\overrightarrow{v_r} \cdot \overrightarrow{\mathrm{d}A} \tag{2.14}$$

where $\overrightarrow{v_r}$ is the menisci velocity , V is the volume , $\overrightarrow{\mathrm{d}A}$ is the cross sectional area, ρ the density and m is the mass. Since the liquid moves, the height of the control volume is to increase however it will always remain inside the CV and therefore relative velocity at the outlet is zero:

$$\frac{\mathrm{d}}{\mathrm{d}t}\int_0^h \rho\pi\,\mathrm{R}^2\mathrm{dz} - \rho\, w(\pi\mathrm{R}^2) = 0 \tag{2.15}$$

where w is the the z-direction velocity and according to the equation it is equivalent to the rate of the meniscus height h, so that w = $\dot{h}$

Taking momentum balance on the control volume in its integral form for the z-direction [45]

$$\sum F_z = \frac{\mathrm{d}}{\mathrm{d}t}\int_V \rho\, w\mathrm{d}V + \int_A \rho\, w\overrightarrow{v_r}\cdot\overrightarrow{\mathrm{d}A} \tag{2.16}$$

Using Leibnitz rule and w = $\dot{h}$, the first integral term could be simplified as:

$$\frac{\mathrm{d}}{\mathrm{d}t}\int_V \rho\, w\mathrm{d}V = \rho\pi\mathrm{R}^2\dot{h} + \rho\pi\mathrm{R}^2\dot{h}^2 \tag{2.17}$$

For solving the second integral term on equation 2.16 one takes into account that the system confined by the CV has only one inlet at z=0 and there is no outlet at z=h:

$$\int_A \rho\, w\overrightarrow{v_r}\cdot\overrightarrow{\mathrm{d}A} = -\rho\pi\dot{h}^2\mathrm{R}^2 \tag{2.18}$$

Now considering the right hand side of equation 2.16, the following forces are identified: gravity force, viscous force and the pressure force which can be split into two: upper pressure force at the menisci z=h and lower pressure force at the entrance at z=0:

$$\sum F_z = F_{menisci} + F_{entrance} + F_{gravity} + F_{viscous} \tag{2.19}$$

The upper pressure force acting on the control volume or meniscus is the capillary suction which is simply the capillary force multiplied by the cross section area dA. Atmospheric pressure also acts on the meniscus so F_{up} becomes :

$$F_{menisci} = -\int_A (p_{atm} - p_c)\mathrm{dA} = -\pi \mathrm{R}^2 (p_{atm} - p_c) \tag{2.20}$$

Pressure force acting at the entrance at z=0 [45] is expressed as :

$$F_{entrance} = \int_A p_0 \mathrm{dA} = \pi \mathrm{R}^2 (p_a - \rho \dot{h^2}) \tag{2.21}$$

$$F_{gravity} = \int_V \rho g \mathrm{dV} = -\rho g \pi \mathrm{R}^2 h \tag{2.22}$$

$$F_{viscous} = \triangle p \cdot \mathrm{A} = -\frac{8\eta}{R^2} h\dot{h}(\pi \mathrm{R}^2) = -8\pi\eta h\dot{h} \tag{2.23}$$

Now substituting all the forces in equation 2.16 and solving for p_c yields :

$$p_c = \frac{8\eta h\dot{h}}{\mathrm{R}^2} + \rho g h + \rho \frac{\mathrm{d}(h\dot{h})}{\mathrm{d}t} \tag{2.24}$$

This is the basic governing equation predicting the meniscus height with time. As apparent the capillary suction pressure on the left hand side of equation 2.24 is balanced by the 3 pressure terms on the right hand side: viscous, gravity and inertial respectively. The capillary pressure as derived earlier is expressed as the Young Laplace equation.

As mentioned before the basic Lucas-Washburn equation neglects gravity and inertial therefore the governing equation is reduced to :

$$p_c = \frac{2\gamma \cos\theta}{R} = \frac{8\eta h\dot{h}}{\mathrm{R}^2} \tag{2.25}$$

This equation when solved for h with boundary condition h=0 at t=0 yield the famous Lucas-Washburn equation:

$$h = \sqrt{\frac{\gamma R \cos\theta}{2\eta} \cdot t} \tag{2.26}$$

When only the inertial term is neglected from equation 2.24 meniscus heigh has the following implicit relation with time:

$$p_c ln \left| \frac{p_c}{p_c - \rho g h} \right| - \rho g h = \frac{\rho^2 g^2 R^2}{8\eta} \cdot t \tag{2.27}$$

As seen above both capillarity model equations 2.26 and 2.27 use height of the moving front as the dynamic quantity changing over time. However the height is not a convenient quantity to be measure in imbibition experiments. A more convenient quantity to be measured is mass against time. This can be obtained using a load cell, and then converting the mass data to height. This conversion assumes that the bulk density of the porous medium is constant through the length of the sample and that there is no entrapped defender (air for the case considered here) behind the wet front. Conversion of mass into height is determined by the following relationship:

$$h(t) = \frac{mass\, of\, oil(t)}{A_{cs}\, \phi \rho_{oil}} \tag{2.28}$$

where h is the instantaneous height at the corresponding measured mass of the porous media sample, A is the cross-section area of the sample and ϕ is the porosity of the sample. The variants of the Lucas-Washburn equation and their accuracy in predicting experimental data of mass against time data for different oils will be discussed in the modeling section of this thesis.

2.8.2 Porous Continuum Model - Darcy Based Model

The physics of flow inside a porous medium is a complex phenomena which is difficult to describe mathematically because of the complicated pore structure and geometry. Solving for flows over an infinitesimal volume at the pore scale level requires expensive computational resources. This approach of modelling flows, called the continuum approach may

be of interest at the fundamental level but for practical applications involving macro sized porous samples it is too expensive to be adopted. Hence the 'up scaling technique of moving to porous continuum approach requires one to use properties that are averaged over an infinitesimal volume of the material/fluid termed as "representative elementary volume" (or REV). This REV is much larger than individual pores/void but much smaller than the size of the porous media sample (see Figure 2.6). There are different theories incorporating averaging approaches but the most commonly used is the volume average approach . Using these theorems one can form a macroscopic description of flow using momentum balance and continuity equations.

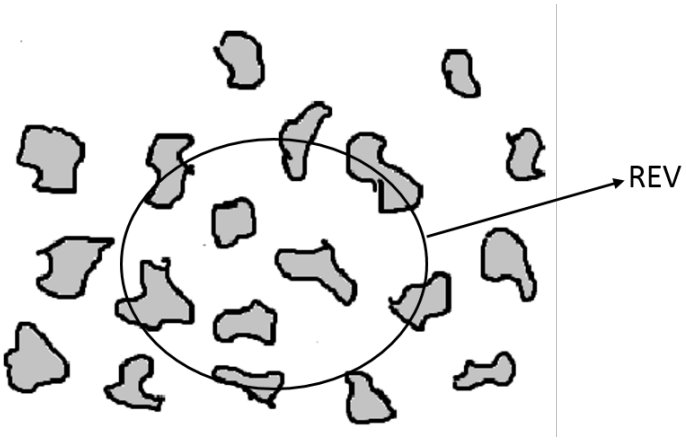

Figure 2.6: A representation of the REV

For single phase flows these balances could be written for a rigid non swelling porous medium using volume averaged velocity and pressure which are point wise integrated quantities over a representative elementary volume :

$$\nabla \cdot \langle \overrightarrow{v} \rangle = 0 \tag{2.29}$$

$$\langle \overrightarrow{v} \rangle = -\frac{K}{\eta}(\nabla P) \tag{2.30}$$

where $\langle \overrightarrow{v} \rangle$ and ∇P are the volume averaged velocity and pore averaged pressure of the fluid respectively. These are most commonly employed flow averaged properties in expressing macroscopic transport equations for porous medium. K is the absolute permeability, η is the viscosity , ρ is the density of the fluid and g is the acceleration due to gravity.

The single phase assumes a clear demarcation between the wet and the dry region of the porous medium. This implies that there is 100% saturation behind the liquid from and 0% saturation in front of the liquid front. The large viscosity contrast between the invading and defending fluid allows one to use this assumption as demonstrated by Lenormand et al. [31]. The mathematical description of this sharp front flow modelling will be discussed now.

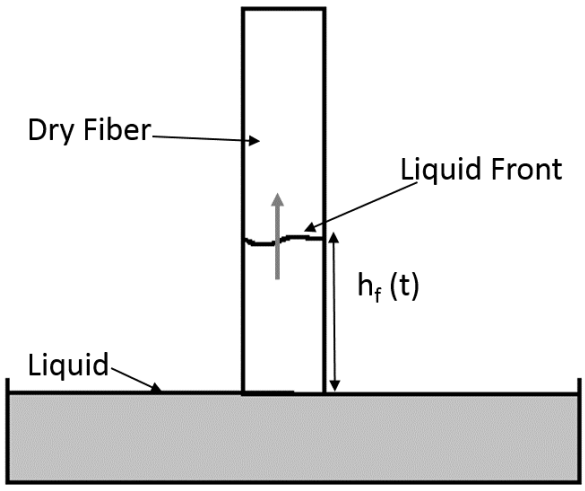

Figure 2.7: Schematic of sharp liquid front

2.8.2.1 Mathematical Theory

Similar to Lucas-Washburn model, here also the objective is to describe model for imbibition of of oil into porous medium to get a relationship between moving front height with time. Momentum balance and continuity equation are applied on the liquid front using volume averaged properties as seen in equations 2.29 and 2.30. This flow description by combining Darcy and continuity equation in porous medium is widely used in predicting flows on a macroscale. Figure 2.7 shows the schematic of the single phase one dimensional flow with a sharp liquid front. The pressure boundary condition is applied on the wetted front and the front height is modeled against time.

Pressure P in equation 2.30 is defined such that it includes the hydrostatic pressure as the liquid front moves along with the hydrodynamic pressure p (pore averaged):

$$P = p + \rho g h \tag{2.31}$$

For one dimensional flow the Darcy and continuity equations becomes:

$$\upsilon = -\frac{K}{\eta}\frac{dP}{dh} \tag{2.32}$$

$$\frac{\mathrm{d}\upsilon}{\mathrm{d}h} = 0 \tag{2.33}$$

Combining the equation above gives the pressure distribution in the wetted region of the porous medium:

$$\frac{\mathrm{d}^2 P}{\mathrm{d}h^2} = 0 \tag{2.34}$$

Integrating the above equation and using boundary conditions for P as:

$$P = p_{atm} \text{ at h} = 0 \tag{2.35}$$

and

$$P = (p_{atm} - P_s) + \rho g h \text{ at h}=h_f \tag{2.36}$$

the following expression of pressure P changes with the moving front height is obtained:

$$P(h) = p_{atm} + \rho g h - p_s \frac{h}{h_f} \tag{2.37}$$

The values of h_f varies as a function of time. Therefore the above equation can be updated by bringing Darcy velocity equation 2.32 and relating it to the front speed and equation 2.37 we get:

$$\frac{\mathrm{d}h_f}{\mathrm{d}t} = \frac{K}{\phi\eta}\left(\frac{p_s}{h_f} - \rho g\right) \tag{2.38}$$

After variable separation and integrating the above equation with the initial h_f= 0 at time t=0 it is possible to get the final form of the governing equation that relates the moving front height with time:

$$p_s\, ln\left|\frac{p_s}{p_s - \rho g h_f}\right| - \rho g h_f = \frac{\rho^2 g^2 K}{\phi\eta} \cdot t \tag{2.39}$$

Here p_s refers to the suction pressure responsible for driving the fluid vertically up in the porous medium sample. By converting the mass imbibed vs time data into height with time data using relation 2.28 one can predict the experimental data using the above equation.

There are different ways in estimating the p_s. It is possible to assume a sharp boundary between the wet and dry region so that frontal saturation is always 100%. By setting p_s

and K as fitting parameters these values for different bulk density of the porous medium can be determined. One expects to find similar K values for same porous medium with different oils. Moreover p_s values must correlate to changes in the contact angle of the fluids. Buckley-Leverret theory might be helpful in interpreting any deviations in the expected trends of these fitted parameters .

2.8.3 Pore Network Model

In the previous models discussed it was assumed that the imbibition front was perfectly flat so that it can be modeled as single phase flow. This assumption eases the macroscopic description of flow but it does not give a true representation of the porous medium . For example it will be seen that the Darcy based capillary models will yield satisfactory fits for the experimental data but the fitting parameters do not give consistent and reliable pore size information. It is in such cases that it is desired to study the flow as two phase phenomena at the pore level and determine its effects at the macroscopic level. Since a real porous medium consists of complex topology of interconnected pores of various sizes it is required to create a virtual representation of a real porous medium so that flow could be modeled at the pore level using the relevant physics. Advanced imaging techniques like computerized tomography are recently being used to reconstruct the porous space into 3-D images that represent the interior of the porous structure.

Chapter 3

Materials and Methods

3.1 Overview

This chapter comprises the experimental methodology with regards to the theory discussed in the previous sections. The materials, sample preparation and the laboratory set up will be discussed here in detail along with recapitulation of some fundamental principles. The scope of the experiments is to characterize a specific kind of short polymer fiber material derived from recycled streams as a suitable material for oil absorption applications, particularly oil spill clean up. The wettability studies are performed in two separate experiments.

The first research task is to find the intrinsic nature of the polymer fiber material, that is to find the preference of a solid material towards a liquid. To quantify this preference of wetting, the contact angle measurements were done with water and different hydrocarbon oils. Surface with different levels of roughness were used and the effect of surface heterogeneities was observed.

The second research task deals with absorption experiments of the polymer fibers. The sorption behavior referred to as spontaneous imbibition was performed and studied in

context of the important parameters that governs it. Since wetting is an initial requirement for spontaneous imbibition therefore contact angles measured in the first set of experiments was useful in interpreting the sorption behavior.

3.2 Materials

Pure deionized water and 4 different hydrocarbon oils were used for both set of experiment. Since oil spill clean up materials is the targeted application the ASTM standard (ASTM F726) for evaluating performance for oil spill sorbents is used as a reference to choose a representative range of hydrocarbon oils. The hydrocarbons used are listed in Table 3.1.

Table 3.1: Hydrocarbons used in experiments

Hydrocarbon type	**Commercial name**	**Supplier**
Kerosene	WOODS Clear Kerosene	Canadian Tire
Diesel		Canadian Tire
Light Lube Oil	Quaker State Motor Oil SAE 5W20	Canadian Tire
Heavy Lube Oil	Quaker State Motor Oil SAE 10W30	Canadian Tire
Crude oil		

The recycled polymer short fibers named Hydra was provided by Clear Blue Sorbents. The samples were a combination of several types of recycle short fiber obtained from tire and carpet recycling. Figure 3.1 shows the Hydra fiber.

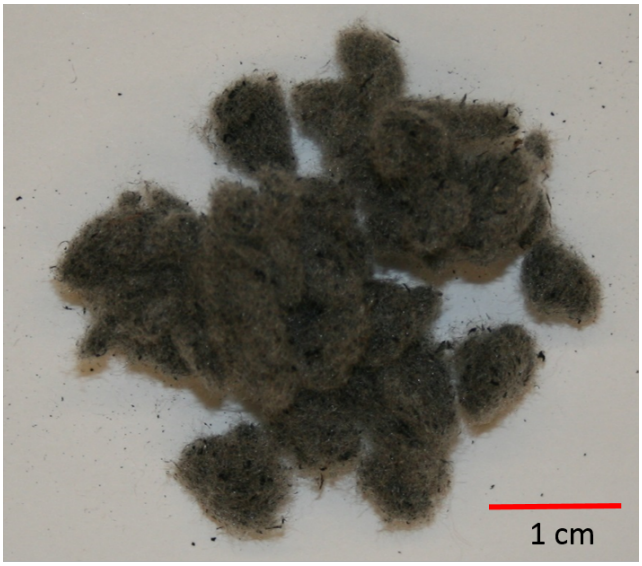

Figure 3.1: Hydra, recycled polymer short fiber

3.3 Materials Characterization

3.3.1 Physical Data of Hydrocarbon Oils

As evident from the equations that describes the motion of liquids inside a porous media accurate measurement of hydrocarbons properties is important for a good agreement between theory and the experiments. These properties are: viscosity, density and interfacial tension.

3.3.1.1 Viscosity

Viscosity of the oils was measured from the Brookfield digital viscometer model DV-E. The measurement accuracy of the instrument for viscosity is $\pm 1\%$. The hydrocarbons oil temperatures was 23^0 ± 2 and the measurements were done in a 600 mL low form Griffin

beaker. Choosing the right spindle is a trial and error process. The guidelines given in the instruction manual were followed to choose the spindle for the hydrocarbon oil. The LV (1-4) spindle range starts from 15 cp therefore to measure the viscosity of kerosene and diesel required using UL adapter which is a precisely machined tube and is used to measure viscosities as low as 0.85 cp. The rpm is selected such that the torque % is always in between 10% and 100%. If it is not in this range the rpm or spindle needs to changed.

The working principle of the instrument is that a spindle is immersed in the liquid upto a predetermined depth. The spindle is rotated at a range of rpms and the viscous drag exerted by the liquid is sensed by a transducer which converts it into a torque signal. The torque and the shear rate data is plotted and by the constitutive equation for Newtonian fluids the value for the viscosity is determined.

3.3.1.2 Density

Densities of oils were calculated by pouring 100 milliliters of oil into a graduated cylinder and weighing it before and after adding the oil. The density was then calculated by taking mass of oil/volume of oil.

3.3.1.3 Surface Tension

Interfacial tensions of water and oils against air as the second phase were measured from pendant drop tensiometer. This method is called axis-symmetric drop shape analysis (ADSA) and is a convenient and reliable method to determine interfacial tensions. An example of the drop file is shown in the figure below.

Figure 3.2: Pendant drop profile of water surrounded by air being fitted by the Young-Laplace equation

The instrument used was VCA 2500 XE, AST product (see Figure 3.4) with its built in software. A drop of 10 microliter is dispensed from the syringe and a typical shape of the drop is shown in Figure 3.2. The density value of the fluids which on our case will be hydrocarbon and air are input into the software. The hanging drop profile is a result of the gravity pulling down the drop and the surface tension pulling the liquid inwards. The software computes the interfacial tension of the pendant drop profile by fitting the Young-Laplace equation.

3.3.2 Properties of the Polymer Fiber Material

The polymer short fibers used in the experiments came from a recycled stream. The fibers had a fluffy behavior and separate easily during handling. Flat and rigid samples were prepared from these fluffy fibers for measuring contact angle. Two processing techniques were used: hot press and injection molding. For thermal processing the fibers it was

important to know the melting point. In this way it could be ensured that the temperatures used in the machines were appropriate for a required task.

3.3.2.1 Melting Point

Melting point of the fibers was found using TA differential scanning calorimeter. A sample weight of 5 mg fiber was used. To remove the thermal history the sample was heated first from 25^0C to 300^0C at 20^0C/min and held there for 5 minutes. It was then cooled to 5^0C at -10^0C/min. It was then heated again to 300^0C at 10^0C/min.

3.3.2.2 Surface Architecture, Size and Porosity of Fibers

Scanning electron microscope (JEOL 6610 SEM) was used to determine the morphology, surface porosity and size of the short polymer fibers. Samples prepared from the hot press and injection molded machine were cut and coated with gold before performing the SEM imaging.

3.3.2.3 Density of the Fiber Material

As mentioned in section 2.4.2 porosity of the fibrous porous media sample is calculated using the density method where bulk density and the fiber material density should be known. The porosity is then calculated by using the Equation 2.4.

The bulk density of the fiber was calculated by knowing the volume of the sample holder and the mass of fiber used to fill that volume. A range of low bulk density samples were prepared that will be discussed shortly in the next section.

The material density of the polymer fiber was found by the Pycnometric method. The sample was prepared by injection molding at high temperatures so that the fibers are completely melted and the injection pressure eliminates any surface and interior porosity/void

space. Pycnometric methods is a precise method of determining the volume of the polymer sample by displacement of an inert liquid like water.

3.4 Wettability Characterization

3.4.1 Sample Preparation

A lab scale hydraulic hot press (Carver, inc.) and injection mold machine (Ray Ran RR/TSMP) show in in Figure 3.3 were used to mold polymer samples with a flat and smooth surface required to measure the contact angles. Before processing the fibers were dried overnight in a vacuum oven to remove any inherent moisture trapped within the polymer fiber. This would ensure that at high temperature the polymer would not get hydrolysed which could degrade its chemical composition. The barrel temperature of the machine was kept at 290^0C and the polymer fiber was held inside the barrel for 20 minutes to melt all the fibers. A pressure of around 100 psi was then applied and the polymer melt flowed smoothly into the mold cavity which was set at 65^0C so that the melt solidifies forming a compact, rigid polymer sample. For the injection molded sample the objective was to eliminate all porosity and make as much a smooth sample as possible.

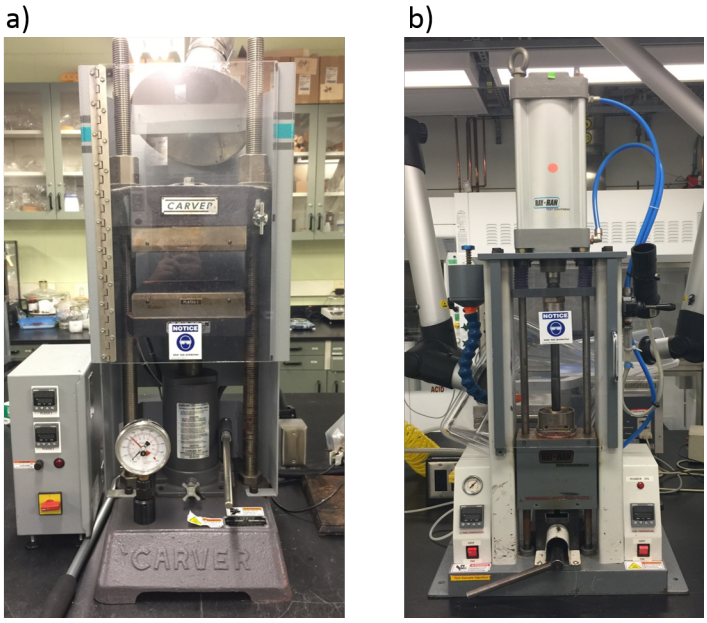

Figure 3.3: a) Hot press and b) Injection molding

A mat of fibers was prepared by compression molding. Fibers were patted into small cakes using molds and then sandwiched between two Teflon sheets before placing them within the platens of the hot press. Samples were pressed at 240°C and force of 2 ton was used. A lower temperature was chosen so that fiber do no melt and the surface produced will still be rough and has some surface porosity.

3.4.2 Contact Angle Measurements

Test liquids for contact angles were deionized water, kerosene, lube oil and crude oil. The instrument used was a contact angle and pendant drop analyser (VCA 2500 XE, AST products) with a high speed precision camera. The same instrument was also used for determining the interfacial tensions of water and oils. The contact angles of liquids against air were measured on both the samples.

The contact angle instrument shown in Figure 3.4 is an ideal tool to study the wetting behaviour of solids and determine interfacial tensions of liquids. A motorized syringe is used to gently dispense a liquid drop of a known volume on the surface of the sample.

Depending on surface porosity liquid might start penetrating into the pores even before the drop has been completely detached from the tip of the syringe needle. If the spreading is time sensitive dynamic contact angles could be measured by setting the instrument software to take snaps at the desired frame rate. If the angles are pinned or equilibrates fast (usually with the non wetting liquid) static angles could be used.

The temperature for the experiment was same as the room temperature ($23^0 \pm 2$) and 3 readings of contact angles were taken for each sample. A 500 µl syringe fitted with a stainless steel needle (N720, 20GA, PT3, 4", chromatographic specialties inc) was used to dispense 10 µl liquid onto the polymer sample. The built-in goniometer software gives option to set 5 points on the edges of the solid/liquid/air interface to fit the drop profile. Based on that it draws a tangent line and gives the contact angle.

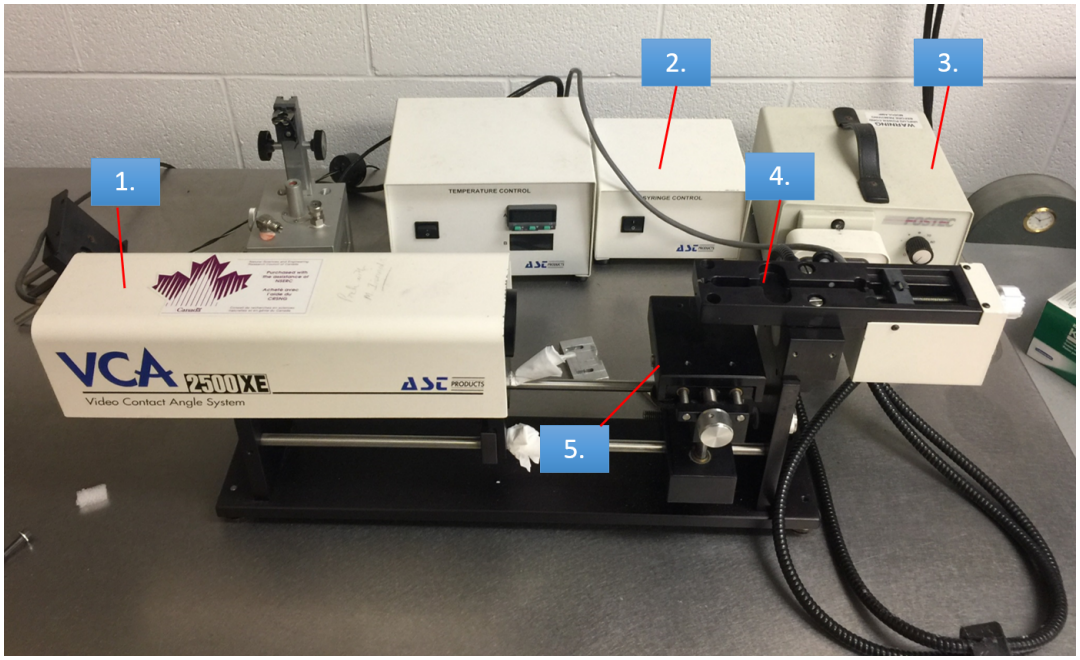

Figure 3.4: Contact angle measuring instrument: 1. High speed camera, 2. Syringe control, 3. Light source, 4. Syringe holder and 5. Sample holder

3.5 Characterization of the Sorption Behavior

3.5.1 Sample Preparation

A special sample holder was developed to study the sorption behavior. The sample holder were prepared using 30 mL graduated plastic syringes with a moving plunger (see Figure 3.5). The tip end was cut open and soldered to a steel wire mesh which had small perforations to allow liquid to penetrate (the invader). The plunger end was drilled with small holes so that the system is not air tight and air (the defender fluid) was allowed to escape during the imbibition process. The top end of the plunger was fitted with a steel hook so that it could be connected to a load cell. A certain mass of the fiber was weighed before

placing it inside the syringe. The plunger was pushed to compress the fiber into a desired volume.

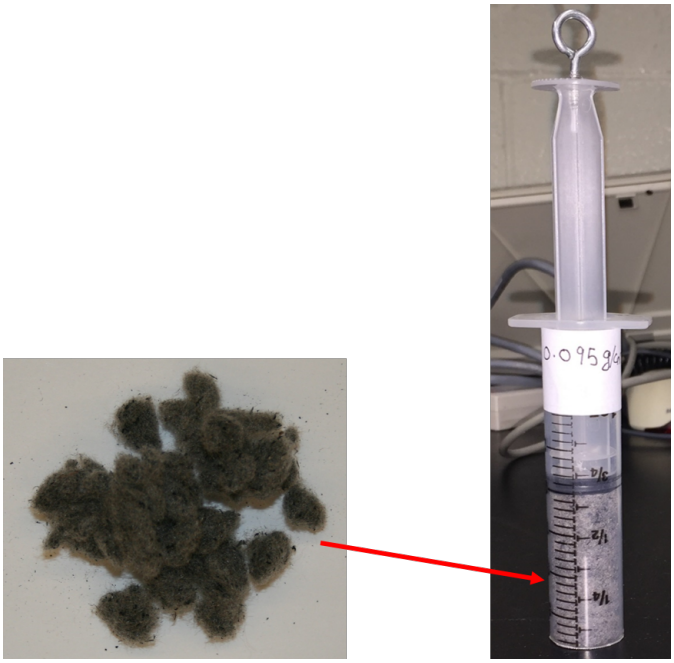

Figure 3.5: Left: Short fibers; Right: Sample holder for porous media

The bulk density of the porous media was controlled by changing the mass of fiber or the volume of the syringe filled with fibers. The range of bulk densities was chosen to represent the bulk density observed in sorbent booms prepared by Clear Blue Sorbents and other reports in the literature. The purpose of choosing different bulk densities was to study the effect of porosity on the rate and on the total mass of the liquid sorbed. The bulk densities were *a*) 0.085 cm^3 *b*) 0.095 cm^3 *c*) 0.11 cm^3 *d*) 0.13 cm^3 and *e*) 0.16 cm^3. The void space and porosity were controlled by varying the bulk density. The porosity was calculated using the Equation 2.4

3.5.2 Imbibition Experiment

The ability of a liquid to penetrate a porous medium due to capillary forces was evaluated by the experimental setup shown schematically in Fig 3.6 .

The sample holder containing the fibers (see Fig 3.5) was attached to the miniature load cell model LSB200 made by Futek, which was wired to a data logger model IPM650 also made by Futek. This load cell has total capacity of 2.5 N and resolution of 0.001 N. The load cell was calibrated by following the Futek IPM 650 product manual.

The hydrocarbon oil was placed in a laboratory dish and located under the sample holder on a moving stage. Figure 3.6 shows a picture of the experimental setup. The moving stage was used to raise the laboratory dish containing the hydrocarbon toward the sample holder until the surface of the hydrocarbon and the steel mesh at the bottom of sample holder entered in contact. The data logger recorded mass data as a function of time sending the data to a computer. The load cell is set to read zero when attached to the sample holder.

As soon as the sample holder made contact with oil it penetrated through the perforations and the mass of the sample holder began to increase because of the slowly imbibing oil. The software could be set to acquire a mass reading automatically after a pre-set time interval. The real time graph helped to indicate as to when the imbibition reaching a maximum thus completing the experiment. Depending on the viscosities of the liquids the time to complete the experiment varied from a few seconds to a full day.

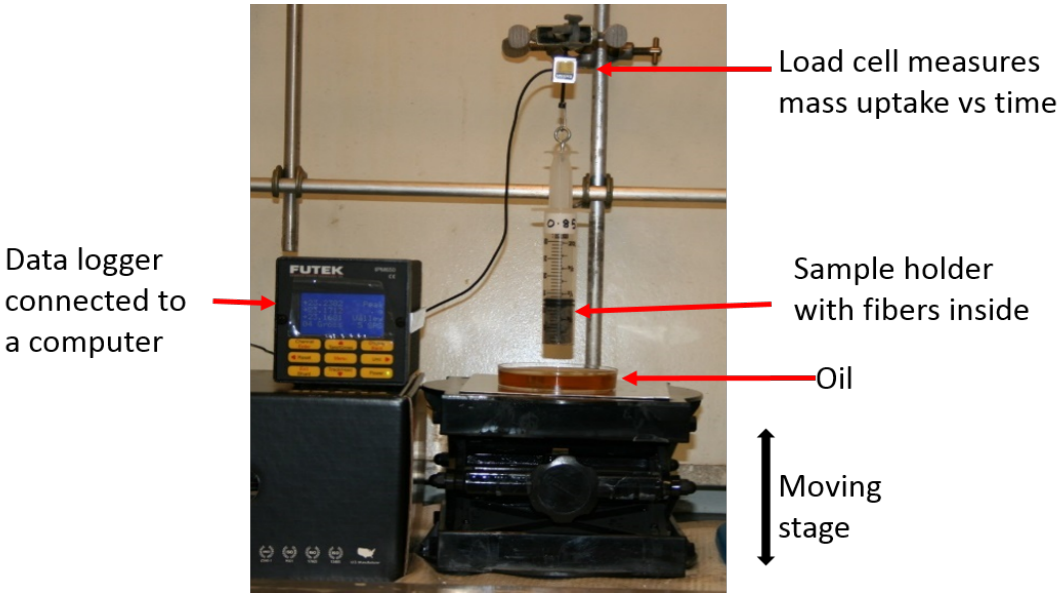

Figure 3.6: Experimental set-up for spontaneous imbibition

Some observations were made that were critical in calculating the correct amount of oil sorbed by the sample. As the moving stage is slowly moved downwards from the sample after plateau has been reached, due to surface tension holding the oil there is a sharp jump on the weight recorded and as the oil detaches the weight falls back below the plateau and this value corresponds to the actual mass absorbed and retained inside the porous sample.

This behavior was seen for each experiment and therefore the sorption curves were adjusted accordingly after subtracting this additional oil due to surface tension effects. Another mass that was subtracted from this final weight was that of the oil retained by a blank sample holder without any fiber material inside. This was due to the oil retained in the steel mesh/wires at the bottom of the sample holder. This was found out by doing a blank test with each of the 5 oils and making the correction for the sorbed mass. Finally the sorbed mass data with time was compiled for all the samples.

In total 5 different bulk densities were tested as listed in table 4.3 and different oils,

thus totaling 25 combinations. Each one of these combination were measured 3 times. The data from 3 measurements were used to calculate an average mass. All subsequent calculations were made using this averaged mass based on 3 experiments. A brief outline for these calculations will be discussed separately.

3.6 Water-Air Capillary Pressure

The non-wetting behavior of water towards the polymer fiber material was further verified by measuring the water-air capillary pressure. The methodology and the instrument used for this experiment have been developed by Gostick et al [46].

The fiber is packed into a specially designed chamber of a known volume. The cylinderical chamber has access to water on its bottom face while the top face is connected to a gas tube. Air can be withdrawn or exerted on top of the sample by a syringe connected to this gas tube.

Since water is a non-wetting liquid and its capillary pressure remains constant for the polymer fiber, external vacuum and positive pressure is required to force water into and out of the porous fiber. In this method capillary pressure is increased in step-wise fashion and the liquid uptake is measured at each step. This yields a saturation versus capillary pressure curve. Further details on the experiment procedure and its working principle are described elsewhere [47].

3.7 Pore Size Information

Computerized micro-tomography was used with a voxel resolution of 5 micrometers. The sample width and diameter was 5 millimeters each. A fiber sample of 0.015 grams was used. Figure 3.7 shows the fiber sample and the sample holder. The interior of the porous

structure was mapped onto high resolution 2-D sections which was them processed through advanced imaging algorithm to a form a 3-D visualization of the fibrous pore structure with varying pore and throat sizes.

The image processing algorithm is based on a technique called watershed segmentation and its source code is written on Python. The working principle and details of extracting pore size and distribution using 2-D tomographic images is dicussed by Gostick [48].

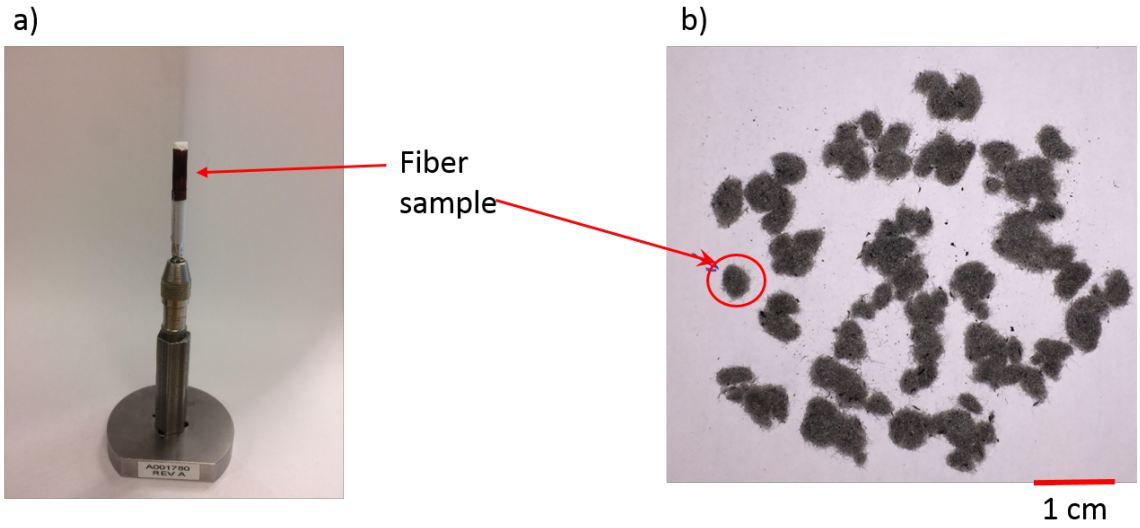

Figure 3.7: a) Kapton tube CT scan sample holder and b) Fiber sample

3.8 Calculations for Oil Sorption

Sorption capacity of the porous sample or mass absorbency as it is referred to as in literature is reported as mass of liquid imbibed divided by the mass of fiber used. However in literature most of these studies involve immersing the whole fibrous sample inside the oil and therefore they use the entire mass of their porous sample. Here in this work since the oil just touches the fiber sample, the mass of only the wetted fiber is used to calculate

the mass absorbency. Therefore absorbency is reported here as as grams of oil sorbed per gram of fiber that has been wetted. Since in all the experiments there was still sufficient amount of dry fiber it cannot be counted as used fiber. The calculation expressions are:

$$\text{Mass Absorbency } \% = \frac{\text{grams of oil}}{\text{grams of wetted fiber}} \tag{3.1}$$

where wetted fiber is the amount of fiber fully saturated with oil. It is calculated by multiplying the wetting phase saturation as calculated from equation 3.3 with the total mass of the sample

It will become apparent that the above definition hinders the comparison between sorption of different oils. It will be seen that this definition makes sense when the performance of a sorbent with different bulk densities and the same oil is compared. However when comparison is made between same bulk densities and different oils this definition doesn't seems to predict the expected behaviour . The reason is that it doesn't account for the density difference between oils. Therefore this problem is overcome simply by using the volume of oil that has been sorbed instead of the mass. Based on that volumetric absorbency is defined as the ratio of volume of the sorbed oil divided by the volume of the solid fiber material used:

$$\text{Volumetric Absorbency } \% = \frac{\text{Volume of sorbed oil}}{\text{Volume of solid fiber material}} = \frac{\text{mass of oil}/\rho_{oil}}{\text{mass of fiber}/\rho_{fiber}} \tag{3.2}$$

Wetting phase saturation or volumetric efficiency of the sorbent sample can be calculated by converting the sorbed mass into sorbed volume and dividing it with the total pore volume of the sample.

$$\text{Wetting phase Saturation} = \frac{\text{mass of oil}}{\rho_{oil}\phi V_{bulk}} \tag{3.3}$$

Since all capillarity model predict height against time therefore the mass data was converted to height by a simple mass balance considering a cylindrical geometry of the porous sample

$$\text{Height } h_{front} = \frac{\text{mass of oil}}{A_{c.s}\phi\rho_{oil}} \tag{3.4}$$

This assumes that the bulk density is constant throughout the length of the sample.

Chapter 4

Results and Discussion

4.1 Wetting Characteristics of Recycled Polymer Fiber

Recycled short fiber were used for preparation of porous media. The objective is to investigate relevant properties of such porous media with regards to applications in removal of hydrocarbon oils from water.

Contact angles were measured in order to investigate the wetting characteristics and the intrinsic preference of recycled polymer fibers toward water or different hydrocarbon oils. As discussed earlier, contact angle measurement is the most intuitive and easily measurable parameter to characterize wettability of a solid surface. Much controversy surrounds interpretation of contact angles. For practical purposes it has been reported that for a liquid to imbibe spontaneously its intrinsic contact angle on a rigid surface must be less than 40^0 [30]. Although there is no consensus as to how smooth a surface should be for the angle to be called intrinsic the idea is to create as much of a rigid and smooth sample as possible (ideal surface).

4.1.1 Evaluating the Surface and Structural Characteristics of the Polymer Fiber

Two methods were used for preparing samples with recycled polymer short fiber: one with the injection molding machine and the other with the hot-press. The injection molded sample is assumed to be a close approximation to the Youngs ideal surface due to minimal surface porosity and rigidity. In this text it will be mentioned as a smooth sample or a smooth surface. The hot-press sample was compressed at a temperature below the melting point of the polymer fiber to avoid melting the fibers. This sample has sufficiently large surface porosity and is considered as a non-ideal. It contains porosity and roughness. It can be easily bent, it is much less rigid than the other sample.

The melting point of the fiber as determined by the DSC, the thermogram is shown in Figure 4.1. It is seen that the melting point of the polymer fiber is around 260^0 C. The sample prepared using the hot-press used the temperature of 240°C (below the melting point); whereas the samples prepared by molding use the temperature of 280°C (above the melting point). As expected, pressing at 240°C did not allow the fibers to melt, but they were compressed forming a mat with relatively good integrity. This mat can be handled without separation of the fibers.

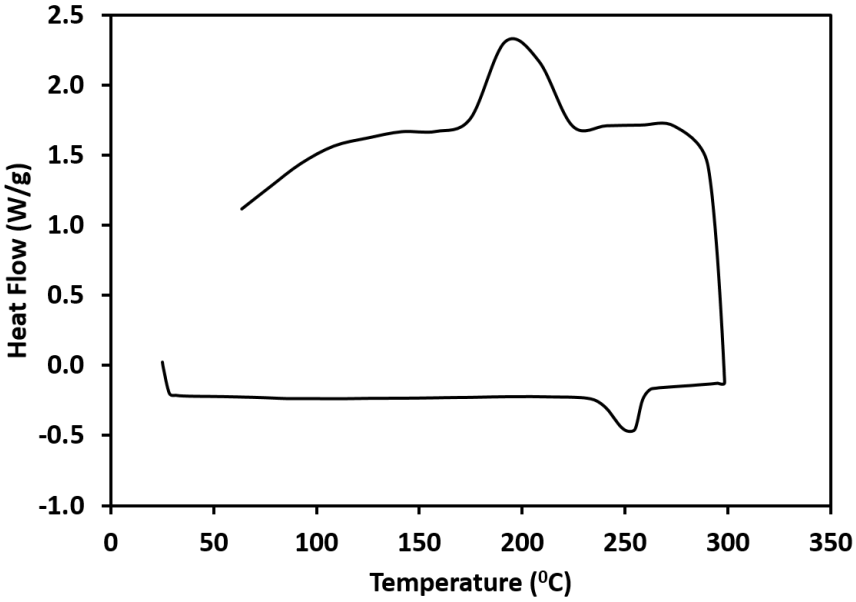

Figure 4.1: Differential scanning calorimetry of the polymer fiber (Hydra)

Figure 4.4 shows images of the sample. The surface morphology of both samples were investigated using scanning electron microscopy (SEM). The size of fibers was also investigated with SEM.

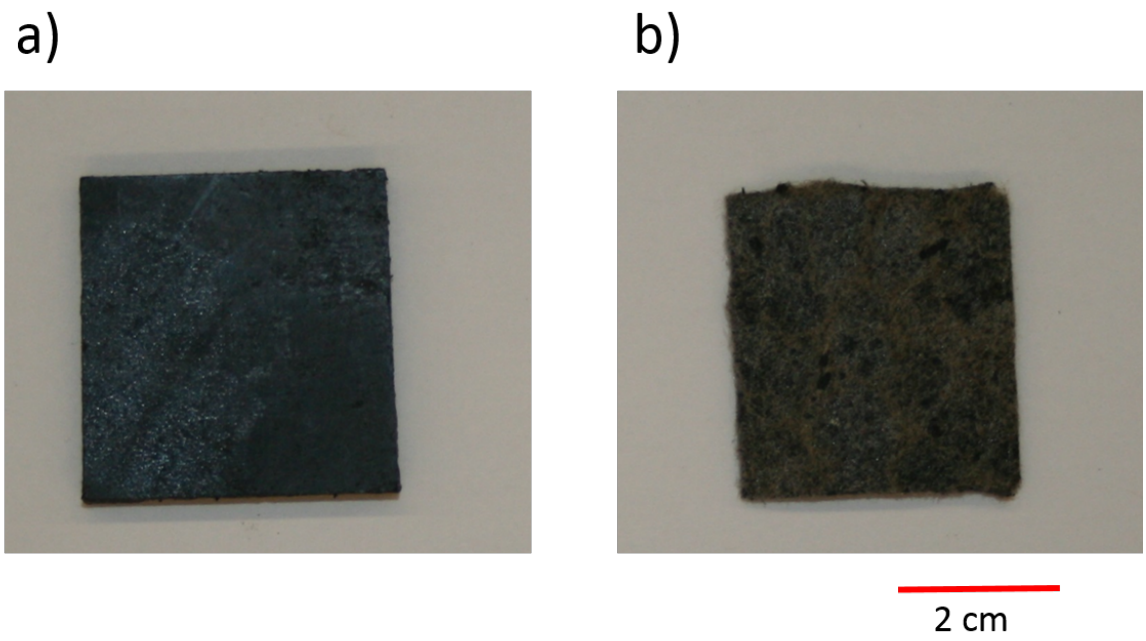

Figure 4.2: a) Injection molded sample and b) Hot press sample

Figure 4.3 shows the SEM image of the raw fibers. The diameter of the fiber can be seen to be around 20 micrometer. It has been reported in the literature that the capillary bridges can be formed by fibers thus creating capillary forces that pulls up the liquid into the open spaces (called as voids/pores) [24]. Other studies reported that some synthetic fibers have hollow lumen which can act as a sink and swell by absorbing liquids such as oils. According to the ASTM F716-09 definition if the fiber swells by 50% the process of liquid uptake is called absorption otherwise it is called adsorption [49]. This distinction is vague and requires separate studies to know the exact amount of swelling and therefore it is advisable to use the more generic term sorption for discussion on liquid uptake [49].

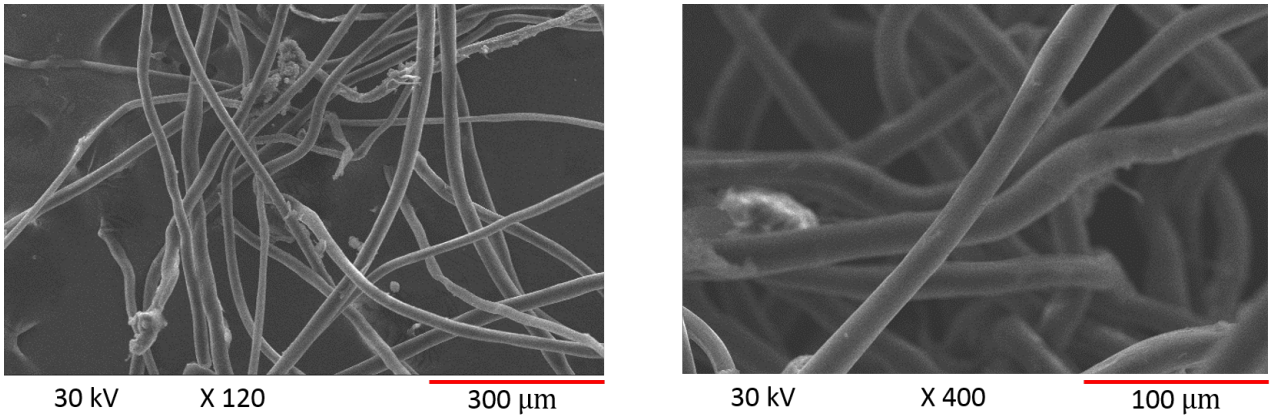

Figure 4.3: SEM micrographs of the polymer fiber

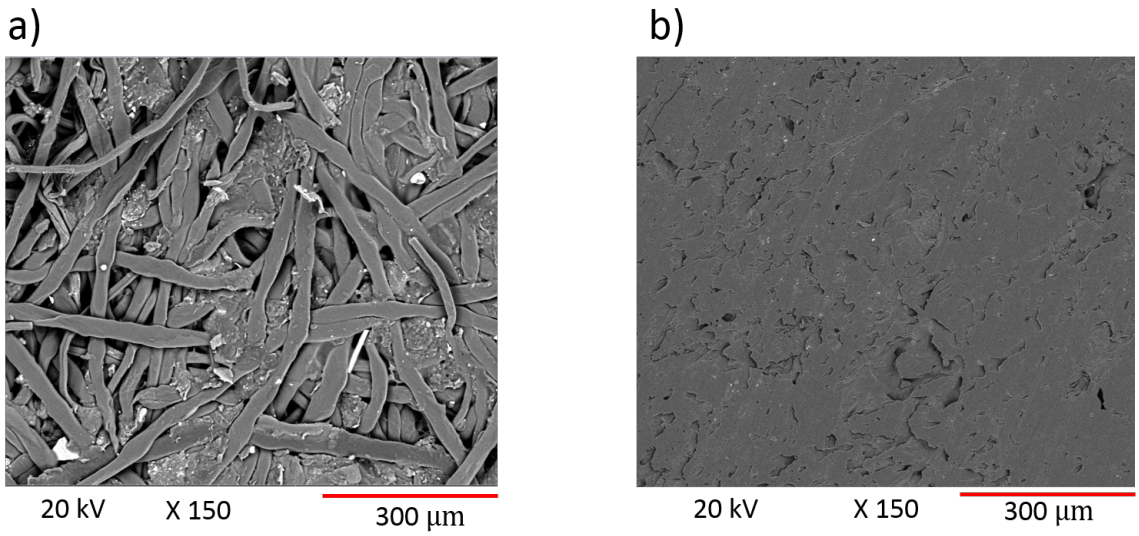

Figure 4.4: SEM micrograph of a) Sample prepared from hot press and b) Sample prepared from injection molding

Figure 4.4 part a) shows the SEM micrograph of the sample surface prepared using the hot-press at a temperature below the melting temperature of the fiber. It can be seen that the fibers were compressed together but maintained the shape of a fiber. The interstices between the fibers gives rise to surface porosity and can easily trap air. This induces dual scale roughness. When a liquid drop is dispensed on such a surface the contact area between the liquid drop and the solid fiber (surface) is greatly reduced. Simultaneously, the contact between the liquid and the trapped air on the surface is increased.

Part b) of Figure 4.4 shows the SEM of the fiber sample prepared using injection molding machine at a temperature above the melting point of the fiber. It can be seen that the fibers have completely melted and fused together to form a rigid sample which is smooth and have no or minimal surface porosity. A minimal amount of surface roughness is presented, but it is much smaller than the amount of roughness observed on the other sample.

4.1.2 Contact Angles

The injection molded sample will be referred to as the smooth surface and the hot-pressed sample as the rough surface.

4.1.2.1 Hydrophobic Behavior

Figure 4.5 shows the image of the drop after contacting the smooth surface and the rough surface. The contact angle was obtained by fitting the shape profile of the drop. The angles were measured thrice with a repeatability of $\pm 2^0$. The apparent water contact angle (WCA) measured here for water against air is 133^0 on the rough surface and 75^0 on the smooth surface. These results are consistent with the literature that the surface roughness with trapped air on surface pores increases the contact angle significantly. Therefore the

measured angles are not a representation of the true surface energetics of the fluid/solid pair as described by the Young-Dupre equation

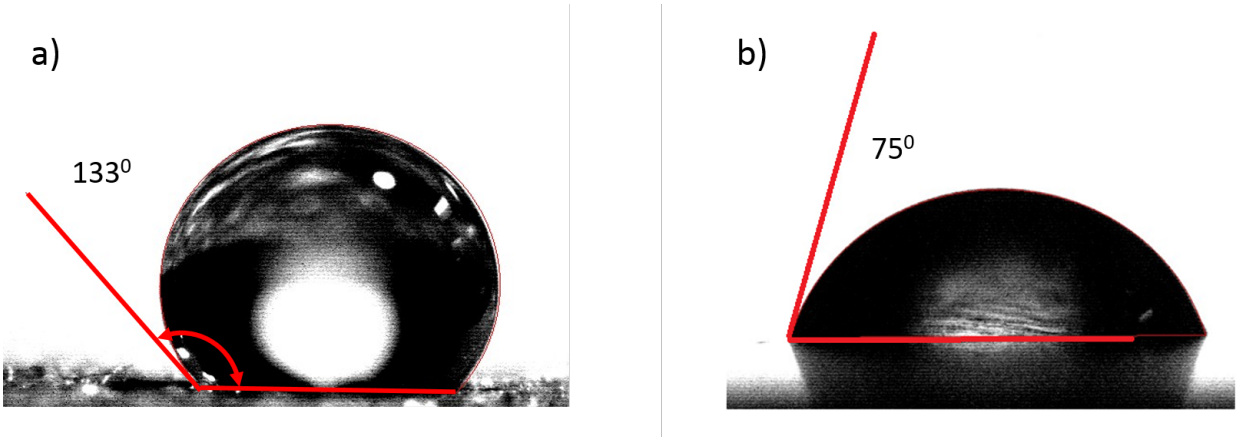

Figure 4.5: Water contact angles against air on a) Rough hot press sample and b) Smooth rigid injection molded sample

The angle on the smooth sample gives a more correct approximation to the intrinsic contact angle. According to Payatakes [30] for spontaneous imbibition into porous structures the intrinsic contact angle should be less than 40^0. This implies that water does not have a tendency to spread against air on the polymer fiber material. Therefore a porous medium made with these polymer fibers will not spontaneously imbibe water which is a useful result for applications like oil absorption from the water surface. These measurements confirm the hydrophobic behavior of the recycled polymer short-fiber.

This non-wetting behavior of water on the polymer fiber will be further confirmed by the water-air capillary pressure curve that have also been reported.

4.1.2.2 Oleophilic Behavior

The same set-up was used for measuring the contact angles with oils (OCA). The angles were measured against air for both the smooth and rough surfaces.

Figure 4.6 shows the image of the contact of kerosene (hydrocarbon oil). It can be seen that the drop spreads spontaneously on the surface as it is being dispensed from the tip of the needle. This observation was seen for kerosene on both the rough and the smooth surface. On the smooth sample it spreads spontaneously against air showing high affinity for the fiber materials and makes an apparent contact angle of 0^0 . Whereas on the rough sample it quickly penetrates into the surface pores due to capillary action. This is because of the high intrinsic oleophilicity of the fiber materials towards kerosene.

Figure 4.6: Kerosene oil being detached from the tip of the needle

Similarly the oil contact angles were measured for lube oil and crude oil on both surfaces. Figure 4.7 below shows the image used for measurement of contact angles of lube oil (Heavy lube oil) and crude oil on the rough surface. The images on the left show the moment of initial contact when the drop is still attached to the tip of the needle. The images on the right show that the droplet has been absorbed inside the surface.

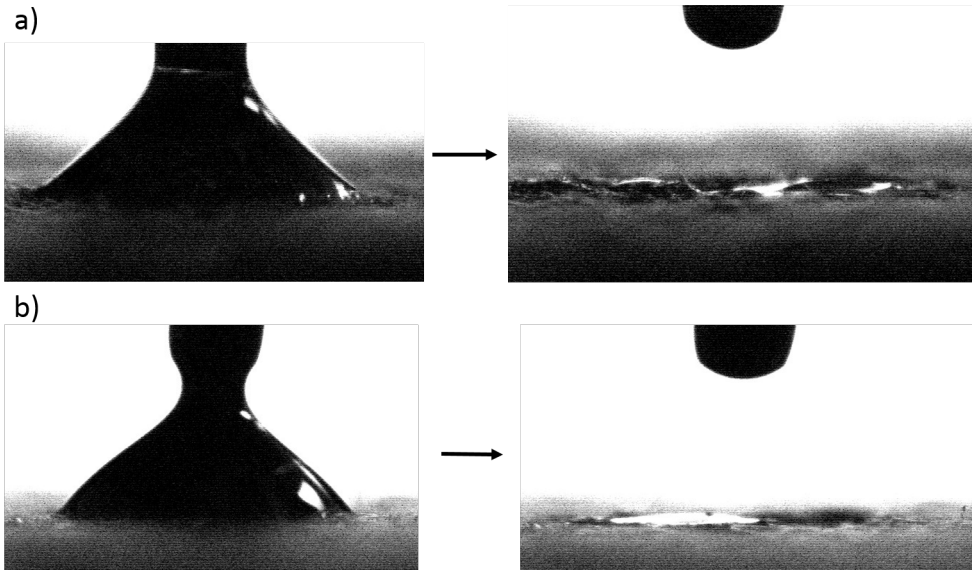

Figure 4.7: a) Lube oil b) Crude oil being dispensed on the rough surface

It is clear that both oils undergo spontaneous pore penetration. This is due to capillary and wetting forces between the hydrocarbon oil and the fiber sample. As mentioned earlier the roughness enhances the oleophilicity by some factor which can be corrected by considering the Wenzel equation of wetting. It is therefore difficult to provide a single value of contact angle between the oil and the rough surface because the oil penetrates the surface and the contact angle changes as a function of time.

The contact angles measured on the smooth sample are more close to the intrinsic contact angle. Figure 4.8 below shows the contact angles on the smooth sample for lube oil and crude oil. The contact angle for lube oil and crude oil were 22^0 and 31^0 respectively. These angles met the requirement for spontaneous imbibition as they are below 40^0.

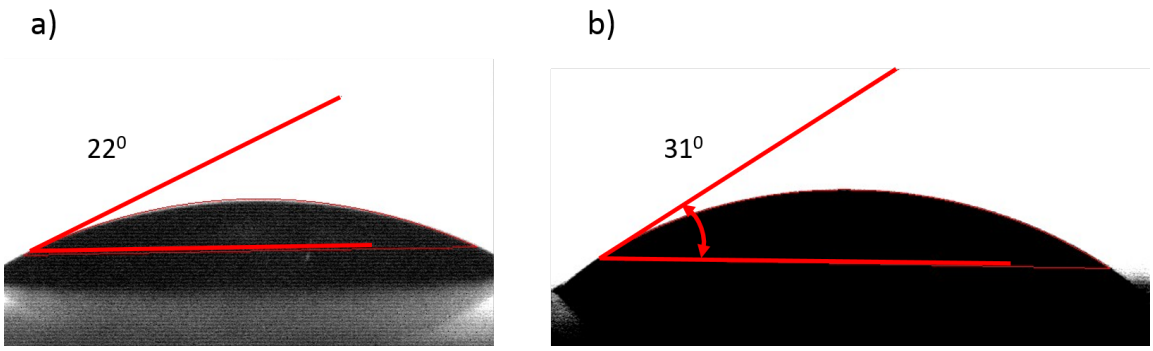

Figure 4.8: a) Contact angle of lube oil and b) Contact angle of crude oil on the smooth sample (injection molded) both against air

Contact angle of Diesel was also measured similarly. However it was observed that the angle formed on the smooth sample (intrinsic) was not zero but was too low to be measured conveniently by fitting the shape profile of the drop. Hence for the purpose of doing calculations a contact angle of 5^0 will be assumed here.

The relative magnitudes of the contact angles can be further verified by characterizing the sorption behavior of these oils. It will become apparent that the sorption kinetics does follow the order of wettability in terms of the contact angles but it is not proportional due to other properties: viscosity, density and surface tension of the oils as it will be discussed next. Table 4.1 shows the contact angles as measured on the smooth sample.

The purpose for doing the wettability analysis was to ascertain that the fiber material exhibits oleophilic and hydrophobic character. In other words it spontaneously attracts oil in preference to air and on the other hand it repels water. Therefore it is expected that a porous medium made of these fibers will not imbibe water without external pressure. That being said the next research task was to perform a quantitative study evaluating the effects of contact angles and other physical properties of oil on the sorption efficiency of the porous structures made using these fibers.

Table 4.1: Contact angles of oil and water on smooth sample against air

Liquid	**Contact Angle** θ	**Surface Tension mJ/m2**
Water	75	0.072
Kerosene	0	0.025
Diesel	5	0.023
Lube Oil	22	0.031
Crude Oil	31	0.035

It is worthwhile to reiterate here that the research task was broadly segregated in two categories. The first is to emphasize solely on the surface characteristics and wettability. The second is to characterize the structural properties like void space and sorption dynamics in relation to porosity and liquid properties. Measuring and interpreting contact angles was a task related to the first category

Researchers have reported to have fabricated superoleophilic and superhydrophobic fibers for oil absorption applications [50]. However other studies have shown that these surface modifications only enhanced the selectivity and had little role to play in increasing the sorption capacity and efficiency which they believe depended more on the structural properties of the porous structure [51].

4.2 Spontaneous Imbibition

The sorbate-sorbent system is described by the process of spontaneous displacement of a non-wetting fluid (air) by the wetting fluid (hydrocarbon oil). In the first chapter it was mentioned that the objective of this thesis work is to evaluate the parameters that enhance the performance of sorbent materials. Wettability in terms of contact angles was one such parameter. Structural parameters in terms of porosity and pore connectivity is another fundamental factor that determines the efficiency of a sorbent. The theoretical framework for studying this problem was discussed in Chapter 2 where it was shown that a combination of transport phenomena, interfacial phenomena and pore structure determines the overall performance of a sorbent-sorbate system. Here it is attempted to form a synergistic overview of these aspects while interpreting the experimental results.

The independent parameters in this experiment are:

a) Hydrocarbon properties

   (i) Viscosity

   (ii) Density

   (iii) Surface tension

b) Porous sample property

   (i) Porosity (by changing the bulk density)

The effects of changing these parameters would be seen in terms of different imbibition rates and the total mass of oil sorbed by the sample. The physical properties of the hydrocarbons are shown in the Table 4.2.

Table 4.2: Physical properties of the test liquids

Type of Liquid	**Density** kg/m^3	**Viscosity** mPa s	**Interfacial Tension** mJ/m^2
Water	1000	0.9321	72
Kerosene	760	1.62	25
Diesel	840	2.1	23
Light Lube	865	95	31
Heavy Lube	890	140	31
Crude Oil	920	550	35

The main objective here would be to comment on the significance of porosity (determined by the bulk density) and the hydrocarbon properties on the sorption efficiency and kinetics of the sorption process. It will be reiterated again that the driving force here is the capillary suction pressure which according to the Young-Laplace has a direct relationship with the contact angle and an inverse relationship with the effective capillary radius. Where as according to the Darcy equation permeability scales with the square of the capillary radius. Therefore a dynamic competition exists between these two superimposing mechanism and will be studied next with help of relevant graphics and various calculations.

It is greatly desired to find a predictive relationship between some representative pore information like effective capillary diameter with easily measured material property like the bulk density of the fiber sample. Bulk density is defined as the mass of fibers that completely occupies a predetermined volume, its units are g/cm^3. Table 4.3 lists the bulk densities with their respective porosities as calculated by $\phi = 1 - Bulk\,density/Material\,density$

Table 4.3: Bulk density/porosity of the porous media sample

Bulk density g/cm^3	**Porosity** ϕ
0.085	0.934
0.095	0.926
0.11	0.915
0.13	0.899
0.16	0.876

4.3 Sorption and Absorbency

The sorption behavior was studied by the spontaneous imbibition experiment which was shown in Figure 3.6. Since all the hydrocarbon oils studied in this experiment have contact angles less than 40°, therefore spontaneous imbibition is expected. It means that oil (on the dish) starts penetrating inside the porous medium as soon as it comes in contact with the fiber surface.

The interfacial pressure difference between the wet and dry regions of the porous material cause a capillary suction force which draws the liquid upwards in the sample and is concurrently opposed by the viscous, gravity and inertial forces. The air residing inside the porous media is gradually displaced by the advancing oil.

The theoretical framework of this immiscible displacement process along with mathematical description was discussed in previous chapters. The wetting oil continues to advance until the capillary suction driving force is balanced by the hydrostatic pressure of the imbibed oil. The mass of the oil imbibed is accurately recorded at a preset time interval by the load cell/data logger. The time to reach the steady state or saturated mass that is

when the mass reaches a plateau depends on the oil properties and the bulk densities of the porous sample. The sorption mass refers to the final steady state mass of the sample. This steady state mass identified as the plateu in Figure 4.9 will be referred as the saturated mass and the terms hydrocarbons and oils will be used interchangeably. Figure 4.9 shows one specific example of the mass versus time data for one bulk density. Similar plots were obtained for the other bulk densities and are shown in Figure 4.10

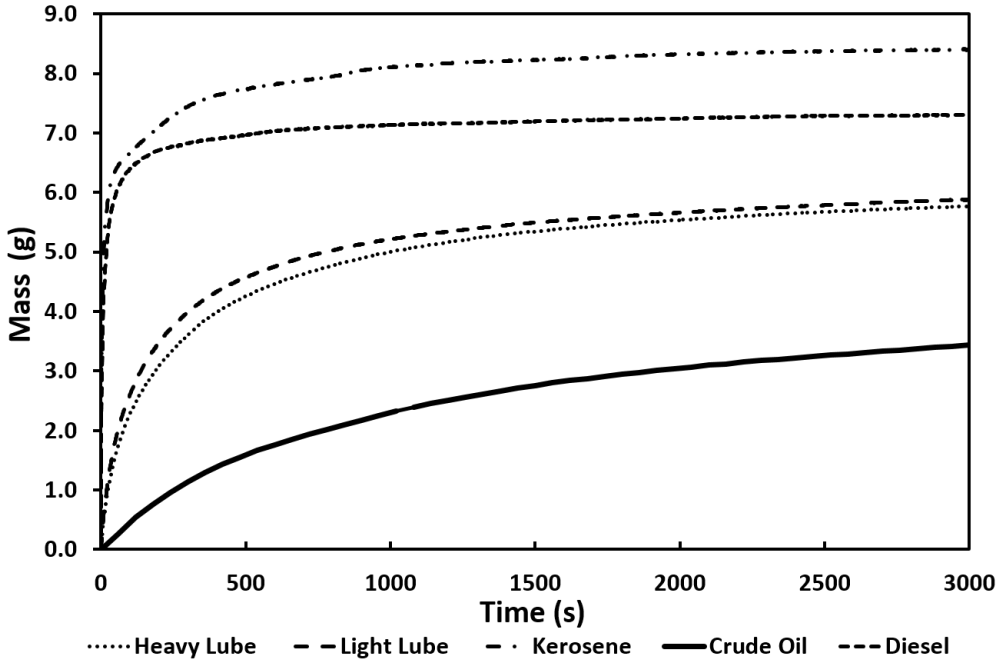

Figure 4.9: Mass sorbed into the porous sample vs time for 0.11 g/cm^3 bulk density

(a) 0.085 g/cm^3

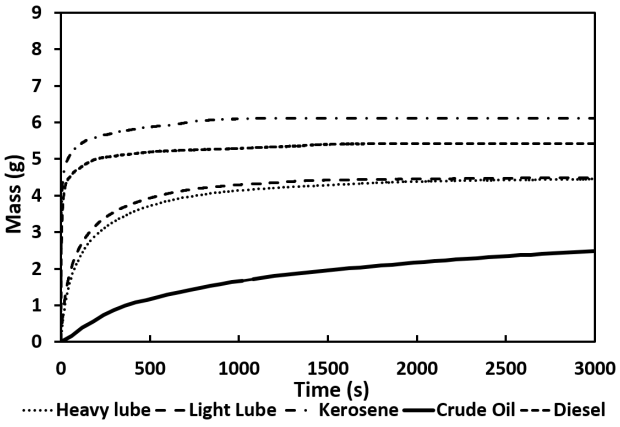

(b) 0.095 g/cm^3

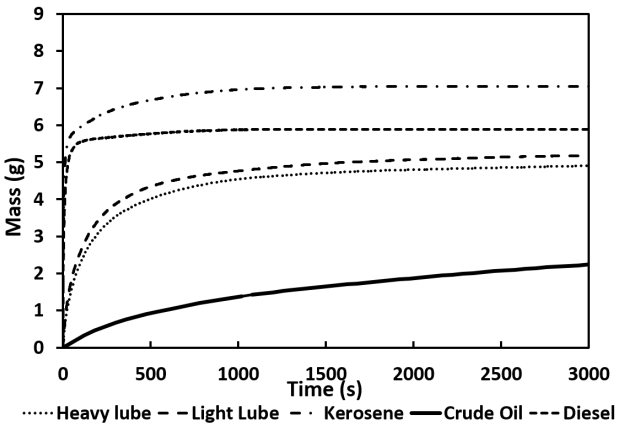

(c) 0.13 g/cm^3

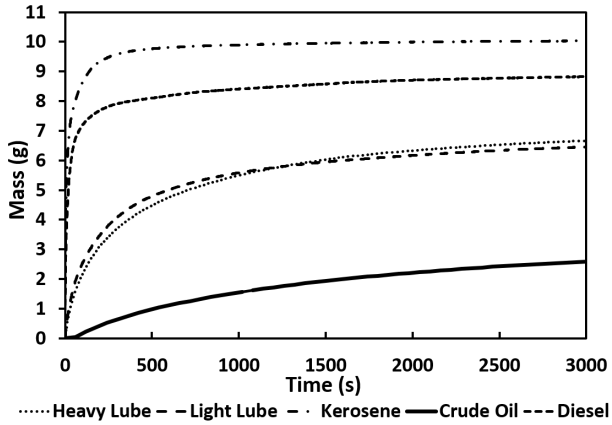

(d) 0.16 g/cm^3

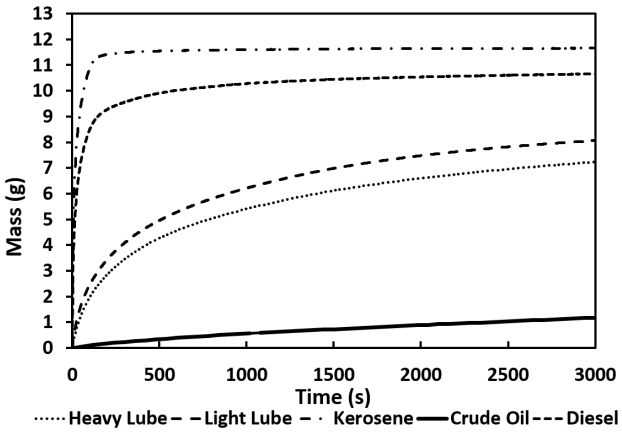

Figure 4.10: Sorption curves for different bulk densities

Effect of increasing the bulk densities on the sorbed oil kinetics can be clearly seen in the above graphs. This section will discuss the saturated mass at different bulk densities. Moreover since the densities of the hydrocarbon oils are different, saturated volume are also computed. These values are tabulated for easy comparison in the Table 4.4.

Table 4.4: Mass and volume sorbed data for different oils/bulk densities

Bulk Density g/cm^3	**Mass Absorbed** grams	**Volume Absorbed** cm^3	**% Mass Absorbency** g oil/ g wetted fiber
		Kerosene	
0.085	6.107	7.800	861
0.095	7.046	8.999	764
0.11	8.376	10.697	651
0.13	10.048	12.833	542
0.16	11.656	14.886	429
		Diesel	
0.085	5.423	6.456	823
0.095	5.882	7.002	819
0.11	7.548	8.986	699
0.13	9.148	10.890	581
0.16	10.745	12.792	460
		Heavy Lube	
0.085	4.558	5.298	945
0.095	5.160	5.999	839
0.11	6.247	7.261	715
0.13	7.531	8.755	595
0.16	9.143	10.628	471

Bulk Density g/cm^3	**Mass Absorbed** grams	**Volume Absorbed** cm^3	**% Mass Absorbency** g oil/ g wetted fiber
		Light Lube	
0.085	4.573	5.342	941
0.095	5.367	6.270	835
0.11	6.199	7.242	712
0.13	7.531	8.798	592
0.16	9.674	11.301	498
		Crude Oil	
0.085	3.951	4.294	1011
0.095	3.994	4.342	897
0.11	5.561	6.045	765
0.13	5.655	6.147	636
0.16	4.581	4.980	504

The above table shows the saturated mass and volume (steady state) of each sorbent sample (averaged over 3 readings) with different hydrocarbon oils. This comparison could be seen more effectively in Figure 4.11 below which shows a combined plot of mass absorbency and the saturated weight against different bulk densities.

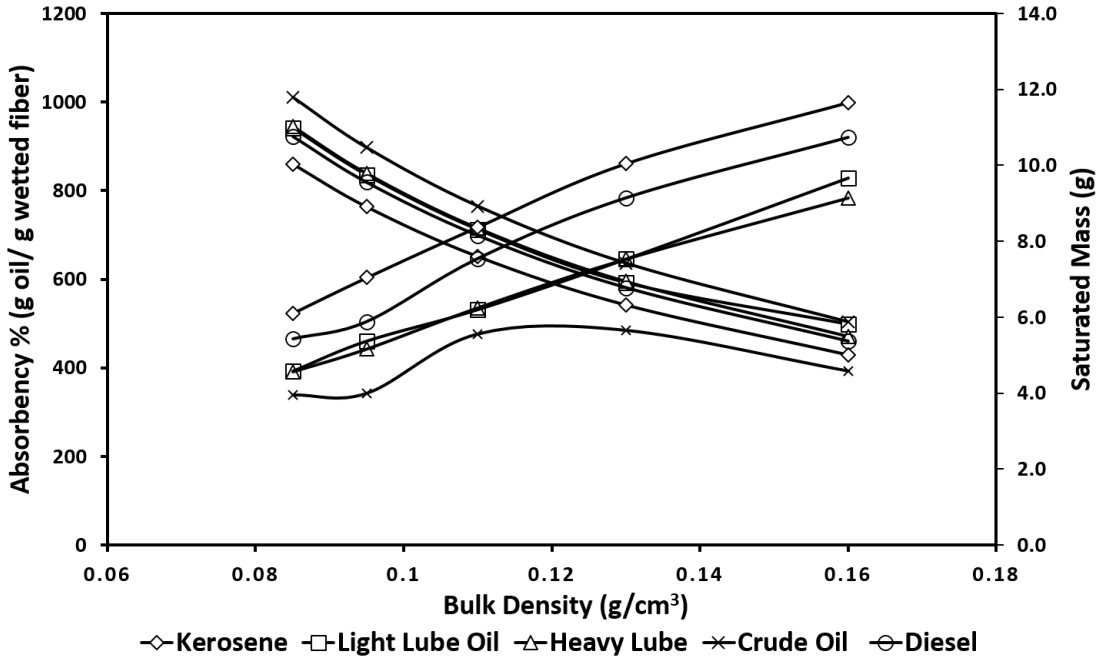

Figure 4.11: Mass absorbency and saturated mass vs bulk density

The general trend seen from the above graph is that with an increase in bulk density the absorbency ratio, as defined by Equation 3.1 decreased whereas the total sorbed mass (saturated mass, see Figure 4.9) increased. This generic behavior exhibited by all the oils at varying bulk densities or porosity is expected. It is known that sorption is a capillary rise phenomenon where the driving force ΔP is inversely proportional to the pore size. It is expected that with increased bulk density the effective capillary radius or pore size is reduced. As a result $\Delta \mathrm{P} = \rho g h_f$ increases and therefore the wetting front h_f will also increase.

The saturated mass data for each oil/bulk density combination was converted into equivalent height reached by the oil using Equation 3.4. This is plotted for each oil/bulk density combination in Figure 4.12. An increase in height corresponds to more fiber coming

in contact with the oil therefore the saturated mass shows an increasing trend with the bulk density.

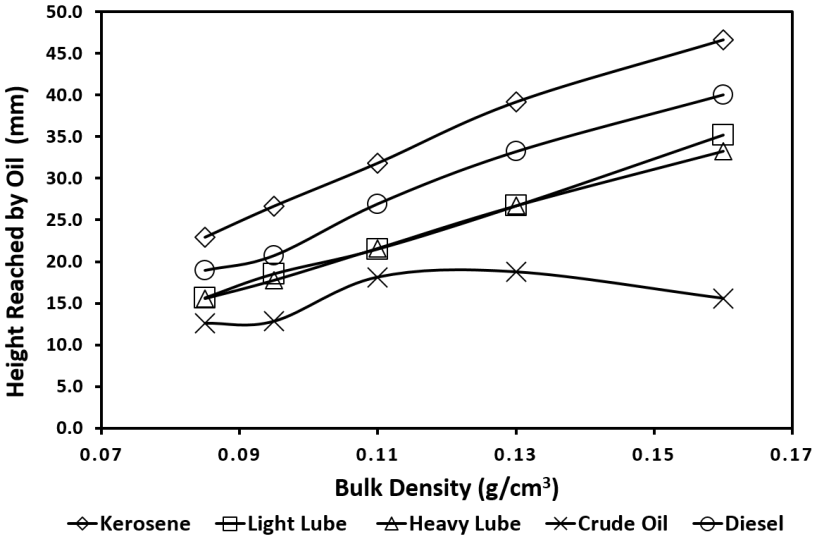

Figure 4.12: Wetted front height vs bulk density (total height of the sample was 55 mm)

On the other hand the declining absorbency ratio with increasing bulk density can be explained by reduction of the overall pore volume available for the oil to occupy. If one wishes to analyze the performance of the sorbents across different bulk densities and oils the following comparison can be made using volumetric absorbency as shown in Figure 4.13

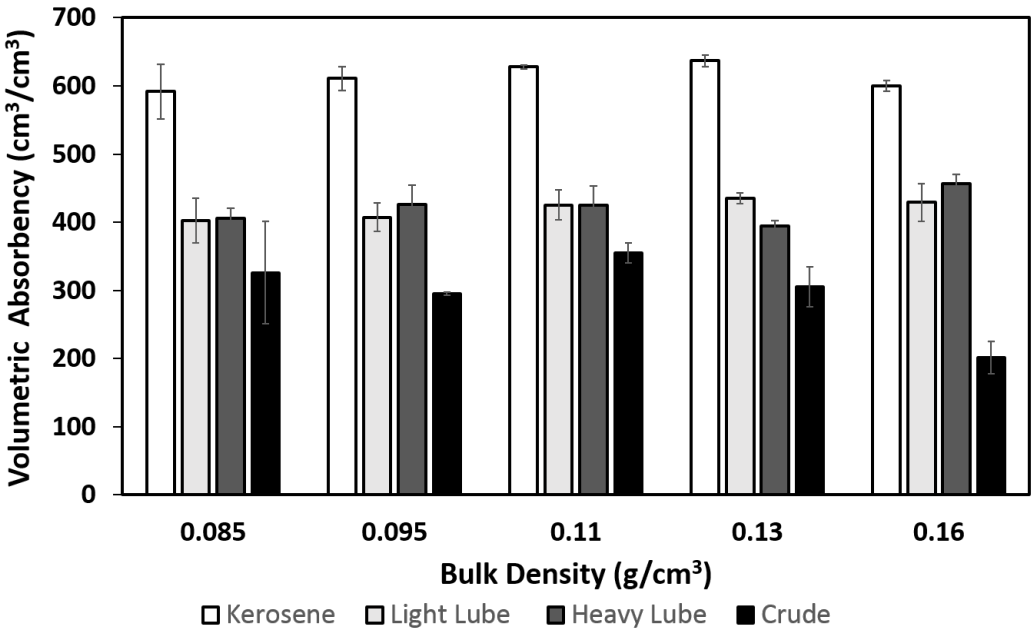

Figure 4.13: Volumetric absorbency comparison of different bulk density and hydrocarbon oils

It is seen here that for the same bulk density the volumetric absorbency for oils differs although the pore volume available for each oil is the same. It appears that for all bulk densities the most sorbed hydrocarbon is kerosene and the worst sorbed hydrocarbon is crude oil. This difference is attributed to the viscosity differences between these oils. As seen from Equation 2.26 the wetted front height is inversely related to the square root of the oil viscosity (see Table 4.2). Moreover because of the large sample size the hydrostatic pressure affects the final front height achieved by the oils.

Since the densities and viscosities increase moving from kerosene to lube oils to crude oil one expects to attain different heights and hence different sorbed volume. As an example Figure 4.14 shows the saturated height reached by the wetting fronts of these oils for the same bulk density of 0.11 g/cm^3

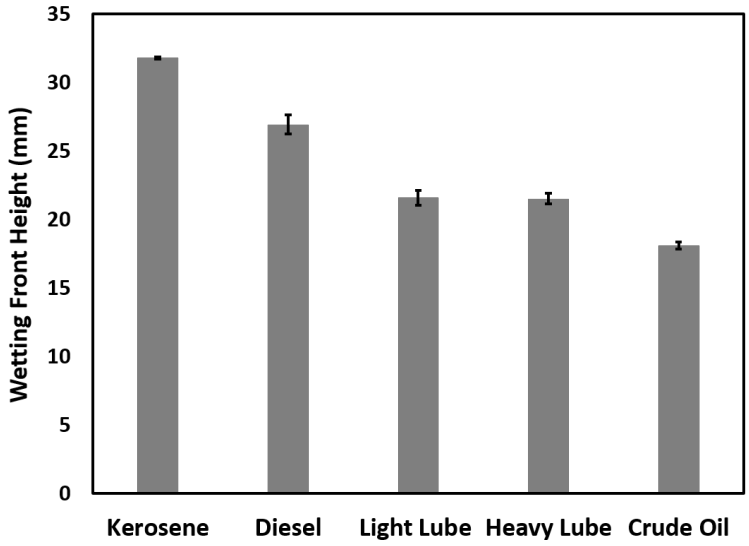

Figure 4.14: Front height for 0.11 g/cm^3 bulk density (total height of the sample was 55 mm)

From Figure 4.13 it is observed that each oil seems to perform the best (in terms of % volumetric absorbency, % cm^3 of oil per cm^3 of fiber) at a certain bulk density. For instance crude oil gets absorbed more into 0.11 g/cm^3 as compared to other bulk densities whereas kerosene is sorbed most by the 0.13 g/cm^3. Since essentially the pore size is reduced by moving to higher bulk densities, it appears that optimal pore size is different based on oil properties. More studies needs to be done to further affirm this interpretation. Structural parameters of the porous samples like: pore connectivity, pore shape and pore size distribution at these bulk densities could be determined using techniques like SEM or CT-scans.

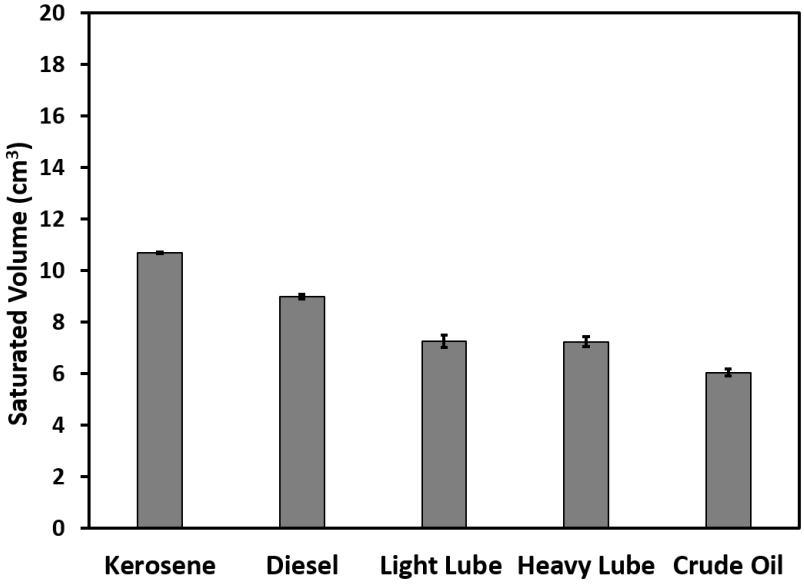

Figure 4.15: Saturated volume for 0.11 g/cm^3 bulk density (total volume of the sample was 20 g/cm^3)

4.4 Saturation and Penetration Kinetics

Another important aspect of determining the efficiency of the sorbents is the wetting phase saturation and the time taken to reach the saturated mass. Wetting phase saturation is an indication of the degree to which the porous sample has been filled with oil. The total volume for fiber sample was 20 cm^2 for all bulk densities. As could be seen from Figure 4.15 there is still substantial volume of fiber that was not wetted by oil, hence unused porous space was filled with air. This can be considered as an inefficiency of a sorbate-sorbent system and could be investigated by studying the wetting phase saturation of oil with different bulk density samples. The time element is also important because in an oil spill scenario it would be desired to have the least amount of saturation time to minimize its environmental impact. Knowing these quantities apriori could be useful in deploying

the correct bulk density sorbent.

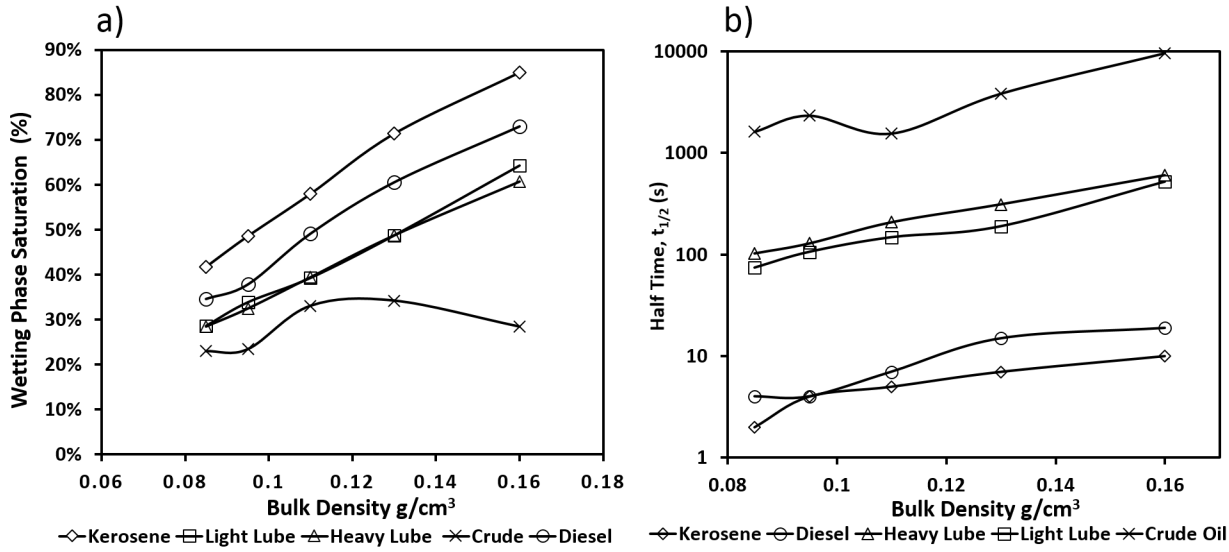

Figure 4.16: a) Wetting phase saturation and b) Half time versus bulk densities of the samples

The wetting phase saturation is also referred to as volumetric soprtion efficiency as it directly tells the fraction of voids or pore volume filled with oil. As expected the increase in bulk densities increase the ΔP which is able to pull the oil to fill up the porous medium. The trend is similar for kerosene and both the lube oils, but for crude oil the maximum saturation is seen at 0.11 g/cm^3 after which it starts to decline gradually.

It is proved elsewhere that this may be due to change in the meniscus velocity which changes the contact angle [52, 53, 44]. In modeling sorption kinetics the flow is assumed to be at the same constant speed and therefore static contact angles are considered. This is the same as measured independently through contact angle measuring equipment. However it is possible as in the case of crude oil here that by densifying the porous material the assumption of constant speed does not hold true. Hence according to Bracke et al the

dynamic contact angle is some function of the velocity which changes with time [54].

The speed of sorption is characterized here as the half time which is determined as the time taken for the oil to reach half of the maximum sorbed mass for that particular bulk density. These half times are different for each type of oil and for any given bulk density the trend is similar as seen in part b of Figure 4.16. It is intuitive to think that same bulk density induce the capillary pressure that should correlate well with the wettability (in terms of contact angles), however the sorption kinetics is not simply proportional to wettability; it forms a complex relationship with other properties like viscosity, surface tension and density of the oil. These relationships are described by several correlations in literature and two of those will be considered here. The full saturation times of oils for 0.11 g/cm^3 bulk density is plotted as the normalized saturated mass as a function of time in Figure 4.17.

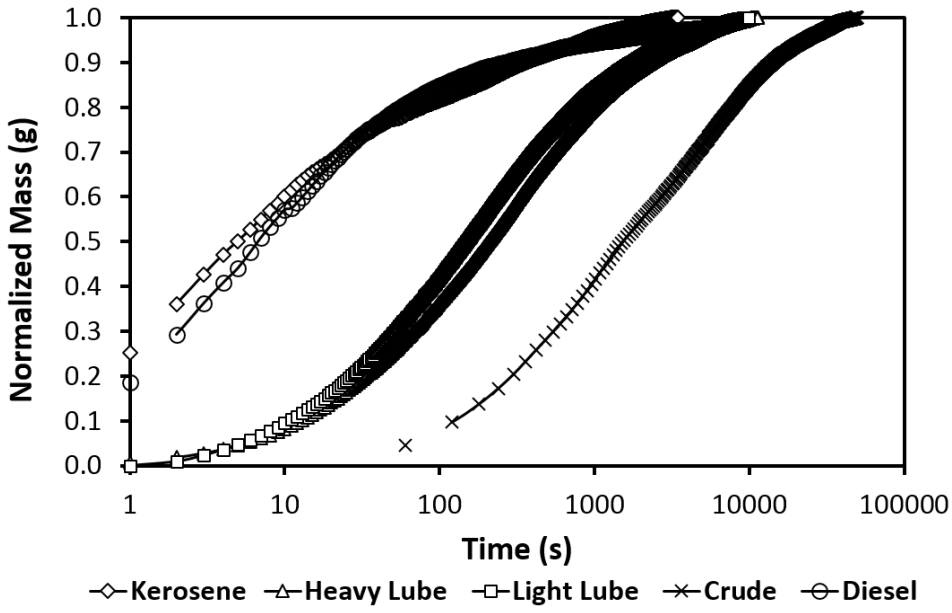

Figure 4.17: Time required for saturation plotted as normalized saturated mass (g) vs time for bulk density 0.11 g/cm^3

As seen from the above plot the penetration of crude oil into the same porous structure (0.11 g/cm^3) is 100 times slower than kerosene and roughly ten times slower than the lube oils. These differences in sorption kinetics will be modeled using traditional theories of imbibition namely: Lucas-Washburn and Darcy Law. It is worthwhile to note that imbibition kinetics qualitatively speaking does follows the expected behavior in terms of contact angles of oils and their ability to wet the porous structure. The static contact angles measured on rigid flat surface as listed in table 4.1 are 0^0, 5^0, 22^0 and 31^0 for kerosene, diesel, lube oil and crude oil respectively. However these differences alone do not explain the significant difference in saturation mass and time required for hydrocarbons to move inside the same porous structure. Figure 4.10 shows the sorption kinetics of oils in the porous sample with different bulk density. The figure below shows one example of a typical sorption curve.

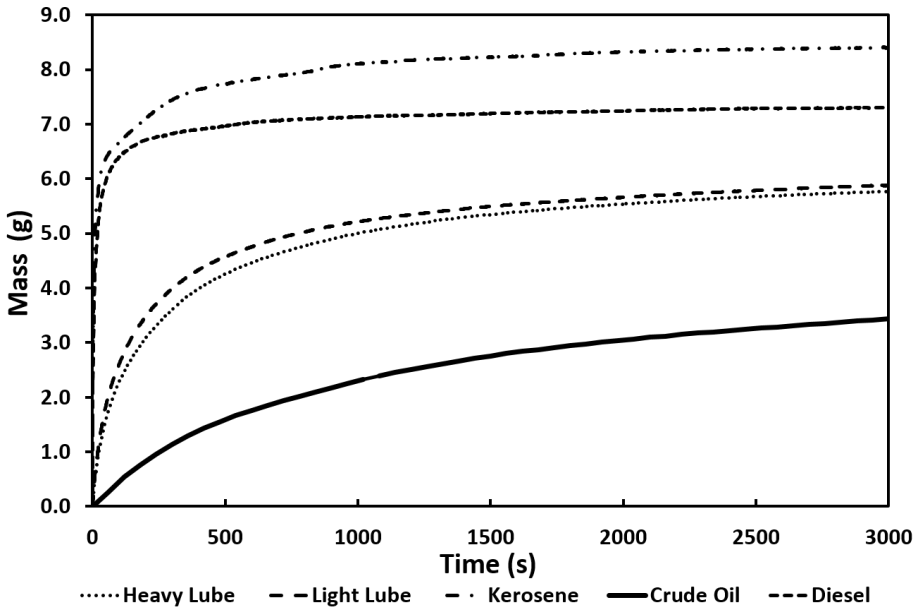

Figure 4.18: Saturated mass vs time at 0.11 g/cm^3

Next the sorption kinetics data for all bulk densities will be evaluated by comparing it with the predictions of the Lucas-Washburn and Darcy based model. As discussed previously these models are based on momentum balance and continuity equation (for Darcy's Law) and correlates liquids properties and porous medium properties to the rate of imbibition. Due to their mathematical simplicity and easy experimental validation they are extensively used in industry and academia as an important tool to characterize macroscopic flow in porous materials.

4.5 Modeling Experimental Data

4.5.1 Lucas-Washburn

This model gives the simplest geometric description of a flow in a porous medium which it considers to be composed of a bundle of capillary tubes of constant diameter. The mathematical theory of the model with its various restrictions are discussed in section 2.8.1. Since the model uses wetted front height, the mass data was converted using the linear relationship shown in Equation 3.4. The final governing equation after simplifying the momentum balance ignoring inertial effect results in an analytical expression relating the wetted front height with time. Equation 2.26 gives an explicit relationship between front height and time when only the viscous forces is considered. An implicit expression 2.27 between front height and time results when both viscous and gravity forces are taken as the opposing force to capillarity. These two cases will be tested against the experimental data; the validation of the models will be discussed.

Lucas-Washburn model with only viscous effects:

$$h_f = \sqrt{\frac{\gamma R_c \cos\theta}{2\mu} \cdot t}$$

Lucas-Washburn model with viscous and gravity effects:

$$p_c ln \left| \frac{p_c}{p_c - \rho g h_f} \right| - \rho g h_f = \frac{\rho^2 g^2 {R_c}^2}{8\mu} \cdot t$$

By examining the experimental data and plotting h_f^2 versus time for the bulk density of 0.11 g/cm^3 results in the following plot. Plots for other bulk densities are attached in appendix A

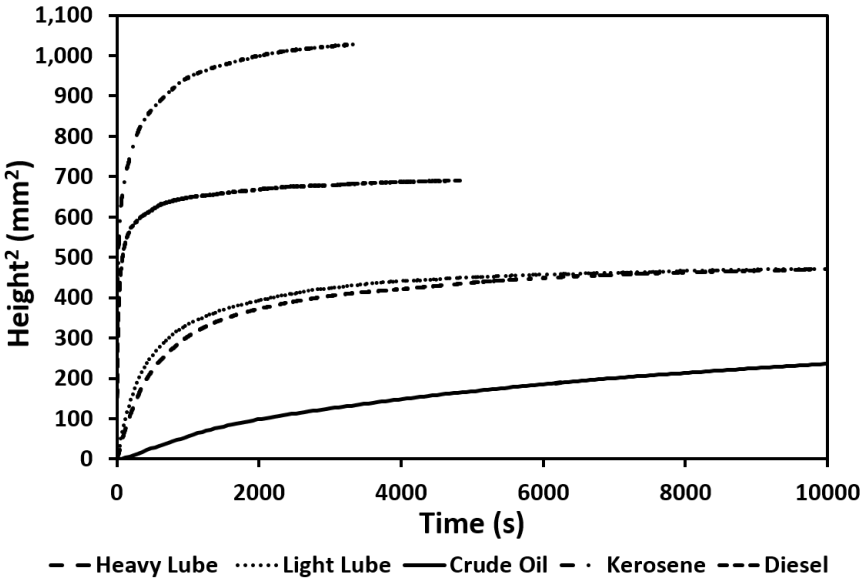

Figure 4.19: Lucas-Washburn model as described by Equation 2.26 at 0.11 g/cm^3 bulk density

It can be seen from Figure 4.19 that all oils deviate significantly from the linear $h^2 \alpha\, t$ Lucas-Washburn behavior. There are a number of factors that can invalidate this model. This will be discussed later together with the second variant of the Lucas-Washburn (LW) model that will discussed next.

The second variant of the LW model takes into account both the gravity and the viscosity effects as the opposing force to the capillary pull. Gravity and viscous effects

together results in the modified Lucas-Washburn (MLW) equation which is a first order non-linear equation that can be solved and the front height is given by the logarithmic relation of the form

$$p_c ln \left| \frac{p_c}{p_c - \rho g h_f} \right| - \rho g h_f = \frac{\rho^2 g^2 {R_c}^2}{8\mu} \cdot t \tag{4.1}$$

This model has been used by Mullins et al [55] to model experimental imbibition data of mineral oils wicked into low bulk densities glass fiber filters. The above equation was rearranged to make 't' as the independent variable. From the Young-Laplace equation it is known that:

$$p_c = \rho g h_\infty = \frac{2\gamma \cos\theta}{R_c} \tag{4.2}$$

Therefore,

$$h_\infty = \frac{2\gamma \cos\theta}{R_c \rho g} = \frac{\beta}{R_c} \tag{4.3}$$

Now, β is a known number since contact angles have already been measured independently and the liquid properties are known. Therefore in modeling equation 4.1 only R_c is let as the fitting parameter. After bringing 't' on left hand side of the equation and substituting the above two expressions results:

$$\mathrm{t} = \frac{16\eta\gamma \cos\theta}{g^2 \rho^2 R_c^3} \cdot \ln\left(\frac{\beta}{\beta - R_c h_f}\right) - \frac{8\eta}{g\rho R_c^2} \cdot h_f \tag{4.4}$$

The least square fitting was performed between the model and the experimental data using the MATLAB function fminsearch, which fitted the data by minimizing the error between observed times and modeled times. The MATLAB code is attached in Appendix B. The fits obtained were not good at all for all oil/bulk density combination. As an example two fittings are shown below for 0.11 g/cm^3 bulk density

(a) Heavy Lube Oil (b) Crude Oil

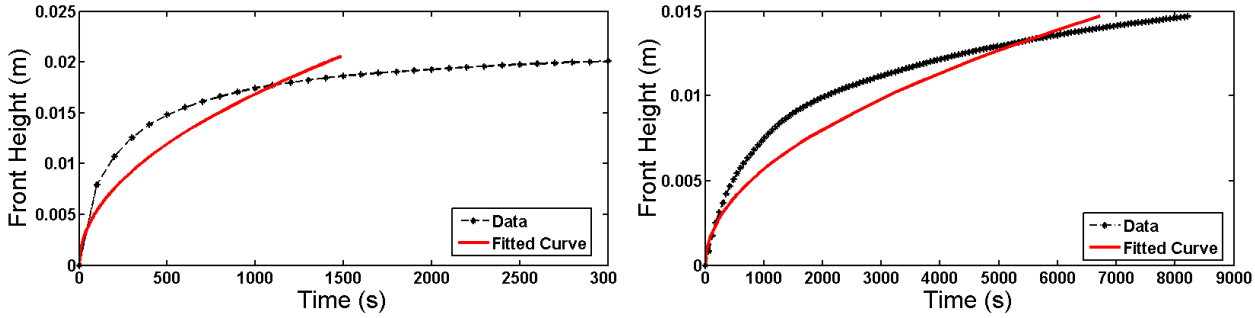

Figure 4.20: Lucas-Washburn model as described by equation 4.4 for (a) Heavy lube oil and (b) Crude oil for 0.11 g/cm^3 bulk density

Thus the Modified Lucas-Washburn model when the contact angle was pinned at the same constant value characteristic of the solid/oil interaction (determined independently) does not agree with the experimental data, hence the fitted R_c, effective capillary radius cannot be related to the porous media using this model. This deviation from the expected Lucas-Washburn behavior has been observed by several researchers [44, 13, 56, 57]. Some of these arise from the theoretical underpinnings of this model which assumes the porous media to be a bundle of aligned parallel tube with constant diameter.

In real porous media used here there is a complex microstructure with pores with various orders of magnitude. Moreover there is obviously lateral flow and the pores are all interconnected whereas in the model the tubes are independent with no interconnection.

Researchers have extended the Lucas-Washburn by adding various corrections and making it more comprehensive to make better predictions. Dullien et al [58] have modified the equation by adding different sized capillaries while Dong et al [59] have proposed adding terms that account for interacting capillaries allowing for cross flow. Cai et al [14] have done a comprehensive review of the variants of the classical Lucas-Washburn equation and has presented a generalized model for predicting rate of spontaneous imbibition in tor-

tuous and variable non circular sized pores. Although these models were presented in a amenable mathematical formulation their usefulness in predicting experimental results is still dubious and merits further investigations.

It is believed that more studies need to be done to find the dynamic effects of liquid and solid interaction within a porous media. Indeed Alava et al [13] has proposed that effects of evaporation and porous media swelling must be studied separately before applying the Lucas-Washburn law. Their work explain that it is very much possible that the moving liquid does not follow the Stokes law the very basis of Lucas-Washburn equation and that it follows another velocity law.

In case of a swelling porous media the fiber filaments can act as a sink. This reduces the average size of the pore and therefore Berg et al [60] have suggested that the effective capillary radius must be adjusted as a function of time. Based on their work they found capillary radius to be independent of the hydraulic radius and through experiments found a linear relationship of hydraulic radius with time. This implies that with time the capillary size will reduce and hence the velocity will change. This correction has to be included for each porous medium based on experimental results and could not be done apriori.

An interesting work has been done by Ahmed et al [57] to overcome some of the discrepancy between experimental results and the Lucas-Washburn model pertaining to the dynamics of the capillary rise. They have postulated that sorption dynamics are not solely controlled by hydrostatic pressure and viscous dissipation but are also controlled by frictional dissipation at the moving line between liquid and solid porous media. They have elaborated on the contribution of each of these energy dissipation channels on the accuracy of the LW model. In their model a retardation coefficient is introduced according to which the contact angle is a function of time and is not a constant value (equilibrium contact angle) as taken in the conventional Lucas-Washburn behavior. They explained the frictional dissipation between the solid and liquid at the 3 phase line by using the molecular

kinetic theory and through experimental work showed range of the capillary radius for which frictional dissipation may be dominant in describing the dynamics of the imbibition process.

4.5.2 Darcy Based Model

The Darcy law as described in section 2.8.2 is also used to model imbibition dynamics in porous media. For the single phase flow where a clearly defined wetting front is assumed momentum balance and continuity equation is applied on the moving interface using the representative elementary volume approach. This upscaling technique ignores pore scale physics and the volume flow of the imbibing liquid per unit area of the porous medium simply becomes the velocity of the interface and leads to the results described in Equation 2.39. The advantage of using Darcy based modeling is that it can be extended easily to 2-D and 3-D flows whereas capillary models like Lucas-Washburn are always 1-D. The 3-D approach can be used effectively in pore network modeling using reconstruction of porous media images and simulating flow directly into the porous medium. Moreover relating macroscopic parameters like permeability and capillary pressure to the porous structure is very important in predicting performance in many engineering applications.

It is reported by Masoodi et al [43] that Darcy based law are more robust and accurate in predicting imbibition dynamics as compared to Lucas-Washburn. The have evaluated the efficiency of imbibition models by fitting experimental data and for Darcy based models have derived a general formula for determining the suction pressure at the moving interface. This model will now be evaluated by fitting the experimental data and the significance of the fitting parameters in relation to the porous structure will be discussed. Expression 2.39 is an implicit equation relating the meniscus height h_f with time. The equation was rearranged to bring 't' to the left hand side of the equation:

$$\mathrm{t} = \frac{\phi \eta p_c}{\rho^2 g^2 K} \ln \left| \frac{p_c}{p_c - \rho g h_f} \right| - \frac{\phi \eta h_f}{\rho g K} \tag{4.5}$$

where K is the permeability of the porous medium, ϕ is porosity, η is viscosity of the liquid and h_f is the saturated front height. With known hydrocarbon oil properties and K and P_c left as fitting parameters a MATLAB code was run using fminsearch to fit the experimental data of t vs h_f. The MATLAB code is attached in Appendix B. Experimental results of three different bulk densities were modeled with Equation 4.5. The fitting trends are shown below for 0.11 g/cm^3 as an example. The fits for the other bulk densities were equally good and have been attached in appendix A for reference.

The Darcy based Equation 4.5 yields a satisfactory fit on the experimental data. The two free fitting parameters: P_c and K were found for each curve by MATLAB. Some interesting comparison between the different porous media can be made using these values. Since the data was modeled for 3 different bulk densities and 5 oils some expected trends both within and across each bulk density have to be verified by comparing the fitted parameters. The fitted parameters for the 3 bulk densities and 5 oils are tabulated in table 4.5:

(a) Kerosene

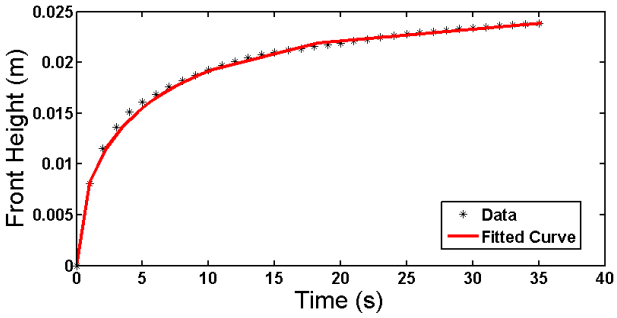

(b) Diesel

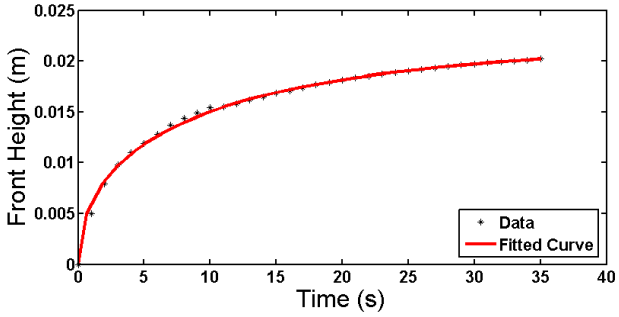

(c) Light Lube

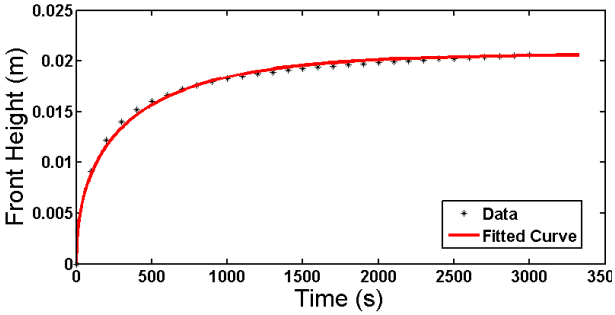

(d) Heavy Lube

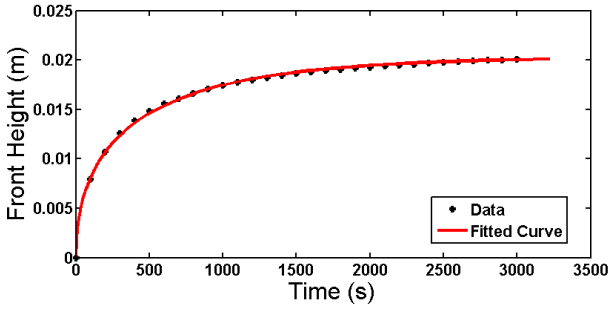

(e) Crude Oil

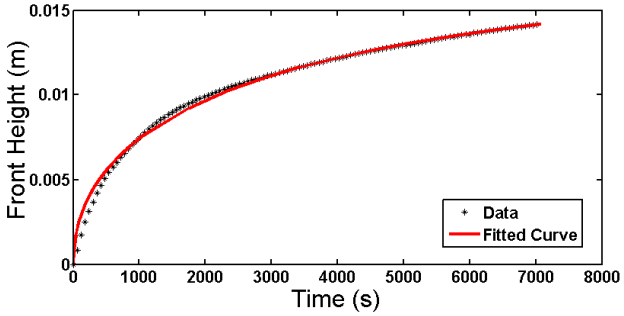

Figure 4.21: Darcy law based curves for 0.11 g/cm^3

Table 4.5: Tabulated values of fitted parameters for different bulk densities/oil

Porosity ϕ	**Oil**	**Viscosity** η **(Pa s)**	**Density** ρ **(kg/m^3)**	**Permeability K (m^2)**	**Capillary Pressure Pc (Pa)**
0.934	Kerosene	0.00165	783	4.87E-10	141.09
0.934	Diesel	0.0021	840	2.96E-10	129.68
0.934	Light Lube	0.095	856	3.58E-10	129.41
0.934	Heavy Lube	0.14	860	4.17E-10	128.28
0.934	Crude	0.55	920	3.58E-10	109.08
0.915	Kerosene	0.00165	783	3.54E-10	188.54
0.915	Diesel	0.0021	840	2.29E-10	180.32
0.915	Light Lube	0.095	856	2.82E-10	173.71
0.915	Heavy Lube	0.14	860	3.39E-10	171.49
0.915	Crude	0.55	920	1.36E-10	152.76
0.899	Kerosene	0.00165	783	3.25E-10	236.94
0.899	Diesel	0.0021	840	1.32E-10	229.04
0.899	Light Lube	0.095	856	2.61E-10	195.09
0.899	Heavy Lube	0.14	860	2.87E-10	206.88
0.899	Crude	0.55	920	5.50E-11	160.45

As could be seen from the Darcy based equation P_c is an important parameter to predict front height with time. Similar to Lucas-Washburn model it can be assumed here too that the fibrous porous sample made is a bundle of vertically aligned capillary tubes with the same diameter, so that the capillary pressure can be equated to the the Young-Laplace equation and using contact angle determined independently find R_c, the effective capillary radius. Table 4.6 shows the calculated effective capillary radius values for the corresponding capillary pressure.

Table 4.6: Effective capillary radius and capillary pressure

Porosity, ϕ	**Oil**	**Pc** **Pa**	**Effective capillary radius** µm
0.934	Kerosene	141.1	354
0.934	Diesel	129.7	353
0.934	Light Lube	129.4	444
0.934	Heavy Lube	128.3	448
0.934	Crude	109.1	550
0.915	Kerosene	188.5	265
0.915	Diesel	180.3	254
0.915	Light Lube	173.7	331
0.915	Heavy Lube	171.5	335
0.915	Crude	152.8	393
0.899	Kerosene	236.9	211
0.899	Diesel	229.0	200
0.899	Light Lube	195.1	295
0.899	Heavy Lube	206.9	278
0.899	Crude	160.5	374

The decreasing effective capillary radius as the porosity is reduced is reasonable to expect. However within the same bulk density the effective capillary radius should be more or less the same. It can be said that even though the model fits the data remarkably the deviation of R_c within same bulk density and different oils cannot be explained by the "bundle of tubes model". In the figure below the effective capillary radius is compared for the same bulk density 0.11 g/cm^3.

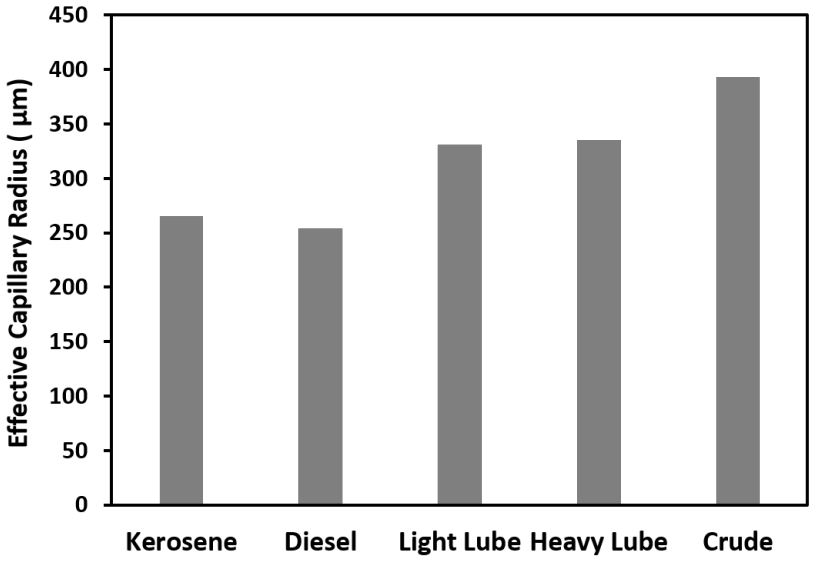

Figure 4.22: Effective capillary radius based on capillary pressure of different oils at 0.11 g/cm^3

There is approximately 48% difference between the lowest and highest predicted R_c values. It is therefore very important to predict the right value for the capillary pressure. One way to predict Pc is by using Buckley-Leverett theory which describes the frontal saturation profile as function of the relative permeabilities of the displacing and the displaced fluids. The flow of the displacing fluid is then defined by a quantity called fractional flow which is a function of saturation. Since the exact value of capillary pressure depends on the

frontal saturation it might be possible that in our case for example kerosene could not be considered as having fully saturated wetted front. Therefore one needs to find the frontal saturation using relative permeabilities and from there determine the adjusted value for Pc.

4.6 Water-Air Capillary Pressure

The non-wetting behavior of water on the fiber material was confirmed by the contact angle measurements. It was determined that the contact angle against air was sufficiently large so that a porous structure made of these fibers will not spontaneously imbibe water. However due to difficulty in interpreting the correct magnitude of the intrinsic contact angle because of surface roughness and the fact that the contact angles is a dynamic property changing as the liquid front moves within a porous medium, it would be preferable to have a measurement by a separate technique to confirm the non-wetting hydrophobic character of the fiber material.

As proposed by Gostick et al [46] the hydrophobic character could be confirmed conveniently by directly measuring the capillary pressure and the subsequent water saturation of the porous medium. The experiment was performed using the set-up described by Gostick et al [46] in which the capillary pressure is increased in step-wise fashion and the resulting water uptake is measured. The capillary equilibrium is achieved at each increase in pressure so that a broad range of saturation was identified with a distinct values for capillary pressure.

Only one bulk density 0.11 g/cm^3 was used here to measure water-air capillary pressure. It was found that a positive pressure was required to force water into the polymer fiber porous medium and similarly a positive pressure required to withdraw the water once the sample has been fully saturated with water. This latter behavior was not expected to us

as earlier it was hypothesized that the fiber material is completely non-wetting to water. Such materials are said to be possessing neutral wettability. Further studies need to be done to confirm this behavior.

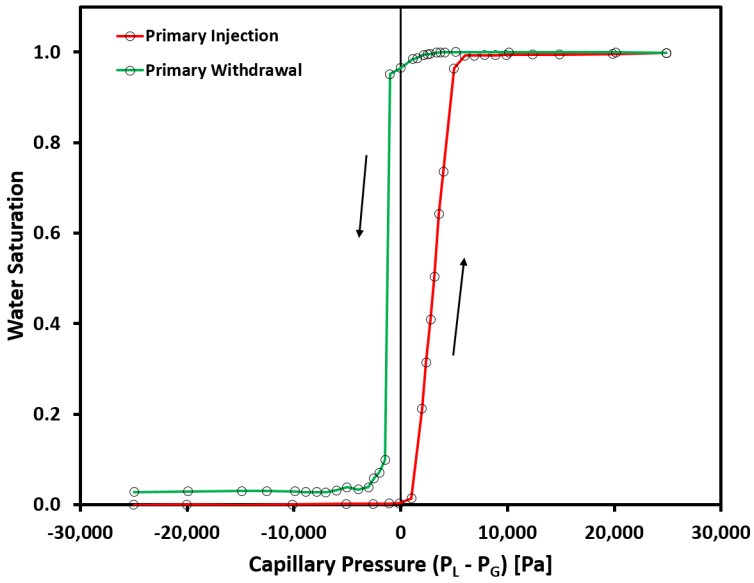

Figure 4.23: Water-Air capillary pressure at 0.11 g/cm^3 bulk density

The graph in Figure 4.23 shows the pressure measured for water injection and removal; the red curve represent water injection. The decreasing gas pressure is used to control the capillary pressure and it could be seen that a positive capillary pressure of around 2000 Pa is required to move water into the porous fiber material. This is a very useful result for oil absorption applications since in an oil spill on water the porous structure could come in contact with water before it contacts the spilled oil.

These results confirm that a sorbent boom made of 0.11 g/cm^3 bulk density would require an external pressure of 2000 Pa to force water into its porous structure. This is a pressure equivalent to approximately 20 cm of water column. These forces could

be experienced in a real scenario by waves, by the hydrostatic pressure and by dragging the sorbent against the water surface. The exact nature and a quantitative analysis of these forces need to be studied separately to further evaluate the suitability of using these polymer fibrous structure for oil spill application.

4.7 Visualization of Porous Structure

Accurate prediction of flow in porous media has been fraught with great difficulties due to the intricate nature of the pore structure. Over the last many years researchers have used traditional transport models like Darcy law and Lucas-Washburn and other theoretical and numerical approaches to study the porous media flow. Despite best efforts there is still a lot of room for improvement and coming up with better techniques.

Pore scale analysis based on statistical models may be very accurate but they are computationally not feasible for analyzing flow in large macro-sized samples with thousands of pores in various directions. Another method which has gained much attention recently is creating a virtual representation of the interior of the porous medium using advanced imaging techniques like computerized tomography scans. The image analysis allows the simulation of flow by incorporating the transport calculations on the simplified porous medium topology.

Pore network modeling depends on the experimental techniques like computerized tomography to get information on the interior of the porous structure. Due to a limitation of resolution available for the images obtained from these imaging tools some simplistic assumptions are made which makes pore network modeling computationally less demanding.

As discussed previously porosity is a macroscopic parameter that alone cannot explain much of the sorption behavior in complex porous media. Pinto et al [51] described that structural parameter like pore size distribution and pore connectivity have significant in-

fluence in evaluating the sorption efficiency of disordered loosely packed fibrous structures. Therefore for many practical applications it is in great interest to extract a true picture of the porous medium consisting of interconnected pores/voids and their size distributions.

X-ray microtomography was used for one of the sample with bulk density (0.11 g/cm^3) to obtain images of the internal porous structure with a 5 micrometer resolution. This resolution was deemed appropriate because the fiber diameter in the order of 30 micrometers. Therefore, with 5 micrometer resolution it was possible to obtain 1000 slices (2-D high resolution images) for a sample with cylindrical volume with diameter of 5 mm and height of 5 mm. Each slice was 5 micrometer in thickness (height) and 5 mm in diameter. Figure 4.24 shows one example of the image for one slice.

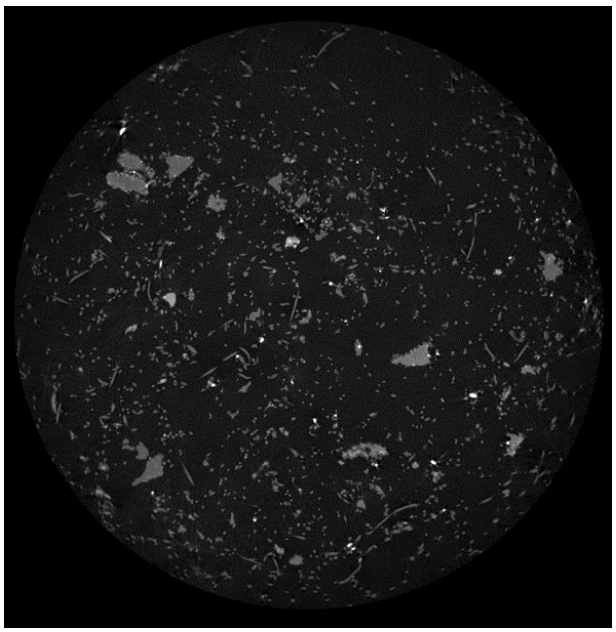

Figure 4.24: Cross sectional view of the porous medium at 0.11 g/cm^3 bulk density

All the images were processed through an image analysis algorithm to produce a 3-D visualization of the porous sample shown in Figure 4.25. In this model a sphere is

made to fit inside each possible pore and the sphere diameter is increased to its maximum size. The colors of the spheres are used to facilitate visualization by classifying sphere of similar size with a certain color. The fiber are identified by gray color. The size of the spheres are subsequently used to evaluate pore size distribution. The pore diameter size and distribution were calculated from the pore network model; the pore size distribution is shown in Figure 4.26.

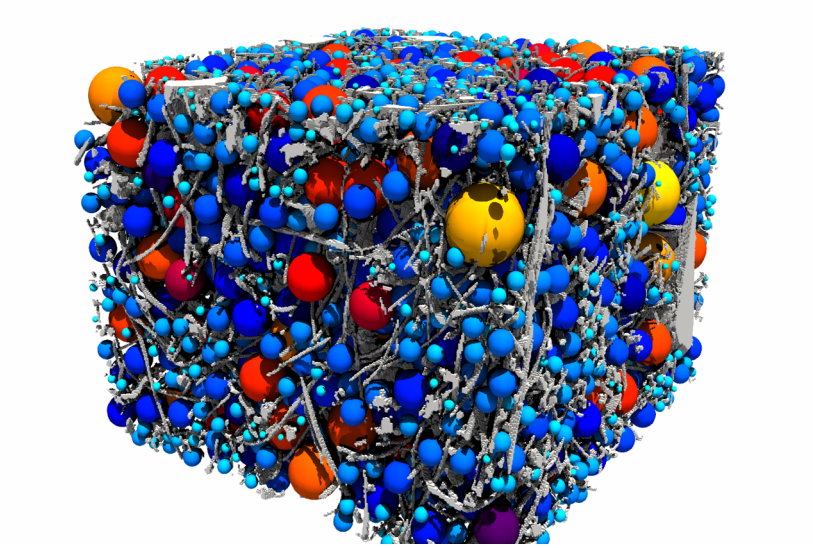

Figure 4.25: 3-D Visualization of the porous medium at 0.11 g/cm^3 bulk density

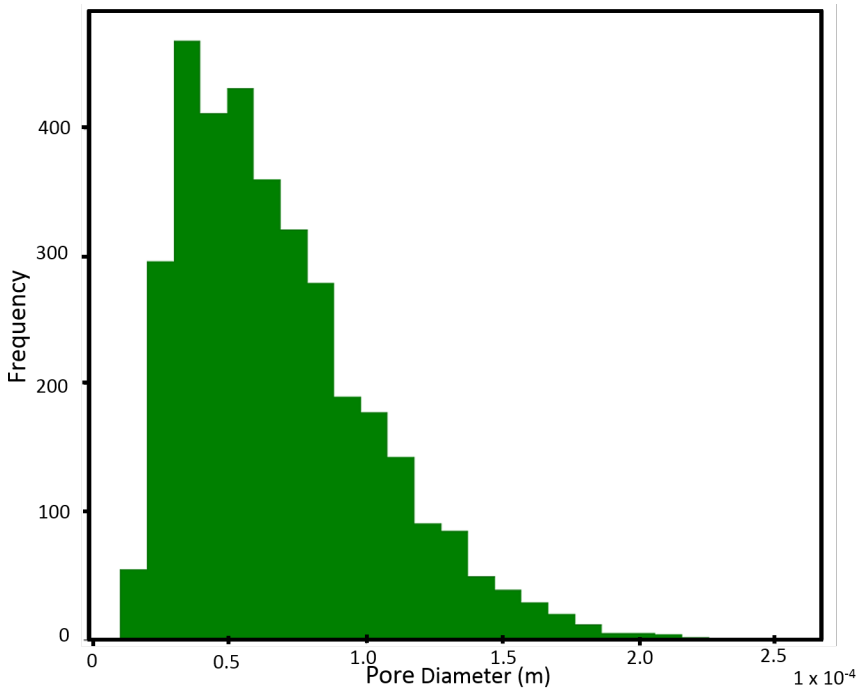

Figure 4.26: Pore size distribution at 0.11 g/cm^3 bulk density

From the above graph it is seen that the highest number of pores are in the range between 40 to 60 micrometer. This size differs considerably from the capillary size calculated from the Young-Laplace equation shown in table 4.22.

Another way of characterizing the pore size is by considering the permeability values. Since for a single capillary tubes it is known that K = $R_c^2/8$ so R_c can be computed from permeabilities as found by the fitting exercise using Darcy based model. The results are shown below:

Table 4.7: Effective capillary radius values calculated from permeability

Porosity ϕ	**Oil**	**Permeability K**	**Rc** $= \sqrt{8K}$ **micrometer**
0.934	Kerosene	4.87E-10	62
0.934	Diesel	2.96E-10	49
0.934	Light Lube	3.58E-10	53
0.934	Heavy Lube	4.17E-10	58
0.934	Crude	3.58E-10	53
0.915	Kerosene	3.54E-10	53
0.915	Diesel	2.29E-10	43
0.915	Light Lube	2.82E-10	47
0.915	Heavy Lube	3.39E-10	52
0.915	Crude	1.36E-10	33
0.899	Kerosene	3.25E-10	51
0.899	Diesel	1.32E-10	32
0.899	Light Lube	2.61E-10	46
0.899	Heavy Lube	2.87E-10	48
0.899	Crude	5.50E-11	21

These values are very different from the ones found by the Young-Laplace equation in table 4.6 but are very close to the values found from the pore network model in Figure 4.26. The values of permeabilities as they vary from one oil to another and across the bulk density is shown in Figure 4.27

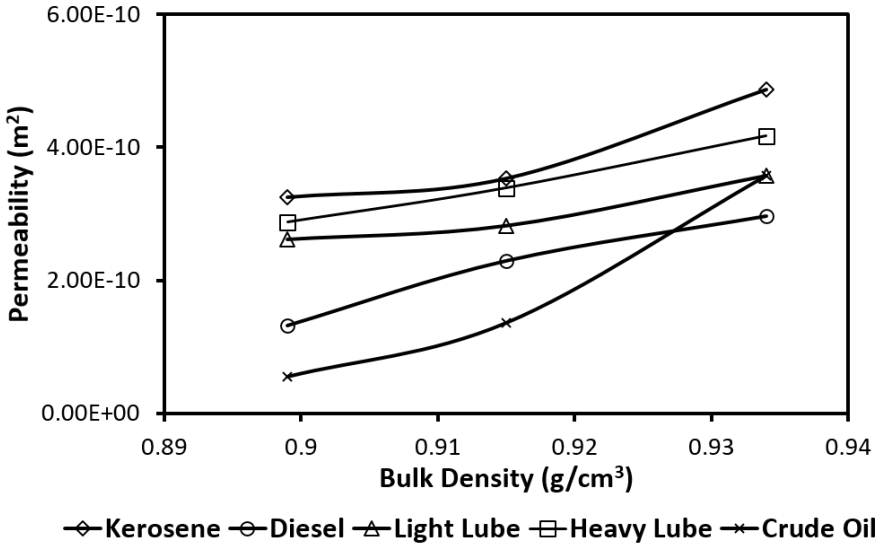

Figure 4.27: Permeability of porous media sample for different oil/bulk densities

Chapter 5

Conclusion and Future Work

5.1 Conclusions

This work investigated several characteristics of sorbents made with recycled polymer short fibers. They have potential for fabricating oil-sorbents with high sorption capacity and efficiency. Different techniques for oil spill remediation were presented and it was discussed that sorbent materials with their exceptional capabilities offers an attractive alternative for advancing research in oil/water separation applications and create a cost effective and environmental friendly product.

This research separates the evaluation of the study in two parts: one having to do with surface characteristics (intrinsic wettability) and the other dealing with the structural or morphological parameters of the porous structure formed by packing of the unconsolidated loosely packed fibers.

Contact angles and imbibition experiments were relevant factors determining the overall efficiency of sorbent materials. Since the surface characteristics of the fiber were not altered the observed differences in sorption study were attributed to the porous structure of the

porous media sample. It was shown that an accurate description of flow into the porous media and hence the performance of the sorbate-sorbent system is strongly dependent on the porous structure properties. This led to study the fundamentals of sorption and the governing equations that describe the transport phenomena in porous media.

The oil absorption phenomena was presented as an immiscible displacement process driven by capillary forces in which the wetting liquid (oil) displaces the non-wetting phase (air). It was suggested that this problem has 3 fundamental aspects: interfacial phenomena, transport phenomena and the pore structure which makes this a very vast field and requires more fundamental research to understand the synergistic effects of all 3 aspects concomitantly.

The porous media was experimentally characterized by studying the dynamics of capillary penetration and the resulting data was modeled using phenomenological laws applied on a macroscale. The models that were used for validating the experimental data assumed a bundle of vertically aligned capillary tubes as a hypothetical representation of the porous structure. The usefulness of these models were discussed pertaining to the macroscopic parameters like effective capillary diameter, capillary pressure and permeability. The deviations from the expected behavior were discussed and interpreted with other theories in literature. More specifically in studying the sorption characteristics of the fibrous polymer porous material the following findings were made:

- The contact angle measurement confirmed the intrinsic hydrophobic and oleophilic character of the polymer fiber. The effect of surface roughness on the magnitude of contact angles were shown and it was assumed that the smooth sample prepared closely approximated the Youngs ideal surface. Since this may not be the case therefore to further verify the non-wetting behavior of water the water-air capillary pressure test was done for one of the samples to show that indeed water does not imbibe spontaneously and a positive pressure was required.

- Spontaneous imbibition of oil was studied as a capillary rise phenomena and the equations describing the dynamics of the process were discussed. The effects of increasing the bulk density and its influence on the driving force ΔP was monitored in terms of the different front heights reached by the oils. The wetting phase saturation was discussed as an important parameters to evaluate the efficiency of the sorbate-sorbent system. It was found that the sorbent could pick up oil upto to 10 times its own mass.

- Darcy based and Lucas-Washburn model equations were fitted to the experimental data. It was found that if the contact angle is fixed to a single value as found from the contact angle measurements the LW behavior was not observed. Where as Darcy based capillarity model with capillary pressure and permeability as free parameters resulted in satisfactory fits. However when P_c was used to find a capillary radius it did not produce consistent results for the same bulk density. The Buckley-Leverret theory was suggested to resolve this issue and adjust the capillary pressure of the wetted front.

5.2 Future Work

- The mechanism of sorption into the porous structure as a capillary rise phenomena taking place in a bundle of capillary tubes with constant diameter was studied. The fibers in the porous media were considered as non swelling, rigid and non deforming under the action of fluid flow. However as Choi [24] argued some fibers have lumens that can absorb the liquid in its core. This would then change the diameter of the fiber hence the effective capillary radius of the pore will reduce with time. This behavior can be studied in future works by using SEM to understand the sorption mechanism. As Berg et al [60] mentions the relationship between hydraulic radius and capillary

radius must be found before applying the classic Lucas-Washburn equation.

- The dynamic nature of contact angle of a moving liquid inside a porous media should be studied. Since the wicking flows may be not be under constant speed therefore contact angle will change with time and this must be incorporated in the governing equations. Hamraoui et al [57] proposed that for some pore size sorption kinetics is dominated by frictional dissipation rather than viscous dissipation, where the latter is associated with a contact angle change.

- Contact angles were measured against air. Since in an actual oil spill scenario water will be present as the third phase therefore, oil contact angles should be measured against water by the reverse dispensing experiment as described in Appendix C.

- As mentioned by Pinto et al [51] in highly porous medium it is very much possible that the performance of the porous structure in terms of sorption efficiency and saturation does not depend on the porosity. Instead it is highly dependent on the pore connectivity and the pore size distribution. Therefore imaging techniques like SEM and micro-tomography should be done on different bulk densities to understand the connectivity of the pores and their relative size.

- It was found that accurate prediction of suction pressure was really important in making consistent prediction for the porous medium. The flow was modeled as single phase flow with sharp moving front. This may not be the case due to the microscopic physics at the meniscus level and therefore the deviation from the Lucas- Washburn behavior. It is recommended to apply fractional flow theory to know the exact saturation of the wetted front. This can be achieved by modeling imbibition as two phase flow in a pore network model and determine the relative permeability.

- Use of tomographic images to construct a 3-D virtual representation of the interior of the porous structure is greatly desired to model fluid flow into the porous medium

directly and predict transport properties like relative permeability much more accurately. This will aid in design of optimal porous structures with precisely known properties.

References

[1] M. Fingas, *The Basics of Oil Spill Cleanup*, CRC press, 2012.

[2] J. Lahann, *Environmental nanotechnology: Nanomaterials clean up*, Nature Nanotechnology, 2008, 3(6), p. 320.

[3] D. Dave and A. E. Ghaly, *Remediation technologies for marine oil spills: A critical review and comparative analysis*, American Journal of Environmental Sciences, 2011, 7(5), p. 423.

[4] Y. Nishi, N. Iwashita, Y. Sawada and M. Inagaki, *Sorption kinetics of heavy oil into porous carbons*, Water Research, 2002, 36(20), p. 5029.

[5] S. Kleindienst, J. H. Paul and S. B. Joye, *Using dispersants after oil spills: impacts on the composition and activity of microbial communities*, Nature Reviews Microbiology, 2015, 13(6), p. 388.

[6] J. Fritt-Rasmussen, S. Wegeberg and K. Gustavson, *Review on Burn Residues from In Situ Burning of Oil Spills in Relation to Arctic Waters*, Water, Air, & Soil Pollution, 2015, 226(10), p. 329.

[7] L. Feng, Z. Zhang, Z. Mai, Y. Ma, B. Liu, L. Jiang and D. Zhu, *A super-hydrophobic and super-oleophilic coating mesh film for the separation of oil and water*, Angewandte Chemie International Edition, 2004, 43(15), p. 2012.

[8] H. Duong and R. P. Burford, *Effect of foam density, oil viscosity, and temperature on oil sorption behavior of polyurethane*, Journal of Applied Polymer Science, 2006, 99(1), p. 360.

[9] R. S. Stein, *Polymer recycling: opportunities and limitations.*, Proceedings of the National Academy of Sciences, 1992, 89(3), p. 835.

[10] R. Siddique, J. Khatib and I. Kaur, *Use of recycled plastic in concrete: a review*, Waste Management, 2008, 28(10), p. 1835.

[11] R. Geyer, J. R. Jambeck and K. L. Law, *Production, use, and fate of all plastics ever made*, Science Advances, 2017, 3(7), p. e1700782.

[12] M. M. Radetić, D. M. Jocić, P. M. Jovancić, Z. L. Petrović and H. F. Thomas, *Recycled wool-based nonwoven material as an oil sorbent*, Environmental Science & Technology, 2003, 37(5), p. 1008.

[13] M. Alava, M. Dubé and M. Rost, *Imbibition in disordered media*, Advances in Physics, 2004, 53(2), p. 83.

[14] J. Cai, E. Perfect, C.-L. Cheng and X. Hu, *Generalized modeling of spontaneous imbibition based on Hagen–Poiseuille flow in tortuous capillaries with variably shaped apertures*, Langmuir, 2014, 30(18), p. 5142.

[15] I. B. Ivshina, M. S. Kuyukina, A. V. Krivoruchko, A. A. Elkin, S. O. Makarov, C. J. Cunningham, T. A. Peshkur, R. M. Atlas and J. C. Philp, *Oil spill problems and sustainable response strategies through new technologies*, Environmental Science: Processes & Impacts, 2015, 17(7), p. 1201.

[16] Q. Ma, H. Cheng, A. G. Fane, R. Wang and H. Zhang, *Recent development of advanced materials with special wettability for selective oil/water separation*, Small, 2016, 12(16), p. 2186.

[17] J. Wang, Y. Zheng and A. Wang, *Effect of kapok fiber treated with various solvents on oil absorbency*, Industrial Crops and Products, 2012, 40, p. 178.

[18] D. Angelova, I. Uzunov, S. Uzunova, A. Gigova and L. Minchev, *Kinetics of oil and oil products adsorption by carbonized rice husks*, Chemical Engineering Journal, 2011, 172(1), p. 306.

[19] R. Sarbatly, D. Krishnaiah and Z. Kamin, *A review of polymer nanofibres by electrospinning and their application in oil–water separation for cleaning up marine oil spills*, Marine Pollution Bulletin, 2016, 106(1), p. 8.

[20] M. A. Zahid, J. E. Halligan and R. F. Johnson, *Oil slick removal using matrices of polypropylene filaments*, Industrial & Engineering Chemistry Process Design and Development, 1972, 11(4), p. 550.

[21] F. A. Dullien, *Porous media: fluid transport and pore structure*, Academic press, 2012.

[22] R. Masoodi and K. M. Pillai, *Wicking in porous materials: traditional and modern modeling approaches*, CRC Press, 2012.

[23] J. Wu, N. Wang, L. Wang, H. Dong, Y. Zhao and L. Jiang, *Electrospun porous structure fibrous film with high oil adsorption capacity*, ACS Applied Materials & Interfaces, 2012, 4(6), p. 3207.

[24] H.-M. Choi and J. P. Moreau, *Oil sorption behavior of various sorbents studied by sorption capacity measurement and environmental scanning electron microscopy*, Microscopy Research and Technique, 1993, 25(5-6), p. 447.

[25] J. Lin, B. Ding, J. Yang, J. Yu and G. Sun, *Subtle regulation of the micro-and nanostructures of electrospun polystyrene fibers and their application in oil absorption*, Nanoscale, 2012, 4(1), p. 176.

[26] M. W. Lee, S. An, S. S. Latthe, C. Lee, S. Hong and S. S. Yoon, *Electrospun polystyrene nanofiber membrane with superhydrophobicity and superoleophilicity for selective separation of water and low viscous oil*, ACS Applied materials & Interfaces, 2013, 5(21), p. 10597.

[27] H. Zhu, S. Qiu, W. Jiang, D. Wu and C. Zhang, *Evaluation of electrospun polyvinyl chloride/polystyrene fibers as sorbent materials for oil spill cleanup*, Environmental Science & Technology, 2011, 45(10), p. 4527.

[28] H. Li, W. Wu, M. M. Bubakir, H. Chen, X. Zhong, Z. Liu, Y. Ding and W. Yang, *Polypropylene fibers fabricated via a needleless melt-electrospinning device for marine oil-spill cleanup*, Journal of Applied Polymer Science, 2014, 131(7), p. 40080.

[29] Q. Wei, R. Mather, A. Fotheringham and R. Yang, *Evaluation of nonwoven polypropylene oil sorbents in marine oil-spill recovery*, Marine Pollution Bulletin, 2003, 46(6), p. 780.

[30] A. Payatakes and M. M. Dias, *Immiscible microdisplacement and ganglion dynamics in porous media*, Reviews in Chemical Engineering, 1984, 2(2), p. 85.

[31] R. Lenormand, E. Touboul and C. Zarcone, *Numerical models and experiments on immiscible displacements in porous media*, Journal of Fluid Mechanics, 1988, 189, p. 165.

[32] J. Bear and Y. Bachmat, *Introduction to modeling of transport phenomena in porous media*, vol. 4, Springer Science & Business Media, 2012.

[33] A. Scheidegger et al., *The Physics of Flow through Porous Media*, University Of Toronto Press: London, 1958.

[34] J. Bear, *Dynamics of Fluids in Porous Media*, Courier Corporation, 2013.

[35] K. N. Prabhu, P. Fernades and G. Kumar, *Effect of substrate surface roughness on wetting behaviour of vegetable oils*, Materials & Design, 2009, 30(2), p. 297.

[36] G. Bracco and B. Holst, *Surface Science Techniques*, Springer Science & Business Media, 2013.

[37] D. Y. Kwok and A. W. Neumann, *Contact angle measurement and contact angle interpretation*, Advances in Colloid and Interface Science, 1999, 81(3), p. 167.

[38] A. Neumann, *Contact angles and their temperature dependence: thermodynamic status, measurement, interpretation and application*, Advances in Colloid and Interface science, 1974, 4(2-3), p. 105.

[39] D. Li and A. Neumann, *Thermodynamic status of contact angles*, Surfactant Science Series, 1996, p. 109.

[40] C. Rulison, *Wettability studies for porous solids including powders and fibrous materials*, Application Note, 1996, (302).

[41] W. A. Zisman, *Relation of the equilibrium contact angle to liquid and solid constitution*, in *Advances in Chemistry*, vol. 43, p. 1, ACS Publications, 1964.

[42] T. Ahmed et al., *Reservoir Engineering Handbook*, Gulf Professional Publishing, 2006.

[43] R. Masoodi, K. M. Pillai and P. P. Varanasi, *Darcy's law-based models for liquid absorption in polymer wicks*, AIChE Journal, 2007, 53(11), p. 2769.

[44] A. Marmur, *Penetration and displacement in capillary systems of limited size*, Advances in Colloid and interface Science, 1992, 39, p. 13.

[45] R. Masoodi, E. Languri and A. Ostadhossein, *Dynamics of liquid rise in a vertical capillary tube*, Journal of Colloid and Interface Science, 2013, 389(1), p. 268.

[46] J. T. Gostick, M. A. Ioannidis, M. W. Fowler and M. D. Pritzker, *Wettability and capillary behavior of fibrous gas diffusion media for polymer electrolyte membrane fuel cells*, Journal of Power Sources, 2009, 194(1), p. 433.

[47] J. T. Gostick, M. A. Ioannidis, M. W. Fowler and M. D. Pritzker, *Direct measurement of the capillary pressure characteristics of water–air–gas diffusion layer systems for PEM fuel cells*, Electrochemistry Communications, 2008, 10(10), p. 1520.

[48] J. T. Gostick, *Versatile and efficient pore network extraction method using marker-based watershed segmentation*, Physical Review E, 2017, 96(2), p. 023307.

[49] A. Bazargan, J. Tan and G. McKay, *Standardization of oil sorbent performance testing*, Journal of Testing and Evaluation, 2014, 43(6), p. 1271.

[50] J. Li, L. Yan, X. Tang, H. Feng, D. Hu and F. Zha, *Robust Superhydrophobic Fabric Bag Filled with Polyurethane Sponges Used for Vacuum-Assisted Continuous and Ultrafast Absorption and Collection of Oils from Water*, Advanced Materials Interfaces, 2016, 3(9).

[51] J. Pinto, A. Athanassiou and D. Fragouli, *Effect of the porous structure of polymer foams on the remediation of oil spills*, Journal of Physics D: Applied Physics, 2016, 49(14), p. 145601.

[52] J. Van Brakel and P. Heertjes, *Capillary rise in porous media. Part III: Role of the contact angle*, Powder Technology, 1977, 16(1), p. 91.

[53] S. H. Davis et al., *On the motion of a fluid-fluid interface along a solid surface*, Journal of Fluid Mechanics, 1974, 65(1), p. 71.

[54] M. Bracke, F. De Voeght and P. Joos, *The kinetics of wetting: the dynamic contact angle*, Trends in Colloid and Interface Science III, 1989, p. 142.

[55] B. J. Mullins, R. D. Braddock and G. Kasper, *Capillarity in fibrous filter media: Relationship to filter properties*, Chemical Engineering Science, 2007, 62(22), p. 6191.

[56] A. Siebold, A. Walliser, M. Nardin, M. Oppliger and J. Schultz, *Capillary rise for thermodynamic characterization of solid particle surface*, Journal of Colloid and Interface Dcience, 1997, 186(1), p. 60.

[57] A. Hamraoui and T. Nylander, *Analytical approach for the Lucas–Washburn equation*, Journal of Colloid and Interface Science, 2002, 250(2), p. 415.

[58] F. Dullien, M. El-Sayed and V. Batra, *Rate of capillary rise in porous media with nonuniform pores*, Journal of Colloid and Interface Science, 1977, 60(3), p. 497.

[59] M. Dong, F. A. Dullien, L. Dai and D. Li, *Immiscible displacement in the interacting capillary bundle model part ii. applications of model and comparison of interacting and non-interacting capillary bundle models*, Transport in Porous media, 2006, 63(2), p. 289.

[60] D. R. Schuchard and J. C. Berg, *Liquid transport in composite cellulosesuperabsorbent fiber networks*, Wood and Fiber Science, 2007, 23(3), p. 342.

[61] Z.-M. Huang, Y.-Z. Zhang, M. Kotaki and S. Ramakrishna, *A review on polymer nanofibers by electrospinning and their applications in nanocomposites*, Composites Science and Technology, 2003, 63(15), p. 2223.

[62] Y. NISHI, G. DAI, N. IWASHITA, Y. SAwADA and M. INAGAKI, *Evaluation of sorption behavior of heavy oil into exfoliated graphite by wicking test*, Journal of the Society of Materials Science, Japan, 2002, 51(12Appendix), p. 243.

[63] J. T. Gostick, M. W. Fowler, M. A. Ioannidis, M. D. Pritzker, Y. M. Volfkovich and A. Sakars, *Capillary pressure and hydrophilic porosity in gas diffusion layers for polymer electrolyte fuel cells*, Journal of Power Sources, 2006, 156(2), p. 375.

[64] A. Torkkeli et al., *Droplet microfluidics on a planar surface*, VTT Technical Research Centre of Finland, 2003.

[65] B. J. Mullins and R. D. Braddock, *Capillary rise in porous, fibrous media during liquid immersion*, International Journal of Heat and Mass Transfer, 2012, 55(21), p. 6222.

[66] S. Giljean, M. Bigerelle, K. Anselme and H. Haidara, *New insights on contact angle/roughness dependence on high surface energy materials*, Applied Surface Science, 2011, 257(22), p. 9631.

[67] B. M. Cummins, R. Chinthapatla, F. S. Ligler and G. M. Walker, *Time-Dependent Model for Fluid Flow in Porous Materials with Multiple Pore Sizes*, Analytical Chemistry, 2017, 89(8), p. 4377.

[68] E. W. Washburn, *The dynamics of capillary flow*, Physical Review, 1921, 17(3), p. 273.

[69] C. D. Volpe and S. Siboni, *Use, abuse, misuse and proper use of contact angles: a critical review*, Reviews of Adhesion and Adhesives, 2015, 3(4), p. 365.

[70] J. Zhao, C. Xiao and N. Xu, *Evaluation of polypropylene and poly (butylmethacrylate-co-hydroxyethylmethacrylate) nonwoven material as oil absorbent*, Environmental Science and Pollution Research, 2013, 20(6), p. 4137.

[71] G. Callegari, I. Tyomkin, K. G. Kornev, A. V. Neimark and Y.-L. Hsieh, *Absorption and transport properties of ultra-fine cellulose webs*, Journal of Colloid and Interface Science, 2011, 353(1), p. 290.

[72] F. A. Coutelieris and J. Delgado, *Fundamentals of Porous Structures*, in *Transport Processes in Porous Media*, p. 5, Springer, 2012.

[73] I. Ltd., *Use of sorbent materials in oil spill response*, Technical information paper, 2012.

APPENDICES

Appendix A

(a) Kerosene

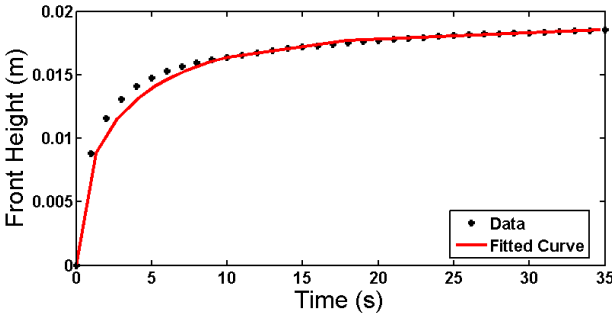

(b) Diesel

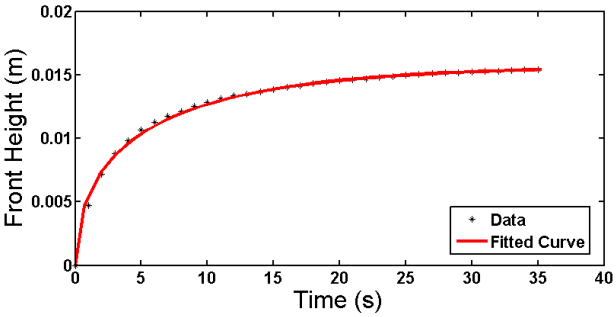

(c) Light Lube

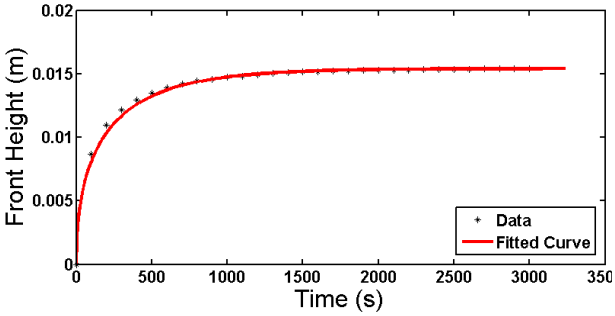

(d) Heavy Lube

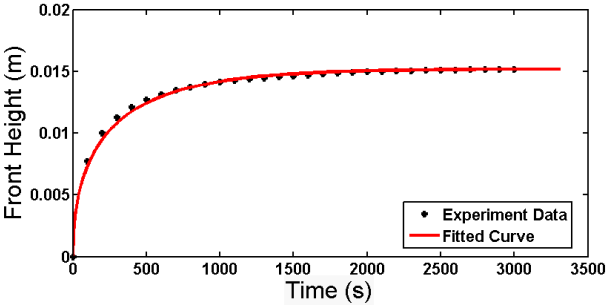

(e) Crude Oil

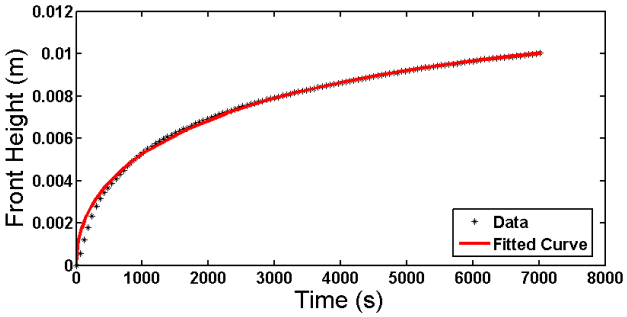

Figure 1: Darcy Law based curves for 0.085 g/cm3

(a) Kerosene

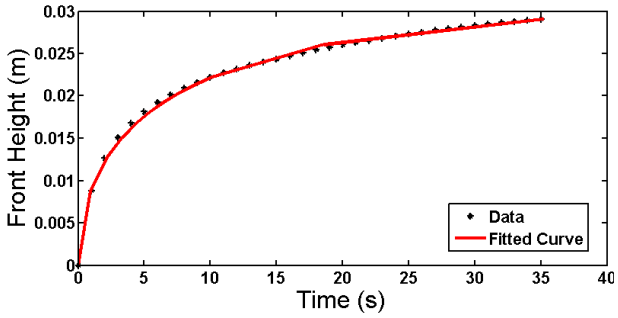

(b) Diesel

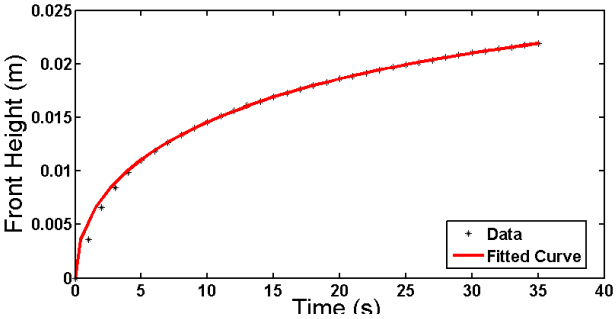

(c) Light Lube

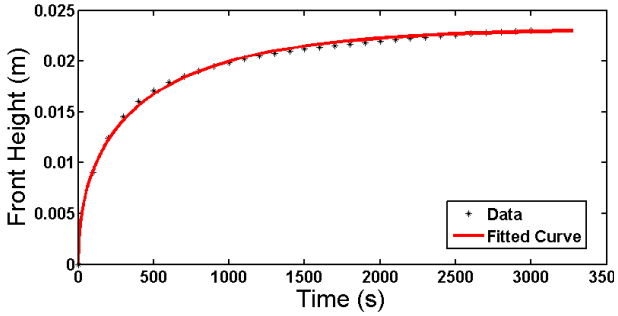

(d) Heavy Lube

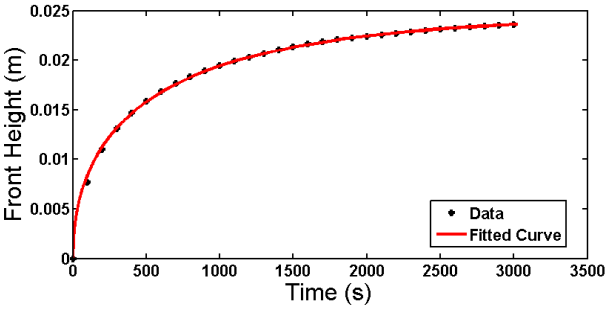

(e) Crude Oil

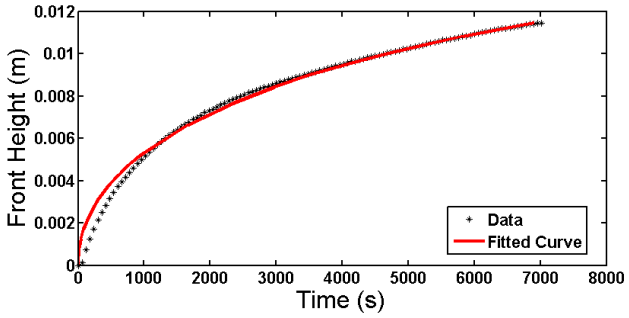

Figure 2: Darcy Law based curves for 0.13 g/cm3

(a) 0.085 g/cm^3

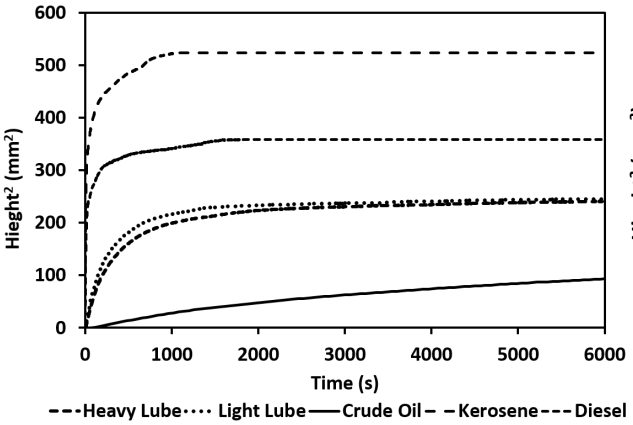

(b) 0.095 g/cm^3

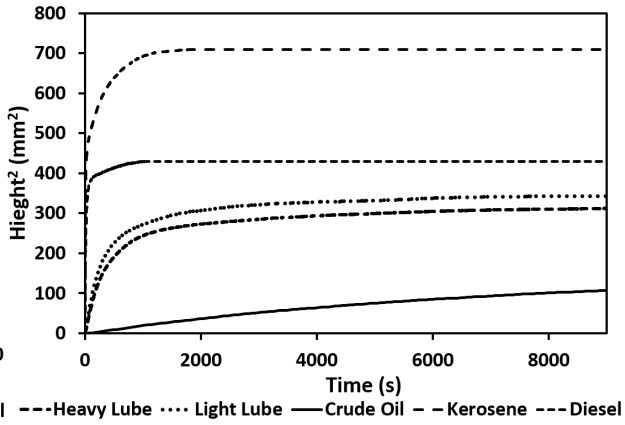

(c) 0.13 g/cm^3

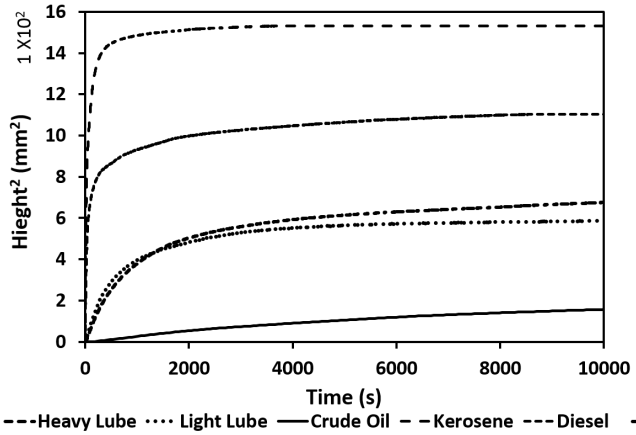

(d) 0.16 g/cm^3

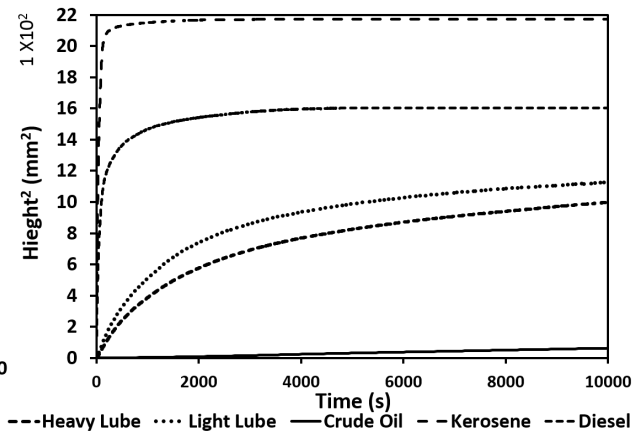

Figure 3: Lucas-Washburn curves for different bulk densities

Appendix B

MATLAB code for Lucas-Washburn model.

% INPUTS xdata = xlsread('LW1.xlsx');

tdata = xlsread('LW1.xlsx');

xdatacalc = xlsread('LW1.xlsx');

tdatacalc = xlsread('LW1.xlsx',);

% FUNCTION fun = @(x)sseval(x,xdatacalc,tdatacalc);

% INITIAL GUESS

c0 = [0.0001]; bestx = fminsearch(fun,c0) n = Oil viscosity; g = gravity; p = oil density; T= Oil surface tension; theta= 31; A=cosd(theta); B= 2*T*A/(p*g);

% Quality check R = bestx(1) % Effective capillary radius R_c

$tfit = (16{*}n{*}T{*}A/(g^2{*}p^2{*}R^3){*}abs(log(B./(B{-}R{*}xdatacalc)))){-}8{*}n{*}xdatacalc/(g{*}p*R^2)$;plot(tdata,xdata,'*'); hold on plot(tfit,xdatacalc,'R'),xlabel('xdata'),ylabel

('Response Data and Curve'); title('Data and Best Fitting Curve') legend('Data','Fitted Curve','Location','Best') hold off

% ERROR OPTIMIZATION

function sse = sseval(x,xdatacalc,tdatacalc) n = Oil viscosity; g = gravity; p = oil density;

T=Oil surface tension; theta= 31; A=cosd(theta); B= 2*T*A/(p*g); $sse = sum((tdatacalc{-}((16{*}n{*}T{*}A/(g^2{*}p^2{*}R^3){*}abs(log(B./(B{-}R{*}xdatacalc)))){-}8{*}n{*}xdatacalc/(g{*}p{*}R^2))).^2)$

MATLAB code for Darcy based model.

% INPUTS xdata = xlsread('LW1.xlsx','1.0','J4:J34');

tdata = xlsread('LW1.xlsx','1.0','I4:I34');

xdatacalc = xlsread('LW1.xlsx','1.0','L4:L529');

tdatacalc = xlsread('LW1.xlsx','1.0','K4:K529');

% FUNCTION fun = @(x)sseval(x,xdatacalc,tdatacalc);

% INITIAL GUESS

c0 = [1000 2e-10];

bestx = fminsearch(fun,c0) n = Oil viscosity; g = gravity; p = oil density; e= Porosity;

P = bestx(1) % Capillary pressure k = bestx(2) % Permeability

$tfit = (P*e*n/(g^2*p^2*k)*abs(log(P./(P-xdatacalc*p*g))))-e*n*xdatacalc/(g*p*k)$;plot(tdata,xdata,'*'); hold on plot(tfit,xdatacalc,'r'),xlabel('xdata'),ylabel('Response Data and Curve'); title('Data and Best Fitting Curve') legend('Data','Fitted Curve','Location','Best') hold off

% ERROR OPTIMIZATION

function sse = sseval(x,xdatacalc,tdatacalc) P = x(1); k = x(2) n = Oil viscosity; g = gravity; p = oil density; e=Porosity; $sse = sum((tdatacalc - ((P*e*n/(g^2*p^2*k)*abs(log(P./(P-xdatacalc*p*g))))-e*n*xdatacalc/(g*p*k))).^2)$;

Appendix C

Contact angle of Oil against water

An experiment was set up to measure the contact angle of oil in the presence of water. Previously in section 4.1.2.2 contact angles of hydrocarbon oils were measured against air. This was useful since in the imbibition experiment the two set of fluids signifying immiscible displacement were oil and water. Therefore oil contact angles against air corroborated with the sorption experiment. However in a real scenario the polymer fiber sample might get soaked with water first, therefore it would be of interest to measure the oil contact angles against water. To this end an experiment was done, schematic of which is shown below:

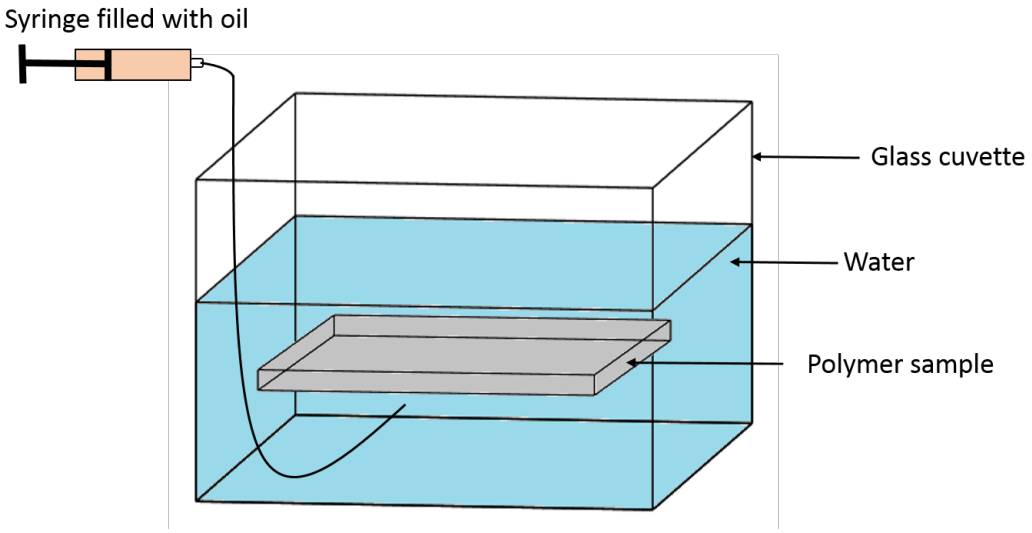

Figure 4: Schematic for reverse measurement of contact angle

The glass cuvette was placed on the sample platform of the contact angle instrument shown in Figure 3.4. However dispensing of oil was done manually which was difficult to control. Moreover the resolution of the images obtained were not sharp. With trial and error some success was made and contact angles were measured for this reverse scenario.

Figure 5 below show contact angle image for kerosene and light lube oil.

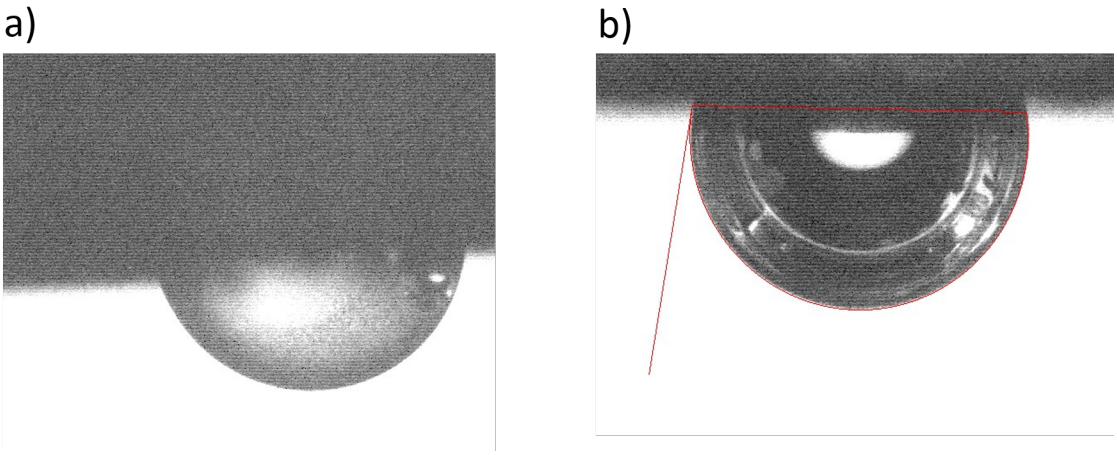

Figure 5: Reverse oil contact angles against water on smooth injection molded sample for a) Kerosene and b) Lube oil